



This is to certify that the

dissertation entitled

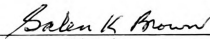
DATA ACQUISITION SYSTEM FOR STUDY
OF IMPACT DAMAGE TO APPLES

presented by

SIAMAK SIYAMI

has been accepted towards fulfillment
of the requirements for

Ph. D. degree in Agricultural Engineering


Major professor

Date OCT 23, 1986



RETURNING MATERIALS:
Place in book drop to
remove this checkout from
your record. FINES will
be charged if book is
returned after the date
stamped below.

~~APR 15 2001~~
000 H308

~~JUL 17 2001~~
APR 06 2001

AUG 07 2001

~~DEC 10 2001~~

DATA ACQUISITION SYSTEM FOR STUDY
OF IMPACT DAMAGE TO APPLES

By
Siamak Siyami

A DISSERTATION

Submitted to
Michigan State University
in partial fulfillment of the requirements
for the degree of

DOCTOR OF PHILOSOPHY

Department of Agricultural Engineering

1986

ABSTRACT

DATA ACQUISITION SYSTEM FOR STUDY OF IMPACT DAMAGE TO APPLES

By

SIAMAK SIYAMI

Impact bruising of apples during harvesting, handling, and transportation, results in major damage and quality loss. A data acquisition system which can be configured as an instrumented sphere (IS) has been developed which permits automatic impact measurement and recording of vector accelerations along with the time of occurrence. The features of this device are as follows:

1. The data acquisition device is a miniaturized, totally integrated, portable, stand-alone system which can fit in a 15 cm cube.
2. The IS is calibrated to provide an accuracy of ± 4.35 g over its full range in the measurement of impact experienced by fruit.

The present IS consists of a 15-cm cube containing a tri-axial accelerometer, a NMOS 8097 micro-controller chip with A/D on board, 64 kbytes of RAM, a real time clock, and a rechargable power supply. The 8097 NMOS chip will be

replaced by a CMOS version when this becomes available. A connector for serial communication is provided to permit program initialization and data transfer to an independent computer.

Impacts were applied simultaneously to Ida-Red apples and to the IS mounted on an impact table. Data were collected to relate the measured impacts and corresponding bruising. A predictive model was obtained by step-wise multiple linear regression which predicted bruise diameter to ± 3 mm with 99 percent confidence. The model could account for 90.2 percent of the bruise diameter variations about the mean. This model was compared with both the Hertz theory and plastic theory, which at best could only account for 65.6 and 66.2 percent of the bruise diameter variation about the mean, respectively. An adjusted Hertz theory was developed which predicted 86.9 percent of the bruise diameter variation.

The IS data acquisition system appears to meet the design criteria. When further developed it should provide insight into bruise prediction and bruise prevention for fruits, vegetables, and damage reduction for fragile non-food articles.

Approved:


Major Professor


Department Chairman

To my wife, Marcy,
for her unending faith and encouragement,
for her love and understanding.
To my parents, Faramarz and Yelena,
whose belief in the value of education
was constant and whose support and sacrifices
toward that end were truly significant.
And to my brothers, Babak and Ramien,
for their patience and tolerance.

ACKNOWLEDGMENTS

I wish to extend my gratitude and appreciation to members of my dissertation committee: Dr. Galen K. Brown, Dr. Gary J. Burgess, Dr. John B. Gerrish, Dr. Bernie R. Tennes, and Dr. Roland H. Zapp. Their collective expertise and constructive comments were invaluable to the completion of this thesis.

A special vote of thanks goes to Dr. Galen Brown for serving as academic advisor and chair of my dissertation committee. His friendship, support, and encouragement helped each step along the way, and his dedication to excellence provides continued inspiration.

I also wish to express my gratitude to Dr. M. Moallemian for his support, advice and encouragement. Sincere thanks and appreciation are also extended to: B. A. Klug, R. J. Wolthuis, D. E. Young, B. Newcome, Y. Chait, J. Clemens, and C. Johnson for their assistance and help.

I also wish to acknowledge Dr. B. R. Tennes and R. H. Zapp for providing an assistantship during the course of this project.

But most of all I wish to express my love and gratitude to my wife marcy, for her gentle understanding, warm support and countless sacrifices.

TABLE OF CONTENTS

	Page
LIST OF TABLES.	vi
LIST OF FIGURES.	vii
Chapter	
1. INTRODUCTION.	1
1.1 Importance of the Investigation.....	1
1.2 Specific Objective of the Study.....	3
1.3 Scope and Limitation of the Study.....	4
1.4 Previous Related Studies.....	5
1.5 Limitations of the Previous Studies.....	9
1.6 Analysis of the Problem.....	10
2. THEORETICAL APPROACH.	12
2.1 Physical Properties of Apples.....	12
2.1.1 Impact of Elastic Bodies.....	13
2.1.2 Impact of Plastic Bodies.....	22
2.2 Artificial Apple (Pseudo-Fruit).....	27
2.2.1 Accelerometer.....	28
2.2.2 Transfer Function Concept.....	33
3. EXPERIMENTAL APPARATUS AND PROCEDURES.	37
3.1 Experimental Apparatus.....	37
3.1.1 Accelerometer.....	38
3.1.2 Microcontroller.....	40
3.1.3 Hardware.....	41
3.1.3.a Power Supply.....	43
3.1.3.b Analog Circuitry.....	45
3.1.3.c Digital Circuitry.....	47
3.1.4 Software.....	52
3.1.5 Impact Table.....	54
3.2 Procedure for Drop Tests.....	56
3.2.1 Half-Sine and Extended Half-Sine Impacts.....	60
3.3 Procedure for Calibration.....	63
3.3.1 Accelerometer.....	63
3.3.2 Impact Table.....	64

Chapter	Page
3.3.3 IS Data Acquisition System.....	64
3.4 Experimental Procedure.....	68
3.4.1 Parameter Selection and Measurement.....	69
3.4.2 Impact Tests.....	72
4. RESULTS AND DISCUSSION.74
4.1 IS Calibration and Precision.....	74
4.2 Statistical Analysis.....	76
4.2.1 Apple Physical Properties.....	78
4.2.2 Methods of Impact Bruise Prediction.....	86
4.3 The Bruise Diameter Versus Hertz Theory.....	87
4.4 The Bruise Diameter Versus Adjusted Hertz Theory...	90
4.5 The Bruise Diameter Versus Plastic Theory.....	95
4.6 The Bruise Diameter Versus MLRA Model.....	100
4.7 Comparison Among Models.....	105
5. SUMMARY	109
6. CONCLUSIONS.111
7. RECOMMENDATIONS FOR FUTURE RESEARCH.113
8. APPENDICES.	114
A.1 Physical Properties of Casting Material.114
A.2 Accelerometer Calibration Charts.	115
A.3 Microcontroller Specifications.	119
B.1 Software Block Diagrams.123
C. Data and Statistical Analysis.126
8. LIST OF REFERENCES.	143

LIST OF TABLES

Table		Page
Table 3.1	Specifications for Vibra-Metrics model No. 3132 Triaxial Piezoelectric Accelerometer.	39
Table 3.2	Definition of Special Select Lines Used in Control and Addressing of the IS Digital Circuitry.	51
Table 3.3	Duration, Maximum Acceleration, Total Velocity Change and Equivalent Drop Height for Half-Sine and Extended Half-Sine.	62
Table 3.4	Simple Statistics for the Lansmont Impact Table Calibration.	66
Table 3.5	CS Type Apple Impact Test Parameters.	70
Table 3.6	CA Type Apple Impact Test Parameters.	70
Table 3.7	U.S.D.A. Guideline for Apple Bruise and Quality Classification, and Present Dollar Value.	71
Table 4.1	Means and Variances for the Apple Physical Properties and Impact Conditions.	79
Table 4.2	Final Statistics for the MLRA Regression Analysis.	102
Table 4.3	Comparison Among All Prediction Methods Based on a First Order Prediction for Bruise Diameter.	106
Table 4.4	Bruise Diameter Prediction Methods and Their Parameters Along With Respective Formulations.	108

LIST OF FIGURES

Figure		Page
Figure 2.1	Physical Parameters Related to Hertz Theory.17
Figure 2.2.a	Hertz Theory Force-Deformation Curve.23
Figure 2.2.b	Plastic Force-Deformation Curve.23
Figure 2.3.a	Maximum Compression and Contact Radius, Before and After Impact.25
Figure 2.3.b	Free Body Diagram of an Apple Impact on a Hard Surface25
Figure 2.4	Instrumented Sphere Shown With All Components Including the Accelerometer.30
Figure 2.5	Physical Arrangement of a Piezoelectric Type Accelerometer.31
Figure 2.6	Electrical Representation of a Piezoelectric Type Accelerometer and Charge Amplifier.31
Figure 2.7	Magnitude Vs Frequency Diagrams for Casting Effects of the Imbedded Accelerometer.36
Figure 2.8	Phase Vs Frequency Diagrams for Casting Casting Effects of the Imbedded Accelerometer.36
Figure 3.1	Circuit Diagram for the Accelerometer Constant Current Source and High Pass Filter.39
Figure 3.2	Block Diagram of the IS Data Acquisition System.42
Figure 3.3	Power Supply Circuit Diagram of the IS Data Acquisition System.44

	Page
Figure 3.4	Analog Conditioning Circuit of the IS Data Acquisition System. 46
Figure 3.5	Block Diagram of the IS Digital Circuitry. 48
Figure 3.6	Digital Circuit Diagram of the IS Data Acquisition System. 49
Figure 3.7	Schematic of an Impact Testing Machine. . . 55
Figure 3.8	Acceleration VS Time Plot for Half-Sine and Extended Half-Sine. 61
Figure 3.9	Magnitude Response of the Triaxial Accelerometer Calibration Used in the IS System. 65
Figure 3.10	Phase Response of the Triaxial Accelerometer Calibration Used in the IS System. 65
Figure 3.11	The {111} Position of the Accelerometer Used in IS System Calibration. 66
Figure 3.12	Measured Bruise and Diameter for Ida-Red Apple. 71
Figure 4.1	IS Calibration Curve for Single Axes Acceleration. 75
Figure 4.2	IS Calibration Curve for the {111} Resultant Acceleration {111}. 75
Figure 4.3	Average of 10 Impacts for 3 Impact Types Collected by IS System at 3.012 kHz Sampling Rate. 77
Figure 4.4	Average of 10 Impacts for 3 Impact Types Collected by Data 6000 as Calibration at 12.048 kHz Sampling Rate. 77
Figure 4.5	Frequency Distribution of Apple Diameters. 80
Figure 4.6	Frequency Distribution of Apple Mass. . . . 81
Figure 4.7	Frequency Distribution of Apple Magness-Taylor. 82
Figure 4.8	Bruise Diameter Versus Maximum Acceleration for 4 Ranges of Magness-Taylor Force. . . . 84
Figure 4.9	Maximum Acceleration Versus Drop Height Mapped for Both Half-Sine and Extended

Figure		Page
	Half-Sine Impacts.	88
Figure 4.10	Maximum Acceleration Versus Velocity Change Mapped for Both Half-Sine and Extended Half- Sine Impacts.89
Figure 4.11	Measured Bruise Versus Hertz Theory Bruise Diameters for All Ida-Red Apples. .	91
Figure 4.12	Hertz Theory and Measured Bruise Versus Maximum Acceleration with First Order Regression Lines.92
Figure 4.13	Measured Bruise Versus Adjusted Hertz Bruise Diameters for All Ida-Red Apples. .	94
Figure 4.14	Adjusted Hertz Theory and Measured Bruise Versus Maximum Acceleration with First Order Regression Lines.96
Figure 4.15	Measured Bruise Versus Plastic Theory Based Bruise Diameters for All Apples.	98
Figure 4.16	Plastic Theory and Measured Bruise Versus Maximum Acceleration with First Order Regression Lines.99
Figure 4.17	Measured Bruise Versus MLRA Prediction Based Bruise Diameters for All Apples. .	.103
Figure 4.18	MLRA prediction and Measured Bruise Versus Maximum Acceleration with First Order Regression Lines.	104

1. INTRODUCTION

1.1 Importance of the Investigation

Increased use of mechanized systems and machinery in harvesting, handling and processing operations for fresh produce has increased the problem of mechanical damage. This type of damage, caused by mechanical impact, is commonly referred to as bruising.

Peleg (1984), estimated that the postharvest losses in some fruit and vegetable crops may reach 30 percent of the total yield. Goff and Twede (1979) concluded that it was difficult to find an unbruised apple in a supermarket. Their studies indicated that about 80 to 100 bruises were found in each 1.4 kg bag of MacIntosh apples (average of 9 bruises per apple) before the apples reached the consumer.

Finney et al. (1975) mentioned that bruising of Golden Delicious apples resulted in approximately 23 percent of the apples being down-graded to grades lower than the best quality. U.S.D.A standards for grades of apples (1964) specify that apples with bruises greater than 12.7 mm in diameter must be down-graded. Bruising can lead to a significant financial loss during storage, handling and

marketing of agricultural commodities, especially apples.

Presently, only limited techniques are available to predict and reduce impact bruising. The sole procedure to assess the quality of apples and the extent of their bruises requires extensive sampling of large quantities of apples at various stages in the handling chain. This method of evaluation is time consuming, costly and subjective. A non-destructive objective method to statistically evaluate bruising at different stages of harvesting, handling and transporting would benefit the apple industry. One such method is to measure and record the impact acceleration (acceleration change caused by a sudden impact) history that apples experience during an entire packing operation. The impact information could then be correlated to actual bruising in order to locate problems and reduce apple bruising at the various handling stages.

The steps involved in bruise prediction using an impact recording system are as follows:

1. Construct a pseudo-fruit capable of identifying probable damage-causing events in different operations.
2. Calibrate the pseudo-fruit to assure accuracy in its measurements.
3. Collect impact data with the pseudo-fruit and correlate the data with physical bruising to identify bruising operations and provide probabilities of bruises occurring.

Various researchers have attempted to predict and

reduce the impact bruising in fruits, but without reliable results. In some cases a system has been developed which lacks in calibration and/or performance (Pullen and Diener (1971), Rider (1969)). In other cases many critical factors were established for bruise prediction, but no pseudo-fruit was developed (Aldred and Burch (1977)).

The purposes of my research were to develop an instrument to measure and store impact accelerations along 3 orthogonal axis, and to use these data to make a model which could predict the extent of bruising. The instrument was to be calibrated against the controlled impacts and apple bruising obtained from a standard calibrated impact table.

State-of-the-art electronics were to be used to obtain great accuracy. The instrument was to be designed to use CMOS technology in order to allow eventual encapsulation of the entire system in a realistic 80-mm diameter sphere.

1.2 Specific Objectives of the Study

Since impact damage to fruit is related to rapid deceleration, the main objective of this study was to develop a device capable of measuring vector accelerations above a damage resulting threshold and storing the resultant vector components in memory for later analysis.

Four specific objectives were identified to achieve the the main objective. The first specific objective was to select the transducer to best detect the impact. The second

objective was to design and fabricate the analog and digital circuits necessary to collect and store the impact accelerations. The third objective was to package the entire system in a compact geometry similar in size to an actual fruit (apple). The fourth objective was to correlate the impact data collected by the device with actual physical damage to apples and develop a predictive model for bruise diameter.

1.3 Scope and Limitation of the Study

This study encompassed the design of a new digital data acquisition system for obtaining and storing critical impact data within the impact instrument. The instrument was designed to measure and store only accelerations which potentially produce impact damage.

The study of apple bruise size caused by impact was based on measuring the bruise diameter, since that is a key element of the U.S.D.A. standards for apple grading. The apple variety Ida-Red was used in all tests.

Rider et al. (1973) indicated that the design and construction of an artificial fruit with the same mechanical properties as a real fruit is complex. With this in mind, the material used to encapsulate the electronics for the impact instrument (hereafter referred to as the instrumented sphere or IS) was chosen to assure that the measured internal acceleration at the IS center was simply

related to the actual surface acceleration at the point of contact with an impacted surface. Tests were conducted to verify the mechanical/electrical properties of the encapsulation material and to establish the transfer function relating surface-acceleration to center acceleration. Since a major CMOS component was unavailable, a functionally equivalent NMOS component was used. As a result, the packaging of the entire power, data acquisition and data storage system inside the IS was impractical. Thus, for initial measurements only the accelerometer was encased in the IS, and three electrical leads connected the accelerometer to an electrical power supply and data storage unit.

1.4 Previous Related Studies

During the past decade many researchers tried to explain and detect bruising in fruits during harvesting and handling. One method they used involved force transducers to measure impacts. Pullen and Diener (1971) developed a miniaturized low cost FET triaxial accelerometer with vector summing capabilities. Three cables were required to transmit the impact data to a recorder. This accelerometer approach was subsequently duplicated by others in recent telemetry systems. Advantages of this system were the vector summing capabilities and the low level of cable noise. Another approach was to use telemetry in a pseudo-

fruit to transmit the variations in accelerations via a FM transmitter. The objective was to remove any sensing cables from the pseudo-fruit in order to enable the pseudo-fruit to simulate the free movement of a fruit. Harrison (1969) used a triaxial accelerometer with three separate FM transmitters and receivers to measure vector accelerations. A chart recorder was used to record the data and provide calibration curves for this system. This system was cumbersome in addition to being unreliable.

Rider (1969), developed a pseudo-fruit using three separate accelerometers mounted in a 57-mm diameter steel shell covered with 9.5 mm of Ensolite material. Cables were used to transfer acceleration signals to a chart recorder. Rider showed that acceleration can be used to predict internal shear stress, if the modulus of elasticity and the radius of the surface impacted by the pseudo-fruit were known. Although physical properties of the Rider pseudo-fruit were similar to those of a peach, the duration of impact did not agree with the values obtained from the Hertz theory. He attributed this to the "bottoming out" of the covering material at relatively high impact values.

Shupe and Lake (1970) placed a miniaturized single axis accelerometer and radio transmitter inside an egg-sized package. The transmitted data were displayed on an oscilloscope, but factors such as transmitter design, inconsistent signal replication and the directionality of a single axis accelerometer limited the usefulness of this study.

O'Brien et al. (1973) used a telemetry system having three separate FM transmitters and a triaxial accelerometer. Data from each accelerometer and transmitter were received by the respective FM receiver and stored on a multi-channel analog tape recorder. The accelerometers were enclosed in a 57 mm fiberglass sphere covered with 10 mm of resilient material. No specific calibration technique was mentioned and accuracy was estimated to be ± 5 percent. The telemetering fruit was not sensitive to accelerations below 0.5 g (gravitational force), or to impacts greater than 0.5 s durations, because both of these conditions were believed to be insignificant for bruise formation.

Aldred and Burch (1977) improved on O'Briens work by using a triaxial accelerometer, with vector summing capabilities, to study impact bruising of peaches. Only one transmitter (for the resultant acceleration) was placed inside a 67 mm sphere. The received data were sent to a computer rather than a recorder. Approximately 2 s of data at a 1 kHz sampling rate were stored and processed for each impact. It was stated that additional tests were necessary to insure pseudo-fruit resemblance to a real fruit and to correlate output of the pseudo-fruit with the actual bruise. No attempts were made to calibrate the output of this system.

Hallee (1981) used a triaxial piezoelectric accelerometer along with a telemetry system inside an artificial

potato to monitor impact accelerations during harvesting and handling. He observed variations in acceleration for different orientations of the potato, which he concluded were due to either the non-homogeneity of the covering material or to its thickness. The maximum acceleration, internal shear stress, and duration of impact could be estimated if radius, modulus of elasticity, mass of fruit, impacting surface and drop height were known. The precision of the output was reported to be ± 7.5 percent based on a 97 percent confidence interval.

Halderson (1983) also used telemetry to predict impact bruises to potatoes. He used a triaxial accelerometer configuration with an improved FM transmitter. The unit operated up to 30 m from the receiver, with a single axis correlation of about 0.8. Multiple axis correlation was not reported. This research, however, lacked both a true calibration procedure and a field test performance analysis.

Kerr and Wilkie (1985) described a triaxial accelerometer and telemetry system, as an automated data collection system, for use on a potato harvester to provide an immediate indication of damage. This unit included a computer on-board the harvester which stored the acceleration, temperature and other critical data for further analysis. No calibration, accuracy or performance results were discussed, however.

Jenkins and Humphries (1982) abandoned the accelerometer system to develop a new technique to assess impact

damage based on water loss, through one-way slit valves mounted in a hollow vinyl sphere. This system resulted in good correlation between drop height on a hard surface and water loss. The only drawback was the lack of a recording system. Anderson and Parks (1984) also developed a pseudo-potato filled with fluid which used pressure sensors as force transducers. They experienced some difficulty with air bubbles, which forced them to convert to air for the internal fluid. This, however resulted in a pseudo-potato which was too light.

1.5 Limitations of the Previous Studies

Previous work utilizing cables or telemetry for transferring impact data to a recorder had many limitations. For instance, the free movement of a fruit could not be simulated when cables were used for data transmission. A major limitation in the telemetry configuration was the need for close proximity of the receiver to the pseudo-fruit, thus limiting its use in addition to requiring an operator. Many of the telemetry systems also suffered from noise produced by the electrical machinery used in typical packing houses. An additional limitation of any telemetry system is that it cannot be used during transportation of fruits, due to the low acceleration sensitivity (high noise ratio) and lack of continuous operation.

Probably the greatest limitation of older impact

measurement systems has been the lack of accurate and miniaturized accelerometers. This limitation has been removed by recent advances in integrated electronics and miniaturized transducers. These advances have also enhanced the performance and reduced the power consumption of most components.

Finally, in most applications where a pseudo-fruit was used, the acceleration was measured inside the sphere which had a soft outer layer. The soft outer shell, which was used to simulate the fruit firmness, resulted in a nonlinear distortion of the acceleration sensed in the center of the pseudo-fruit. A slightest change in the impact surface or in the temperature could alter the response of the outer-layer. Such affects were neglected in earlier research, but could in fact explain the poor performance of such systems.

Many researchers have neglected to validate the accuracy and performance of their pseudo-fruit through actual field tests or laboratory drop tests. In most cases there are no functions to relate bruising to impact data sensed by the pseudo-fruit.

1.6 Analysis of the Problem

Impact bruising caused during apple handling and harvesting operations has created a need for an accurate method of predicting this type of bruising in order to

establish means for preventing it. Previous instruments used in bruise prediction lacked in accuracy and reliability and no general calibration procedures were outlined. The focus of this dissertation was to develop a totally integrated, portable, and stand-alone data acquisition system (IS) which could be cast in a 15 cm cube. The IS is fully calibrated and calibration charts were provided for single axes and the triaxial resultant vector sum. A complete calibration procedure was developed based on the transfer function of the IS.

An impact table was used to generate two types of impacts, half-sine and extended half-sine representing very hard and hard surfaces, respectively. These impacts were used to bruise Ida-Red apples.

The IS was then used in impact tests along with apples to identify critical bruise parameters that are highly correlated with impact bruising. Such parameters were to be identified and then incorporated into a model to predict apple impact bruise diameter based on measurable parameters and IS recordings.

This predictive model was then compared with existing elastic and plastic theories for accuracy of bruise diameter prediction.

2. THEORETICAL APPROACH

2.1 Physical Properties of Apples

The physical properties of the apple enable it to absorb only limited dynamic inputs or free fall impacts without the tissue being bruised. The bruising of an apple begins with immediate softening of the impacted tissue resulting from the rupture of cell walls and consequent loss of turgor. Browning in apples results from oxidation of cellular contents by enzymes, because when cells rupture their contents are exposed to the intercellular air which results in enzymatic oxidation.

Many of the measurable physical properties such as fruit size, firmness and coefficient of restitution, as well as drop height and impact surface conditions, have been recognized by various researchers to be of importance in bruise formation. Nelson and Mohsenin (1968) and Schoorl and Holt (1974) predicted that high modulus of elasticity values were a good indication of the bruise resistance of apples. Hammerle and Mohsenin (1966) reported that the area and volume of bruise increased with an increase in drop height. Diener et al. (1977) studied the coefficient of

restitution of apples and concluded that it is not a good parameter to estimate bruise resistance of fruits since it does not change with maturity.

The physical properties used in this study were limited to apple mass (AM), horizontal diameter (AHD), vertical diameter (AVD) and Magness-Taylor values (MT). Additional critical parameters such as maximum acceleration, total velocity change, bruise depth, bruise volume and bruise energy were used to quantify bruising as the result of impacts.

2.1.1 Impact of Elastic Bodies

Impact differs from static rapid loading because the forces created by the collision are exerted and removed in a very short time (duration of impact), and the collision produces stress waves which travel away from the region of contact. For the case of apples, the physical characteristics of the fruit demonstrate viscoelastic-type behavior. Thusfar, no general impact damage theory has been developed. The current theories are based on wave theory and Hertz relations, which incorporate contact phenomenon for elastic bodies. Various linear and nonlinear models, however, have been developed to describe the impact behavior in fruits. Pao (1955), Goldsmith (1960) and Yang (1966) have demonstrated that a good approximation of the Hertz contact problem may be obtained for nonlinear viscoelastic bodies if

the modulus of elasticity E is considered to be time dependent ($E(t)$): Such models require extensive experimentation for evaluating the time dependency and cannot be used in this study.

Horsfield (1972) used a theoretical approach developed from Hertz contact theory to predict the level of damage from two impacting bodies by considering the modulus of elasticity, surface radii, impact energy and shear strength. Hertz contact theory was used in his study to predict bruise diameter in apples as well as peaches. The results obtained from his study justified use of the Hertz theory, and in particular the linear viscoelasticity assumption that is the basis of this theory. Use of the Hertz theory provided a good approximation to apple contact and bruising, as well as an exact solution to the contact for a pseudo-fruit constructed from elastic material.

Fridley et al. (1967) reported that the Hertz contact theory (theory of elasticity) satisfactorily described the behavior of many fruits and vegetables during impact. Horsfield et al. (1972), Rider et al. (1973), and Hallee (1981) have also verified the use of this theory and its assumptions on various fruits.

In 1896 Hertz proposed a solution for contact stress in two elastic bodies. The following assumptions were used in the derivation of this theory:

1. The material of the contacting bodies is homogeneous.

2. The applied loads are static.
3. Hooke's law holds (linear viscoelasticity).
4. The radius of curvature of the contacting solids is very large compared with the radius of the contacting area.

This study was later extended by Timoshenko and Goodier (1951) to include spheres of similar sizes and properties. Since the contact time of the two bodies is very long compared to the period of lowest mode of vibration of the two spheres, internal vibrations can be neglected and the theory developed for static conditions can be applied to impact conditions. This theory, which holds for the general case of impact of two spheres of similar material, is used in this study.

From Timoshenko and Goodier (1951), the approach distance of two spheres under impact at the point of maximum compression is given by;

$$\chi_m = \left(\frac{5}{4} \frac{V^2}{n n_1} \right)^{2/5} \quad [2.1]$$

where n and n_1 are;

$$n_1 = \frac{M_1 + M_2}{M_1 M_2} \quad [2.2]$$

$$n = \left[\frac{16}{9\pi^2} \frac{R_1 R_2}{(K_1 + K_2)^2 (R_1 + R_2)} \right]^{1/2} \quad [2.3]$$

with;

$$K = \frac{1 - \mu_n^2}{\pi E_n} \quad [2.4]$$

and

X_m = approach at maximum deformation from centers

V = relative approach velocity of bodies at impact

R_n = radius of curvature of body n

μ_n = Poisson's ratio of material n

E_n = modulus of elasticity of body n

M_n = mass of body n

where $n=1$ for fruit, $n=2$ for impact surface and/or for the puncturing object. Figure 2.1 displays two cases of impact, showing each parameter for the fruit and the impacting surface or puncturing object, respectively.

Substitution of equations 2.2 and 2.3 into equation 2.1 results in;

$$X_m = \left\{ 5/4 V^2 \frac{M_1 M_2}{M_1 + M_2} \frac{1}{\left[\frac{16}{9\pi^2} \left(\frac{1}{K_1 + K_2} \right)^2 \frac{R_1 R_2}{R_1 + R_2} \right]^{1/2}} \right\}^{2/5} \quad [2.5]$$

If one body is stationary while the other is free falling with acceleration G , V can be defined as:

$$V = \sqrt{2GH} \quad [2.6]$$

where G is the gravitational acceleration and H is the drop height. By substitution of equation 2.6 in 2.5 and simplifying:

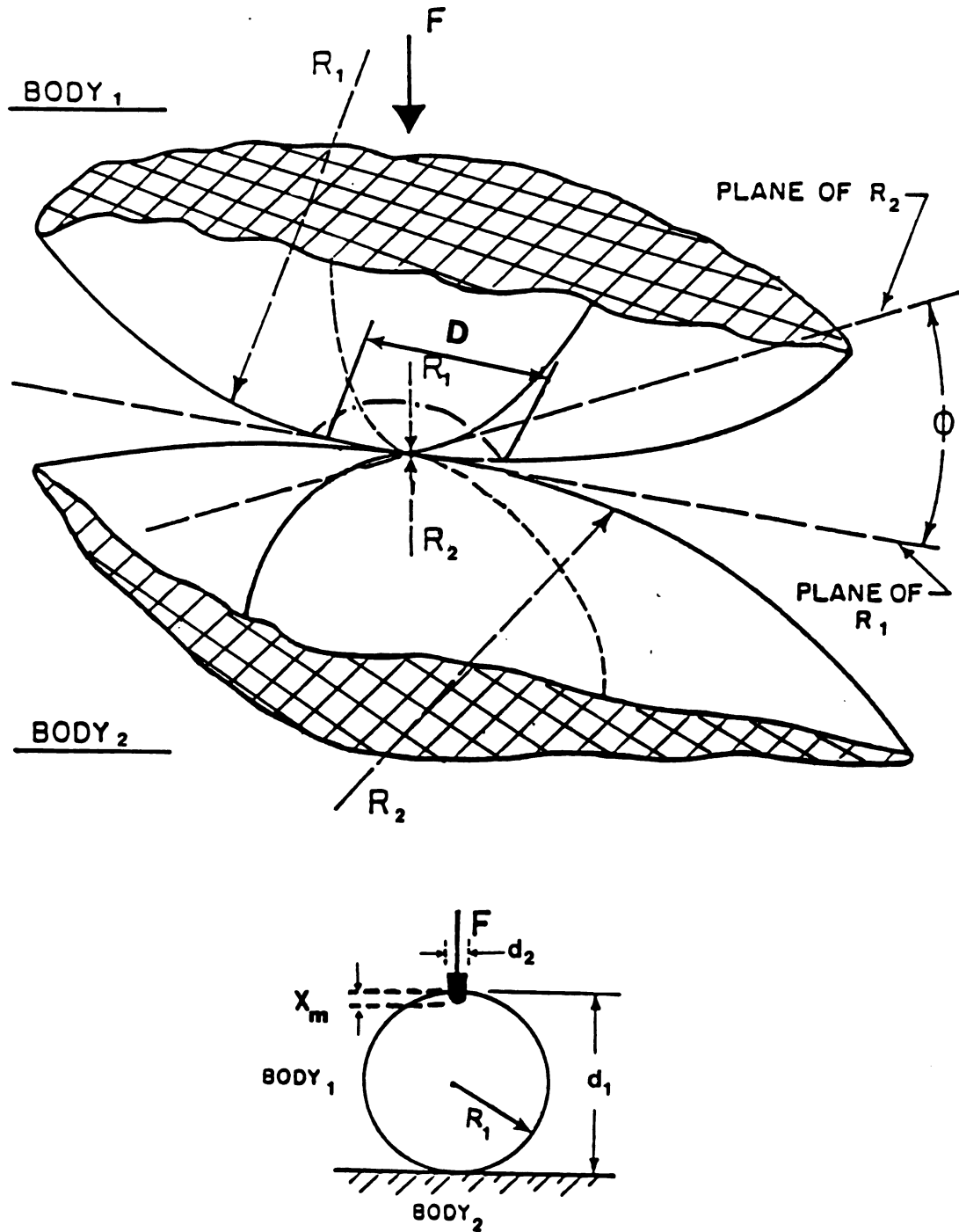


Fig. 2.1 Physical Parameters Related To Hertz Theory For 2 Cases of a) Impact of Spherical Object With a Flat Surface and b) Indentation Caused by the Magness-Taylor Indenter.

$$\chi_m = \left[\frac{15}{8} \pi GH \frac{M_1 M_2}{M_1 + M_2} \left(\frac{R_1 + R_2}{R_1 R_2} \right)^{1/2} (K_1 + K_2) \right]^{2/5} \quad [2.7]$$

For the impact of an apple with a rigid flat surface further assumptions on R_2 and M_2 are necessary. the mass of an apple is negligible compared with the mass of the impacting surface or $M_1 \ll M_2$, then:

$$\frac{M_1 M_2}{M_1 + M_2} \Big|_{M_1 \ll M_2} \approx M_1$$

For a flat surface having $R_2 = \infty$, it follows that:

$$\frac{R_1 + R_2}{R_1 R_2} \Big|_{R_2 = \infty} \approx \frac{1}{R_1} \quad [2.8]$$

Now substituting the above reductions into 2.7 results in:

$$\chi_m = \left[\frac{15}{8} GH M_1 \left(\frac{1}{R_1} \right)^{1/2} (K_1 + K_2) \right]^{2/5} \quad [2.9]$$

The approach distance χ_m and the radius of contact, r , are given by Timoshenko and Goodier (1951) in the form:

$$r = \left(\chi_m \frac{R_1 R_2}{R_1 + R_2} \right)^{1/2}$$

which, by substitution from equation 2.8, reduces to:

$$r = \left(\chi_m R_1 \right)^{1/2} \quad [2.10]$$

Finally, equations 2.9 and 2.10 are used to obtain:

$$r = \left(\pi \frac{15}{8} M_1 GH \right)^{1/5} R_1^{2/5} (K_1 + K_2)^{1/5}$$

Since $W_1 = M_1 G_1$, where W_1 is the weight of the apple, we have:

$$r = \left[\left(\pi \frac{15}{8} W_1 H \right)^{1/5} R_1^{2/5} (K_1 + K_2)^{1/5} \right]$$

Therefore the contact diameter, D , which is just twice the radius, r , is given by:

$$D = 2 \left(\pi \frac{15}{8} W_1 H \right)^{1/5} R_1^{2/5} (K_1 + K_2)^{1/5} \quad [2.11]$$

According to equation 2.11, D , the diameter of the contacting area, can be calculated for the case of a falling apple impacting on a flat surface. The parameter values needed are weight of the apple, the radius of curvature of the apple, the drop height, and the values for K_1 and K_2 which represent the rigidity of the apple and impact surface, respectively. K_n , defined by equation 2.4, is a material property and function of the Poisson ratio (μ) and the modulus of elasticity (E). For a hard impact surface this value can easily be calculated. For example using aluminum with:

$\mu_2 = 0.334$ and $E_2 = 70.3 \times 10^3$ MPa, the value for K_2 is:

$$K_2 = 3.99 \times 10^{-6} \text{ MPa}^{-1}.$$

The task of evaluating K_1 for apples can be accomplished by the use of the Hertz theory. With this approach, the Magness-Taylor force reading, from each apple, is used to obtain an estimate for K_1 which is then used in

equation 2.11. Using the relation from Mohsenin (1970), the χ approach of the two bodies (also depth of an indenter) can be written as:

$$\chi_m = \frac{\kappa}{2} \left[\frac{9F_1^2 A_1^2}{\pi^2} \left(\frac{1}{R_1} + \frac{1}{R'_1} + \frac{1}{R_2} + \frac{1}{R'_2} \right) \right]^{1/3} \quad [2.12]$$

where R_n and R'_n are the maximum and minimum radius of curvature, respectively. F_1 is the Magness-Taylor force, κ is a constant to be tabulated and A is defined as:

$$A = \frac{1 - \mu_1^2}{E_1} + \frac{1 - \mu_2^2}{E_2}$$

Equation 2.12 can be used to obtain a relation in terms of E_1 using the assumption $\kappa_2 = 0$ (large E_2 value) for the case where a steel rod is used as an indenter in the Magness-Taylor test. Thus,

$$E_1 = 0.338 \frac{\kappa^{3/2} F_1 (1 - \mu_1^2)}{\chi_m} \left(\frac{1}{R_1} + \frac{1}{R'_1} + \frac{4}{d_2} \right)^{1/2} \quad [2.13]$$

where d_2 is the diameter of the indenter.

Values for the constant κ are tabulated and given by Kosma and Cunningham (1962), for a given value of $\{\cos(T)\}$ defined as:

$$\cos(T) = \frac{\left[\left(\frac{1}{R_1} - \frac{1}{R'_1} \right)^2 + \left(\frac{1}{R_2} - \frac{1}{R'_2} \right)^2 + \left(\frac{1}{R_1} - \frac{1}{R'_1} \right) \left(\frac{1}{R_2} - \frac{1}{R'_2} \right) \cos 2\phi \right]^{1/2}}{\left(\frac{1}{R_1} + \frac{1}{R'_1} + \frac{1}{R_2} + \frac{1}{R'_2} \right)} \quad [2.14]$$

where ϕ , as shown in Fig. 2.1 is the angle between the

normal planes containing the principal curvatures.

For Ida-Red apples it can be assumed that R_1 and R'_1 will approach one another, and furthermore that they are very large. This is true because, in the dynamic Magness-Taylor test, the points with least radii of curvature are selected, and after peeling this area a flat surface is created. Thus, $1/R_1$ and $1/R'_1$ can be considered negligible. It can also be assumed that $R_2 = R'_2$ because of the spherical shape of the indenter. With the above assumptions it is possible to calculate the value of $\{\text{COS}(T)=0\}$ which results in the value of $\kappa = 1.3514$ from the table provided by Kosma and Cunningham (1962). Therefore E_1 is reduced to:

$$E_1 = \frac{0.531 F_1 (1-\mu_1^2)}{\chi_m^{3/2}} \left(\frac{4}{d_2}\right)^{1/2} \quad [2.15]$$

which has also been used by McDonald and Delwishe (1983) as a measure of the apple's modulus of elasticity. This relation is useful since for a given Magness-Taylor apparatus, values of χ_m and d_2 are known and F_1 (Magness-Taylor force) can be measured directly. The only unknown is a relation in terms of E_1 and μ_1 which can be rewritten to form the unknown parameter K_1 :

$$K_1 = \frac{1-\mu_1^2}{\pi E_1} = \frac{1}{\pi} \frac{\chi_m^{3/2}}{0.531 F_1} \left(\frac{d_2}{4}\right)^{1/2} \quad [2.16]$$

Substitution of equation 2.16 into 2.11 will result in the final form which can be used to calculate the diameter of the contact area (bruise diameter) based on the physical properties of each apple and the drop height. This is given by:

$$D = 2 \left(\pi \frac{15}{8} W_1 H \right)^{1/5} R_1^{2/5} \left[K_2 + \frac{\chi_m^{3/2}}{\pi 0.531 F_1} \left(\frac{d_2}{4} \right)^{1/2} \right]^{1/5}$$

further simplification results in:

$$D_1 = 4.624 (W_1 H)^{1/5} \left(\frac{D_1}{2} \right)^{2/5} F_1^{-1/5} \quad [2.17]$$

2.1.2 Impact of Plastic Bodies

Hertzian theory (based on Hooke's law) holds true when the impact force-deformation curve is in the elastic region as shown in figure 2.2.a. This condition exists, only for very low drop heights where no permanent deformation occurs in the apple tissue. For most impacts, however, the force-deformation curve of impact exceeds the elastic region and passes through a yield point (microstructure failure) and reaches a rupture point (macrostructure failure). I will assume that in apples the yield and rupture point are very close; this means that apples will bruise when the force-deformation curve exceeds the yield point as shown in figure 2.2.b. The elastic behavior of apple is followed by a

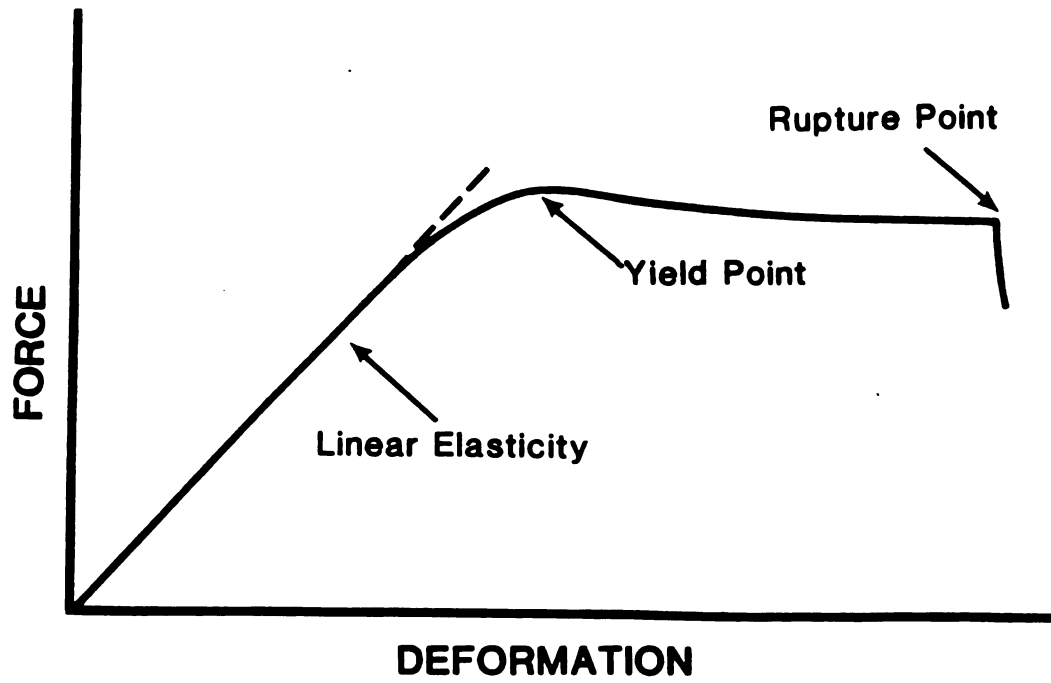


Fig. 2.2.a Hertz Theory Force-Deformation Curve.

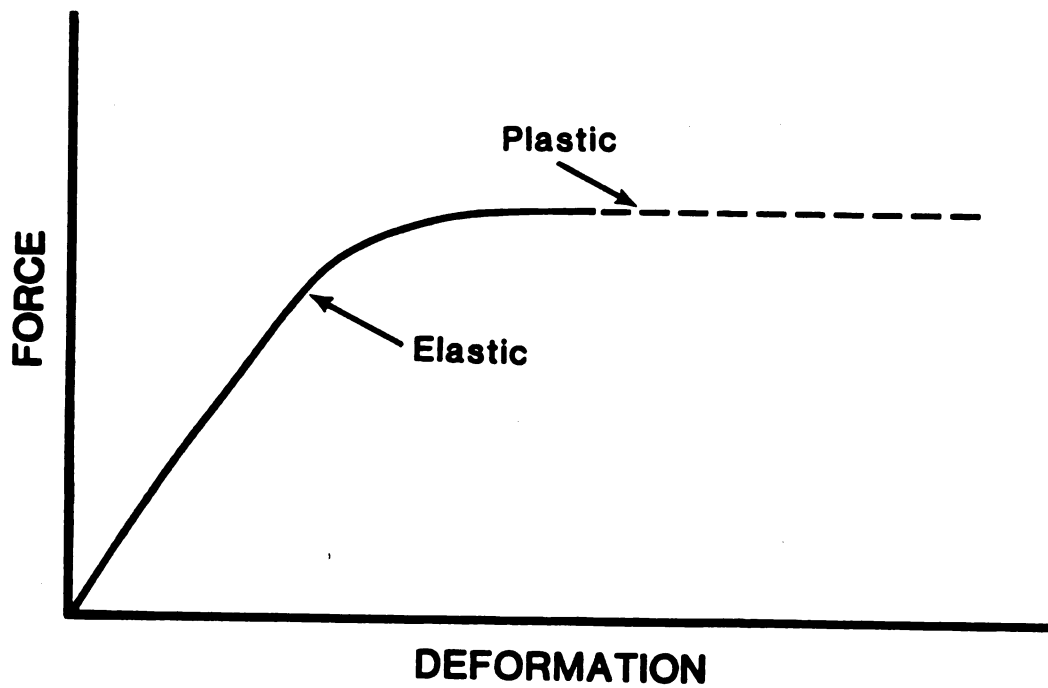


Fig. 2.2.b Plastic Force-Deformation Curve.

plastic type response, which is the basis for plastic force-deformation characteristics. It is possible to consider the Magness-Taylor force of each apple as a measure of its yield point. The purpose of this approach is to introduce a plastic theory which may predict impact bruising with knowledge of Magness-Taylor force, apple diameter, apple weight and drop height. [I am indebted to Dr. G. Burgess for suggesting this approach].

When an apple is dropped on a hard surface, forces acting on the contacting surface compress the tissue to a maximum when the apple reaches zero velocity. This compression is displayed for just before and after impact in Fig. 2.3.a. The radius of contact, r , can be measured if radius of the apple, R_1 , and the maximum compression, χ_m , is known. This relation is simply given by:

$$r^2 = R_1^2 - (R_1 - \chi)^2 = 2R_1\chi - \chi^2 \quad [2.18]$$

Assuming that during impact all points on the contacting surface are yielding, the apple free-body-diagram can be considered as shown in Fig. 2.3.b. The only forces that are acting on the apple are the surface resistance force, F_s , and apple's weight, W_a . Therefore, the following relations are derived:

$$F = \sigma A = \sigma \pi r^2 \quad [2.19]$$

where F is the yielding force (Magness-Taylor force), σ is the yield point stress from (Magness-Taylor force) and r is

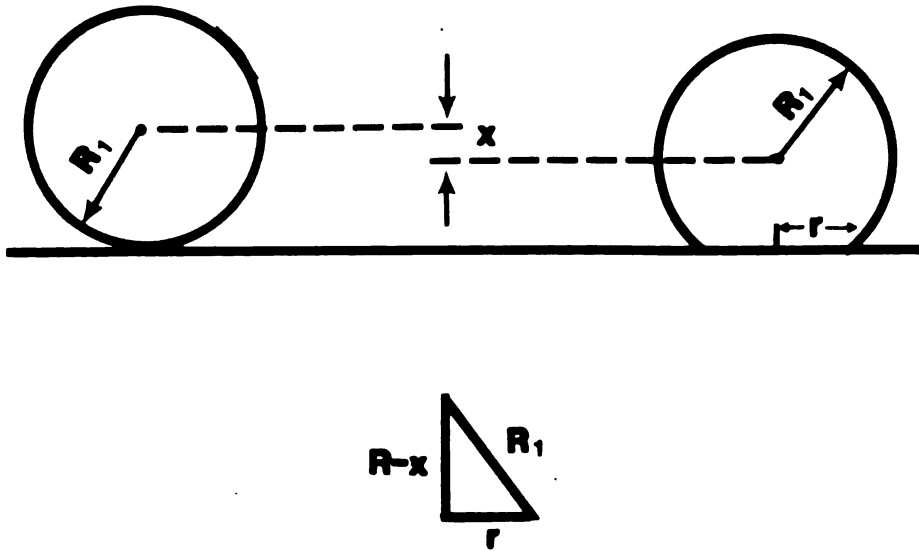


Fig. 2.3.a Maximum Compression and Contact Radius, Before and After Impact.

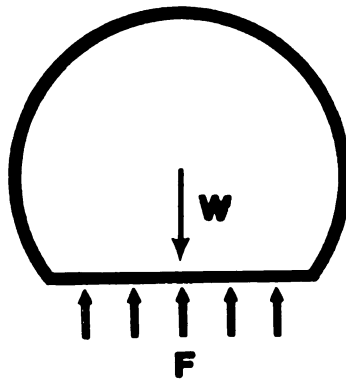


Fig. 2.3.b Free Body Diagram of an Apple Impact on a Hard Surface.

the contacting radius. Let's substitute equation [2.18] in [2.19] then:

$$F = \pi\sigma(2R_1\chi - \chi^2) \quad [2.20]$$

Summing all forces in the free body diagram results in the following:

$$\Sigma F\downarrow = W - \pi\sigma(2R_1\chi - \chi^2) = \frac{W}{g}\ddot{\chi} \quad [2.21]$$

let $\dot{\chi} = v$, Then:

$$\ddot{\chi} = \dot{v} = \frac{dv}{dt} = \frac{dv}{d\chi} \frac{d\chi}{dt} = v \frac{dv}{d\chi}$$

by substituting the above relation in equation [2.21] the following is obtained:

$$W - \pi\sigma(2R_1\chi - \chi^2) = \frac{W}{g} v \frac{dv}{d\chi} \quad [2.22]$$

For impact of an apple, the left hand side of equation [2.22] is a function of χ , which varies from zero compression to maximum compression χ_m , and the right hand side is a function of v , which also varies from approach velocity v to zero. By integration of both sides with respect to χ and v and simplifying, the following relation is obtained:

$$W\chi_m - \pi\sigma\left(R_1\chi_m^2 - \frac{\chi_m^3}{3}\right) = -\frac{W}{g} \cdot gH \quad [2.23]$$

Equation [2.23] can be solved for χ_m , which can then be substituted in equation [2.18] to calculate the contact radius of the apple during impact.

$$\frac{\pi\sigma}{W} \left(R_1 \chi_m^2 - \frac{\chi_m^3}{3} \right) - \chi_m = H \quad [2.24]$$

$$\left(\frac{d}{2} \right) = r^2 = 2R_1 \chi_m - \chi_m$$

Further simplifications of these relations is possible if contributions from the second and third order terms of χ_m are considered to be negligible in equations [2.23] and [2.24]. Then the following approximations are obtained:

$$\chi_m = \sqrt{\frac{HWA}{\pi FR_1}}$$

$$d \approx 2\sqrt{2R_1 \chi_m - \chi_m^2} = 2\sqrt{2R_1 \chi_m}$$

the above relations result in a final simple form of:

$$d = 2\sqrt{2R_1 \left(\frac{HWDA}{\pi FR_1} \right)^{1/2}} = 5.63(\pi)^{1/2} \left(\frac{HWD}{F} \right)^{1/4} \quad [2.25]$$

which shows the response of bruise to each of the parameters. When equation [2.25] was compared with the exact solution of equation [2.24], it turned out to be very accurate and always within 1 percent of the exact value.

2.2 Artificial Apple (Pseudo-Fruit)

The pseudo fruit (IS) consisting of a microcontroller with internal CPU (central processing unit), ROM (read only

memory) and external RAM (random access memory), battery supply and accelerometer was to be encapsulated inside a 75 mm sphere. But, as mentioned previously, the lack of a CMOS microcontroller has presently limited the miniaturization process. Thus, in order to obtain a transfer function for the casting material, an initial IS was made with the accelerometer alone Fig. 2.4.

The casting material (clear epoxy casting resin) is a water clear two-part epoxy compound. The physical properties of this material as well as the casting procedure are specified in Appendix A.1.

2.2.1 Accelerometer

An accelerometer is a transducer that produces an electrical output proportional to its acceleration input. The ratio of this output to input is referred to as sensitivity in units of mV/g, with g being 9.81 m/s^2 .

Accelerometers are basically seismic piezoresistive or piezoelectric devices which are made of either resistive strain gages or piezoelectric materials, respectively. Comparison of the two types reveals the following:

1. Piezoelectrics are smaller and can be made in a subminiature design which is essential for this study.
2. Piezoelectrics are active or self-generating transducers that produce an electrical output proportional to acceleration, without the use of an external power source

or carrier voltage. The piezo material generates an electrical field when it is strained due to a change in acceleration. Therefore it operates with no input current so that an over all lower supply current will suffice.

3. Piezoelectrics have much higher sensitivity and lower output impedance. Thus they require less amplification and fewer components.

4. Piezoelectrics have a very high natural frequency and thus they are ideal for high frequency application. Since at zero frequency no mechanical energy is put into the system, no electrical energy can be removed. Hence this type of accelerometer does not respond well to very low frequencies and should not be used to measure constant accelerations. It is well suited for transient type measurements such as accelerations caused by an impact.

Figures 2.5 and 2.6 show, respectively, the physical arrangements and the electrical representations of a piezoelectric type accelerometer. Based on the above discussion this type of accelerometer was selected for this study.

Circuit analysis of a piezoelectric crystal can be represented as a charge generator of capacitance C_p . The open circuit voltage output, E_o , of the crystal is:

$$E_o = \frac{q}{C_p} \quad [2.26]$$

in which q = the charge generated by straining the crystal.

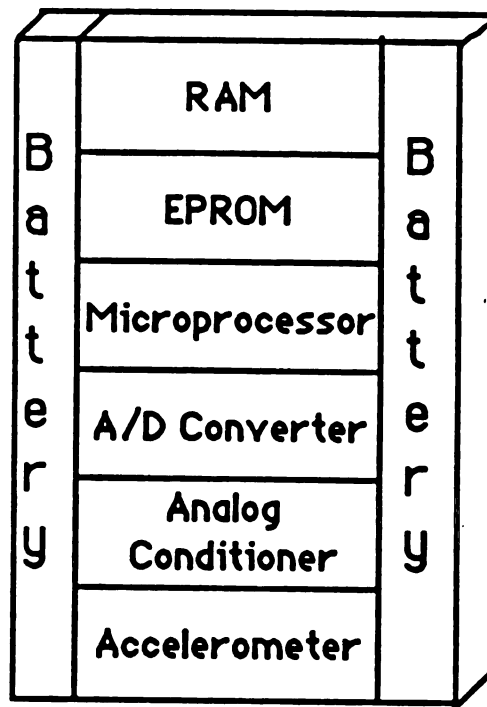


Fig. 2.4 Instrumented Sphere Shown With All Components, Including the Accelerometer.

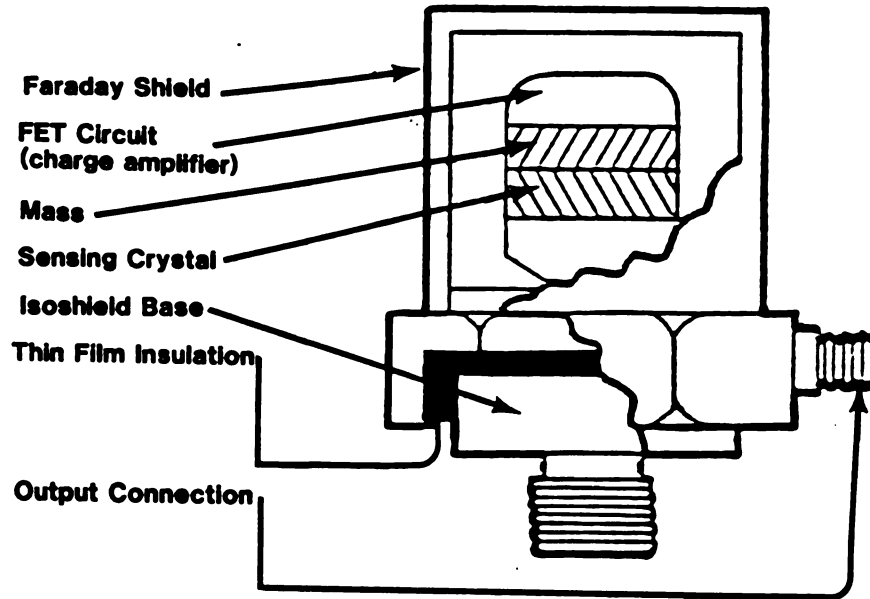


Fig. 2.5 Physical Arrangement of a Piezoelectric Type Accelerometer.

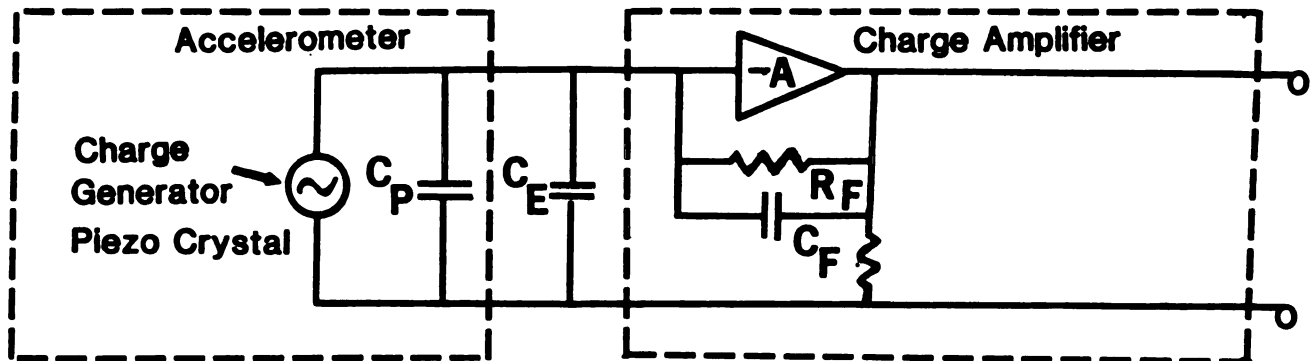


Fig. 2.6 Electrical Representation of a Piezoelectric Accelerometer and Charge Amplifier.

When the crystal is connected externally, the loaded voltage due to the addition of the external capacitance, C_E , becomes:

$$E_0 = \frac{q_p}{C_p C_E} \quad [2.27]$$

Thus, the voltage output of a given piezoelectric crystal varies inversely with the total capacitance of the system. The accelerometer response will change with any slight variations in the external capacitance. However, a charge amplifier consisting of a voltage amplifier and feedback loop is used to convert the input charge into an output voltage. This charge amplifier has recently been integrated into the design of accelerometers, which greatly improves the transducer performance. When the accelerometer is cast inside of a pseudo-fruit, the loading from the accelerometer will be affected and the resonance frequency of the system will be modified. The frequency change is given by:

$$\Delta F_n = F_n \left(1 - \sqrt{\frac{m_1}{m_1 + m_n}} \right) \quad [2.28]$$

where

F_n = resonance frequency of the accelerometer

ΔF_n = reduction in resonance frequency

m_1 = mass of the pseudo-fruit (180 g)

m_a = mass of the accelerometer (7 g)

Given $F_n = 90$ kHz, then a new resonance frequency of 88.3 kHz is calculated which is close to the original value. According to Rhodes (1960) when a piezoelectric accelerometer is used for transient measurements the accelerometer sensitivity is essentially constant for frequencies equal to, or less than, 0.2 of the accelerometer's natural frequency. Hence, the mentioned accelerometer operates linearly up to one fifth of the resonance frequency which is = 17.7 kHz. This translates into impacts with durations as low as 57 μ s. The lower operating frequency is determined by external circuitry, and will be discussed latter.

2.2.2 Transfer Function Concept

The accelerometer is cast inside the pseudo-fruit made from hard plastic epoxy which has a tensile strength of 41.4 MPa. The impact acceleration travels through the pseudo-fruit to reach the accelerometer, thus, verification of the sensed and surface accelerations is necessary. To estimate the amount of distortion caused by the casting the Transfer Function concept is introduced.

The transform ratio of output to input is described by the transfer function, if input and output are related in time by a linear differential equation whose coefficients are constants in the form:

$$A_n \frac{d^n c}{dt^n} + \cdots + A_1 \frac{dc}{dt} + A_0 c = B_m \frac{d^m r}{dt^m} + \cdots + B_1 \frac{dr}{dt} + B_0 r. \quad [2.29]$$

The Laplace transform of Equation [2.29] is:

$$(A_n s^n + \cdots + A_1 s + A_0)C(s) = (B_m s^m + \cdots + B_1 s + B_0)R(s). \quad [2.30]$$

The ratio $G_S = C_S/R_S$, or transfer function, can be expressed as a ratio of two polynomials:

$$G(s) = \frac{C(s)}{R(s)} = \frac{B_m s^m + \cdots + B_1 s + B_0}{A_n s^n + \cdots + A_1 s + A_0}. \quad [2.31]$$

In general, this ratio of polynomials is a property of the system only, and is not affected by the excitation.

If the pseudo-fruit is considered as a system, then by this method it is possible to determine the exact relation between the impact acceleration and the sensed acceleration. Thus, before casting the accelerometer inside the pseudo-fruit it was mounted on a shaker table along with an NBS (National Bureau Of Standards) calibrated accelerometer. After casting it was again exposed to the same shaker table conditions. The shaker table along with other instrumentation is specified in Appendix A.2.

The shaker table produced a low 'g' sinusoidal waveform. At each discrete frequency the ratio of magnitudes and the phase differences were obtained by respectively dividing and/or subtracting the output signal (accelerometer

or pseudo-fruit) by/from the input signal (NBS accelerometer). The magnitude ratio and the phase difference of the pseudo-fruit transfer functions are shown in Figs. 2.7 and 2.8. These graphs represent the change in the transfer function caused by the casting process. When the cast sphere was dropped on very hard, hard and soft surfaces the resulting impact frequencies fell in the range of 1 kHz to 100 Hz (1 to 10 ms durations). It is clear that the difference is very small, less than 5 percent, and it can be neglected. This means that the acceleration sensed by the pseudo-fruit represents the true impact acceleration.

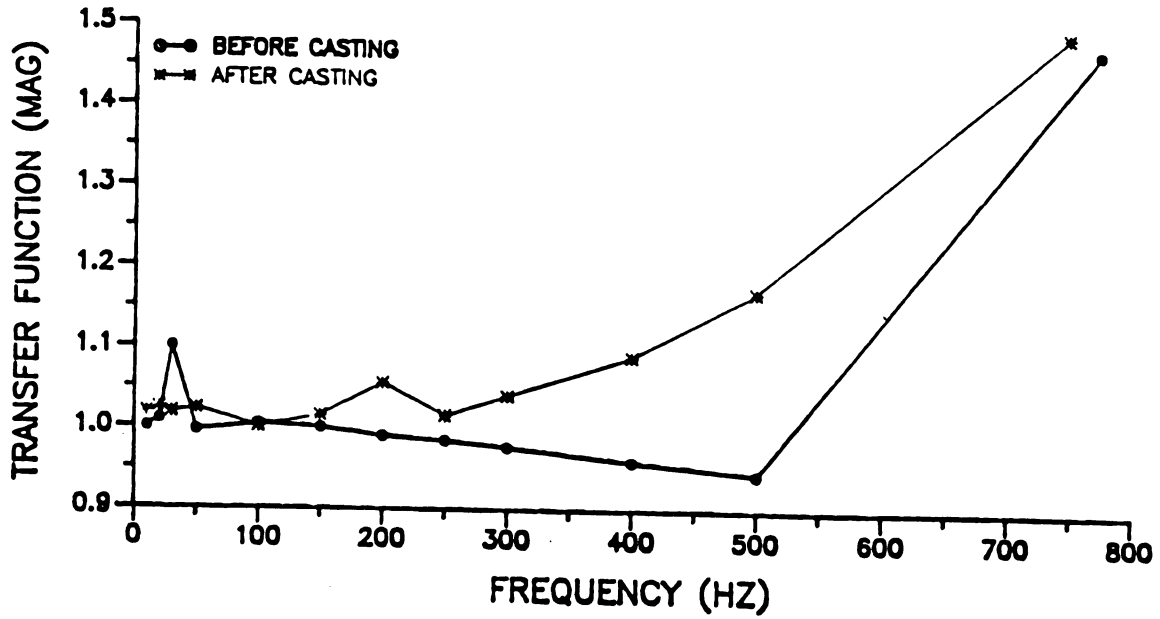


Fig. 2.7 Magnitude Vs Frequency Diagrams for Casting Effects of the Imbedded Accelerometer.

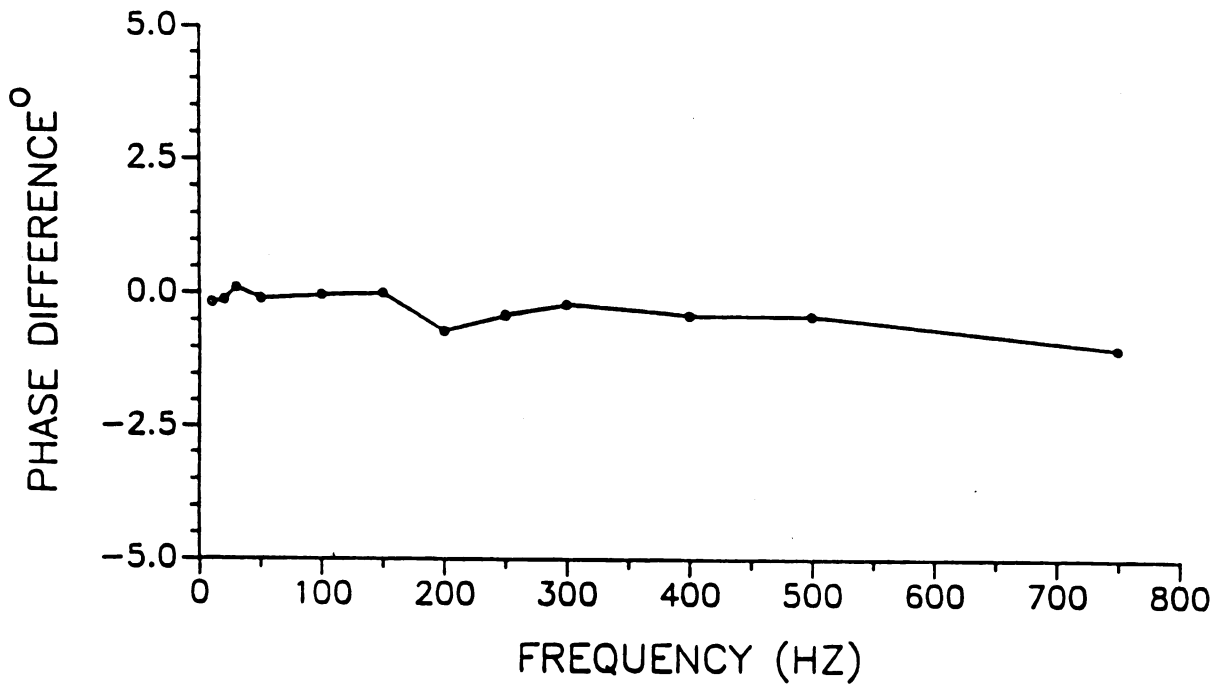


Fig. 2.8 Phase Vs Frequency Diagrams for Casting Effects of the Imbedded Accelerometer.

3. EXPERIMENTAL APPARATUS AND PROCEDURES

3.1 Experimental Apparatus

The application of a stand alone IS data acquisition system as described by Tennes et al. (1986), to agricultural products is a new concept. Materials, test equipment and components used in this design were either fabricated or purchased (when suitable commercial components were available). Initial design requirements for the IS data acquisition system were set for maximum flexibility and expandability. These requirements were:

1. Portability for easy use in agricultural environments.
2. Multi-channel inputs to allow for triaxial data measurements.
3. Impact amplitude recording range of ± 270 g to cover the bruising range of most fruits and vegetables.
4. Impact duration recording as low as 1.0 ms to permit collection of impacts on rigid surfaces.
5. At least 8-bit analog-to-digital (A/D) conversion for high accuracy.
6. Variable sampling rate up to 4 kHz (per channel for the current 3 channel A/D) to permit sufficient data for accurate analysis.

7. Communication link to a host computer to facilitate off-line processing of collected impact data.
8. Miniaturized accelerometer with high linearity and accuracy in the range of 5 Hz to 2kHz.
9. Overall error of less than 5 percent.

3.1.1 Accelerometer

The triaxial accelerometer is the basic sensing element of the IS. This unit provides the information necessary to evaluate the damage potential in impact bruising. As described previously a piezoelectric triaxial accelerometer was selected for best performance and its characteristics are presented in Table 3.1. Although the effective acceleration causing impact damage can be related to the resultant acceleration, presently three axes are monitored and stored in the RAM. The resultant acceleration could have been stored, thus reducing the data storage by two thirds, but to preserve relative direction this was not done.

A JFET preamplifier incorporated along with the accelerometer provides isolation to the attached circuitry. The unit requires a constant power input with 9 to 24 V for its operation. As shown in Fig. 3.1, the accelerometer charge amplifier bias requirement of 1.0 to 2.2 mA constant current source is achieved with a zener current-limiting diode. Therefore, the output of the accelerometer will be biased at 9 to 24 V which requires DC blocking (high pass

Table 3.1 Specifications for Vibra-Metrics model No. 3132
Triaxial Piezoelectric Accelerometer.

Sensitivity (at 100 Hz, 1.0g).....	10mv/g (nominal)
Frequency range.....	3-10,000 Hz $\pm 5\%$
Amplitude linearity.....	$\pm 2\%$
Maximum peak (at 15 Vdc).....	750g
Maximum shock (w/o damage).....	5000g
Transverse sensitivity max.....	5%
Temperature sensitivity.....	$\pm 5\%$ (-20 to 65 C)
Output impedance.....	1000 Ω
Weight (w/o cable).....	7.0 grams (nominal)

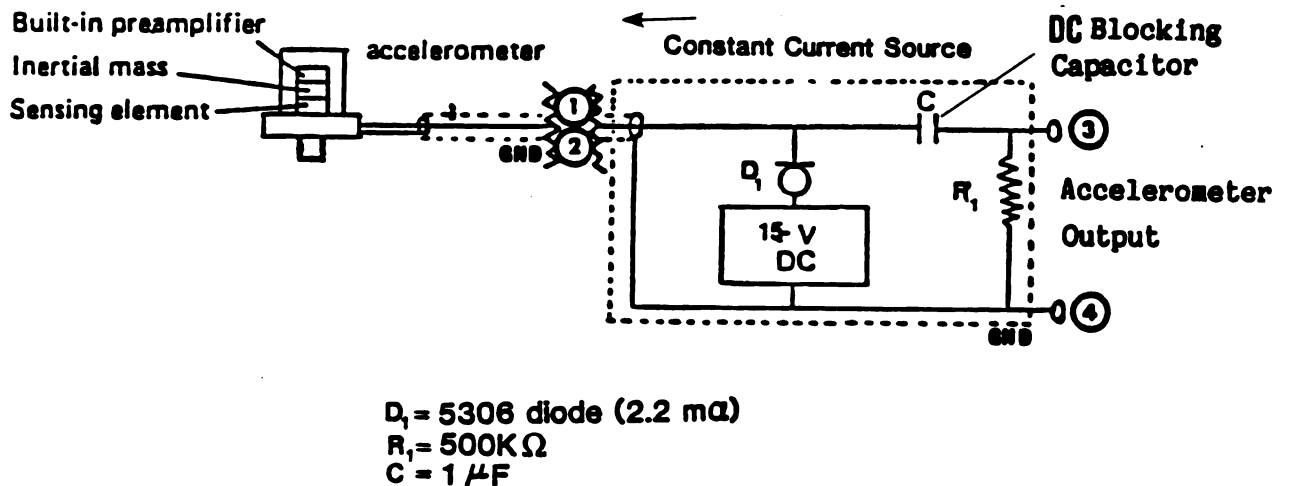


Fig. 3.1 Circuit Diagram for the Accelerometer Constant Current Source and High Pass Filter.

filtering) of this voltage before it can be amplified or sensed by the A/D (Analog To Digital Converter). Thus, as shown in Fig. 3.1, a first-order passive filter is used to AC couple the accelerometer. This filter dictates the low frequency response of the accelerometer. Equation 3.1 describes the mathematical relation between the components of this RC filter with f_c (-3 dB cut-off frequency):

$$f_c = \frac{1}{2\pi RC} \quad [3.1]$$

where R = shunt resistance (ohm)

C = series capacitance (farads)

which is set for $f_c = 0.16$ Hz.

3.1.2 Microcontroller

The main consideration in the microprocessor selection was to identify a high-performance, single-chip, 16-bit central processing unit (CPU) which would minimize the number of external components needed to achieve the IS data acquisition requirements. The Intel 8097 microcontroller (MCS-96 family) provides a 16-bit NMOS CPU with eight multiplexed channels of 10-bit A/D (22 μ s conversion time). In addition, this microcontroller includes two 16-bit timers, a full duplex serial port, a 16-bit multiplexed address/data bus, 256 bytes of internal RAM, 8 kbytes of internal EPROM (Erasable Programmable Read Only Memory) and

an internal clock operable at frequencies up to 12 MHz. This microcontroller requires 1.0 W at 12 MHz, but, future CMOS versions of this chip will guarantee a lower power requirement.

The specifications, instruction set, and additional information on the 8097 microcontroller are supplied in Appendix A.3.

3.1.3 Hardware

The hardware design of the IS data acquisition system is shown in the block diagram of Fig. 3.2. It should be noted that the analog circuitry is required to condition the accelerometer output signal before it is sampled by the A/D onboard the 8097 microcontroller. The component categories of power supply, analog circuitry and digital circuitry are explained in the following sections.

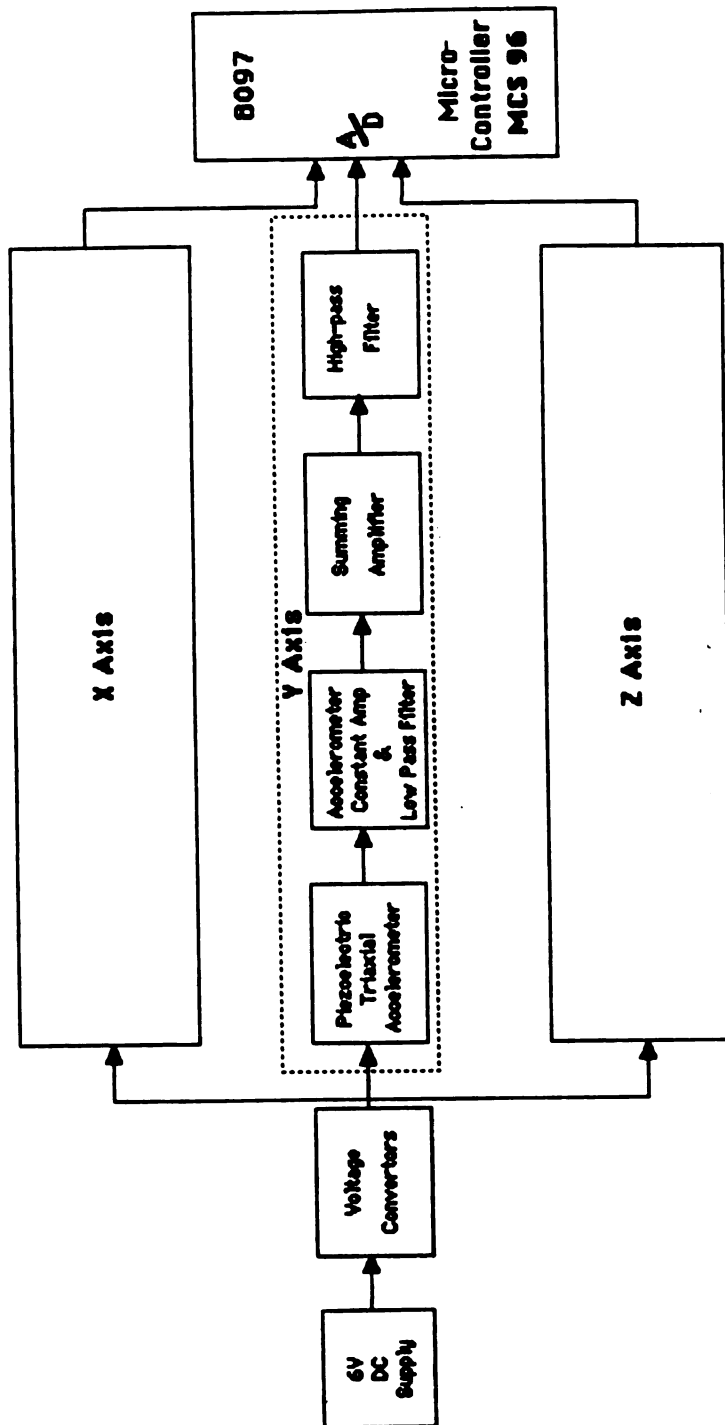


Fig. 3.2 Block Diagram of the IS Data Acquisition System.

3.1.3.a Power Supply

The power supply circuit is shown in Fig. 3.3. The average power requirement for the NMOS digital circuitry is 1.5 W (5 Vdc at 0.3 A). The accelerometer requires 0.1 W (15 Vdc at 6.6 mA) and the analog circuitry requires 0.75 W (± 15 Vdc at 50 mA). Since three voltage levels are required (+5 V for digital and ± 15 V for analog), either three batteries or several voltage converters are necessary. To better achieve the IS size requirement, a single rechargeable lead-acid jell-type battery at 6 Vdc and 10 Ah (4h operation) was chosen for the 8097 NMOS microcontroller. The use of NMOS components requires 2.35 W which can be reduced to 0.4 W when CMOS components are available. The excess power needed for NMOS has increased the power supply size, which in turn has increased the final size of the NMOS pseudo-fruit. For this reason the 10 Ah batteries were selected to ensure at least 4 h of operation for the NMOS version and 25 h of operation with the CMOS version. The conversion of 6 Vdc into ± 15 Vdc is accomplished with an ICI 371515DB (Integrated Circuits Inc.) switching regulator which generates in excess of 200 mA current with a typical efficiency of 75 percent. A monolithic low drop voltage regulator, LM 2935 (Motorola), is used to provide the digital voltage along with a 10 mA standby supply to shut off the IS unit in cases where the buffer memory is full or when the batteries are discharged.

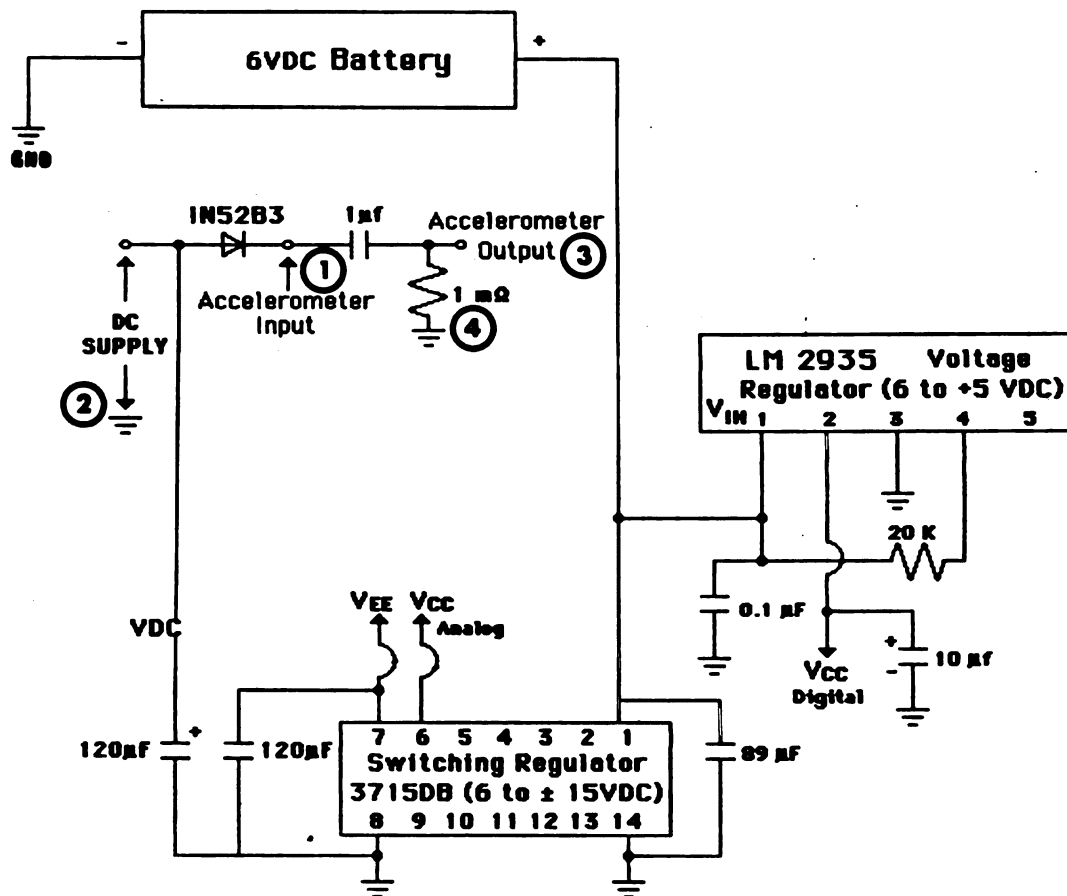


Fig. 3.3 Power Supply Circuit Diagram of the IS Data Acquisition System.

3.1.3.b Analog Circuitry

The overall diagram of the analog circuit is shown in Fig. 3.4. The analog circuit consists of a conditioning stage to scale and offset the accelerometer signal for conversion by the 8097 A/D which has an input range of 0 to 5 Vdc. This is achieved by using an operational amplifier LF 356 (Motorola) in a non-inverting summing mode. Based on Fig 3.4 the Kirchhoff nodal equations at node E_a and E_b are:

$$E_A \left[\frac{1}{R_1} + \frac{1}{R_0} \right] = \frac{V_0}{R_0} + \frac{V_{EE}}{R_1} \quad [3.2.a]$$

$$E_B \left[\frac{1}{R_{NS}} + \frac{1}{R_{N1}} \right] = \frac{V_{ACC}}{R_{N1}} \quad [3.2.b]$$

Let

$$R_A = R_0 \parallel R_1 = \left[\frac{1}{R_1} + \frac{1}{R_0} \right]^{-1} \quad [3.3.a]$$

$$R_B = R_{NS} \parallel R_{N1} = \left[\frac{1}{R_{NS}} + \frac{1}{R_{N1}} \right]^{-1} \quad [3.3.b]$$

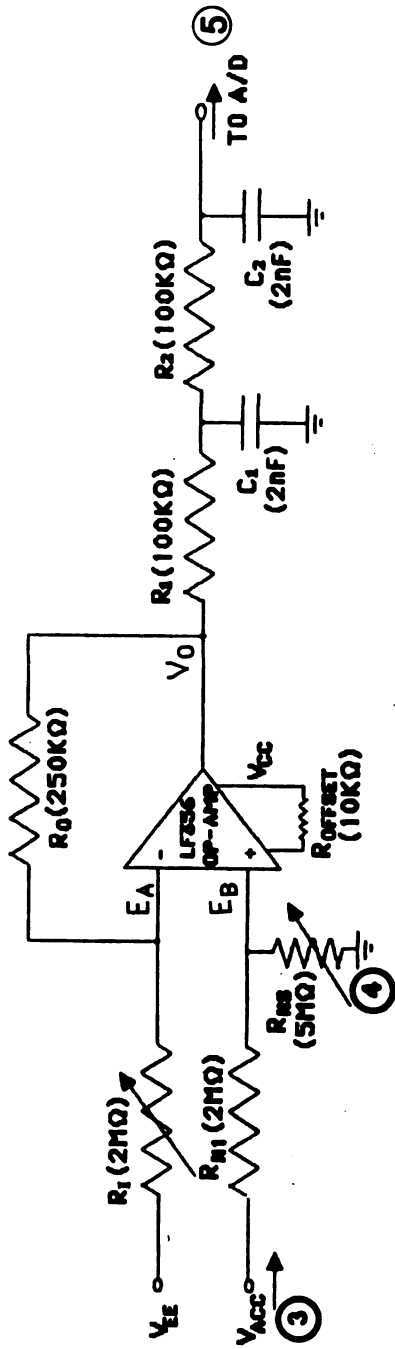
For an ideal operational amplifier,

$$E_A \approx E_B \quad [3.4]$$

Therefore by using equation [3.3] in [3.2] we obtain the Kirchhoff voltage sum for nodes E_a and E_b as:

$$\frac{E_A}{R_A} = \frac{V_0}{R_0} + \frac{V_{EE}}{R_1} \quad [3.5]$$

$$\frac{E_B}{R_B} = \frac{V_{ACC}}{R_{N1}} \Rightarrow E_B = \frac{R_B V_{ACC}}{R_{N1}} \quad [3.6]$$



$$V_0 = -\frac{R_0}{R_1} V_{EE} + K_N V_{ACC}$$

$$K_N = \frac{R_B}{R_A} \frac{R_0}{R_{N1}}$$

$$R_A = R_0 \parallel R_1$$

$$R_B = R_{N1} \parallel R_{MS}$$

$$R = R_1 = R_2$$

$$C = C_1 = C_2$$

$$T = \frac{R_1 R C_1}{R_1 + R_2}$$

3 db cutoff at 10 kHz

Fig. 3.4 Analog Conditioning Circuit of the IS Data Acquisition System.

Now by substituting equation [3.4] in [3.5] and [3.6]:

$$\frac{R_B V_{ACC}}{R_A R_{N1}} = \frac{V_0}{R_0} + \frac{V_{EE}}{R_1}$$

$$V_0 = -\frac{R_0}{R_1} V_{EE} + \frac{R_0 R_B}{R_A R_{N1}} V_{ACC} \quad [3.7]$$

where V_{EE} = offset voltage

V_{ACC} = accelerometer output voltage

and R_0 , R_1 , R_{N1} and R_{NS} are resistors used to set the amplification level.

Since the piezoelectric accelerometer is biased at 15 Vdc, ac coupling is required to remove this dc-bias level. As explained before, the ac coupling is achieved by using a one pole, high-pass RC filter. Finally, because voltage converters create high frequency noise (20 to 50 kHz), a 3 pole low-pass filter having a cutoff frequency of 10 kHz is employed. This filtering operation does not affect the impact signal, which is limited to 0.24 ms duration.

3.1.3.c Digital Circuitry

The digital circuits for the IS are shown in Figs. 3.5 and 3.6. The 16-bit multiplexed (address/data) bus is controlled with the select lines ALE, RD, WR, BHE and AD0. A list of these select lines and their functions is given in Table 3.2. Two transparent Latches (274LS373) are

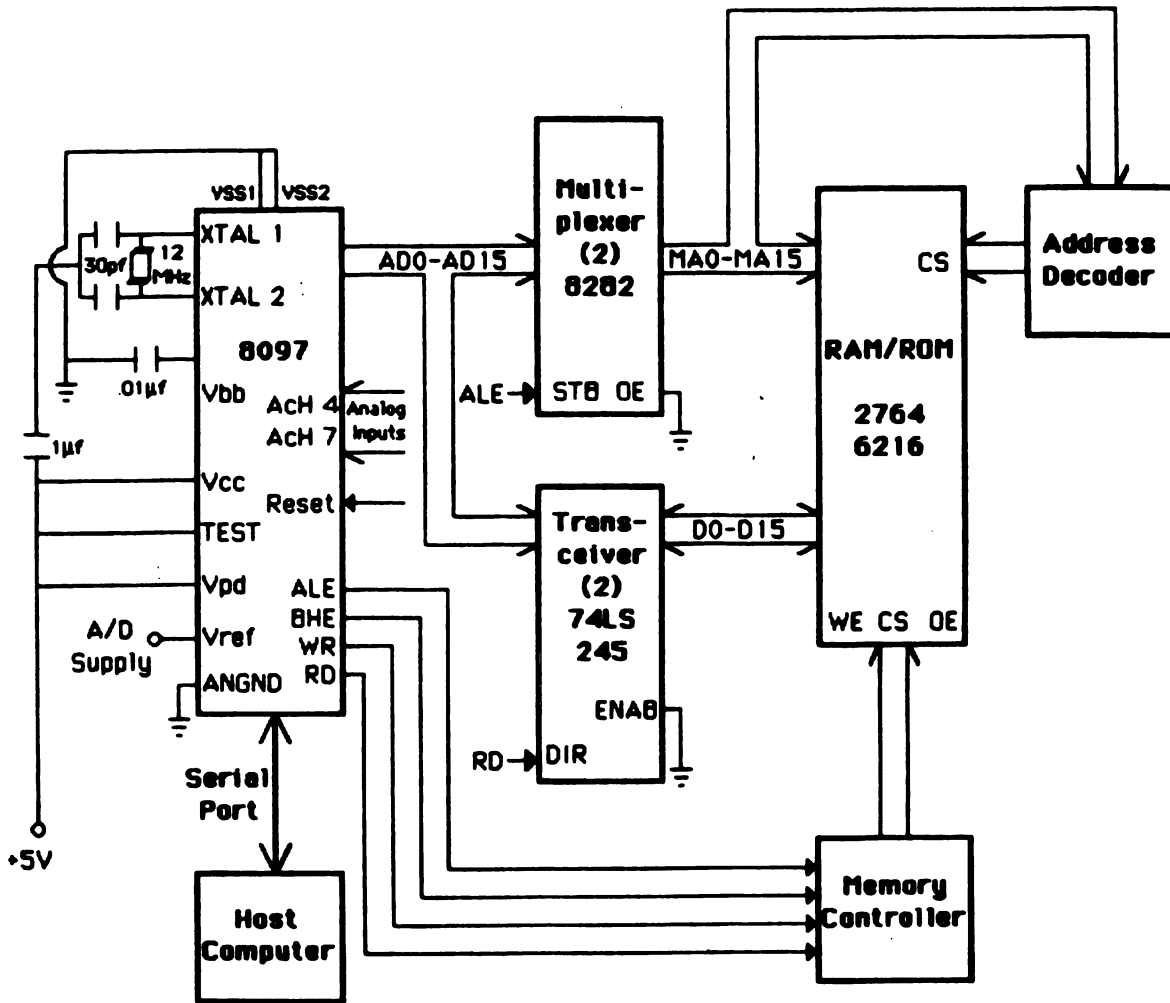


Fig. 3.5 Block Diagram of the IS Digital Circuitry.

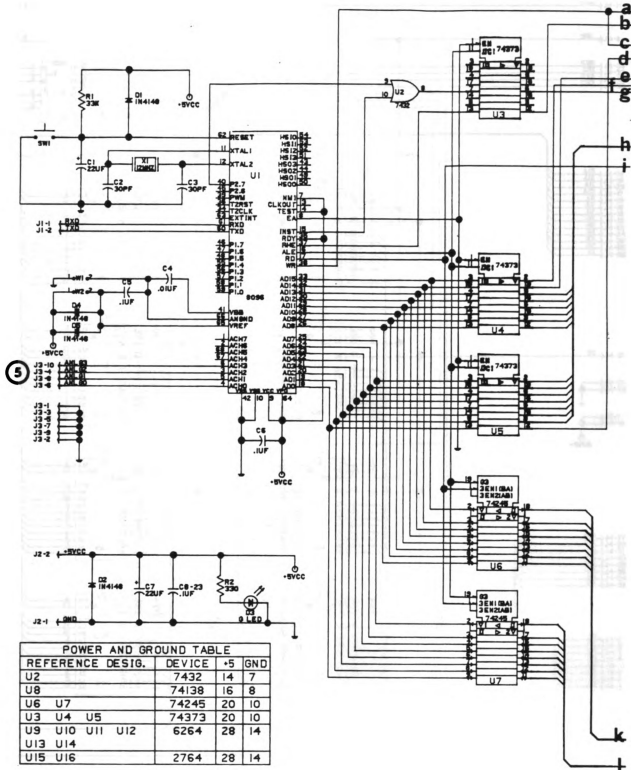


Fig. 3.6 Digital Circuit Diagram of the IS Data Acquisition System.

Table 3.2 Definition of Special Select Lines Used in Control and Addressing of the IS Digital Circuitry (obtained from Microcontroller's Handbook Intel Corp. (1986)).

<u>PIN Description</u>	<u>Function</u>
RD, WR	Read, Write signal output to external memory, active only during external operations.
$\overline{\text{BHE}}$	Bus High Enable signal used to select the high byte of the data bus.
AD0-AD15	Multiplexed Address/Data bus used when accessing external memory.
Port2.6,2.7	Quasi-bidirectional Ports.
INST	Used during external read to indicate that read is an instruction fetch.
$\overline{\text{EA}}$	Input for memory select for (External-accessing).
ALE	Address Latch Enable used to latch the address from the multiplexed AD bus.
V_{in}	Input voltage sensed by A/D.
V_{ref}	A/D reference voltage.
AN_{gnd}	Analog ground voltage.

used to demultiplex the address/data bus to generate the memory address bus. Two transceivers (74LS245) are used as drivers and receivers to drive the data bus. The external memory (RAM) is decoded for a minimum of 64 kbytes addressing with controls MA0 to MA15 and BHE to select even and odd (8-bit wide each for 16-bit operation) memory banks of 32 kbytes each. For extended data collection, the IS system is capable of selecting up to 192 kbytes of RAM. This is accomplished by using one of the two bidirectional ports (2.7 or 2.6) along with the INST to select 64 kbytes of auxiliary RAM pages. The NMOS microcontroller contains 8 kbytes of internal EPROM which contains the instructions needed to operate the IS. The CMOS version, however, initially would not contain internal EPROM and appropriate provisions are made such that an external EPROM can be used with a minimum amount of modification. The system is capable of A/D conversion for up to 8 channels, but currently only 3 channels are used for the triaxial accelerometer. A fourth channel is also provided to monitor any analog signal, like temperature.

3.1.4 Software

A single-board emulator (iSBE-96) along with an Intel Series IV Development System was used as a debugging tool for generation of the IS software. Therefore, real-time emulation was possible prior to hardware assembly. The

software design for the IS is based on the MCS-96 instruction set (ASM96, an assembly language) and a high level programming language (PLM96, a compiler language). The software developed by Klug et al. (1986), includes a monitor program consisting of 15 modules and 30 subroutines which allow interactive selection of the threshold triggering acceleration, sampling frequency and baud rate for data transmission. Interactive commands for IS initialization consist of keywords used to input the sampling frequency in Hz, the threshold acceleration in g, the baud rate in bits/s and the start of the data collection process are provided at the start-up time. The collected data transmission is also accomplished by use of keywords to terminate the data collection process and transfer the data from the IS to a host computer for analysis. Each 8-bit impact datum is transferred into 2 hex digits such that ASCII characters can be used in data transfer. Both initialization and data transfer are entered through a host computer via the 8097 serial port. As discussed by Klug et al. (1986) the IS upper sampling rate for 3 channels is limited to 4.25 kHz. According to the Nyquist sampling theorem this is sufficient for sampling impacts of up to 2.125 kHz or greater than 0.235 ms durations. Actual duration of impact for an apple with a very hard surface is much greater than 0.235 ms. Block diagrams of the IS software are displayed in Appendix B.1.

3.1.5 Impact Table

One of the methods used in impact testing of agricultural products is the calibrated drop test. During a drop test either a mass is dropped upon the product or the product is dropped onto a rigid surface. In either case transducers are mounted on one surface to sense the impacts.

Hammerle and Mohsenin (1966) developed a drop test apparatus for impact testing of agricultural products. Piezoelectric accelerometers and load cells were used to monitor the impact force and displacement of a falling plate on the fruit. Later Mohsenin (1970) used a similar system with a force transducer mounted to a rigid plate on to which fruits would fall. Flucke and Ahmed (1973) developed a falling mass device to capture the impact-time curves for a variety of agricultural products.

In general the drop testing apparatus lacks the requirement of accuracy and repeatability, which are critical when impact bruise analysis is studied for perishables. In recent years impact testing machines (impact tables) which were developed and used by the packaging industry, have become more useful to study impact bruising of fruits and vegetables. The impact table is used to simulate the impact conditions on various surfaces and is similar to a falling mass apparatus except that the test sample is placed on the falling mass as shown in Fig. 3.7. Kusza (1979) used an impact table to study the effect of time in a CA storage on bruising of apples. Turczyn et al. (1985) also

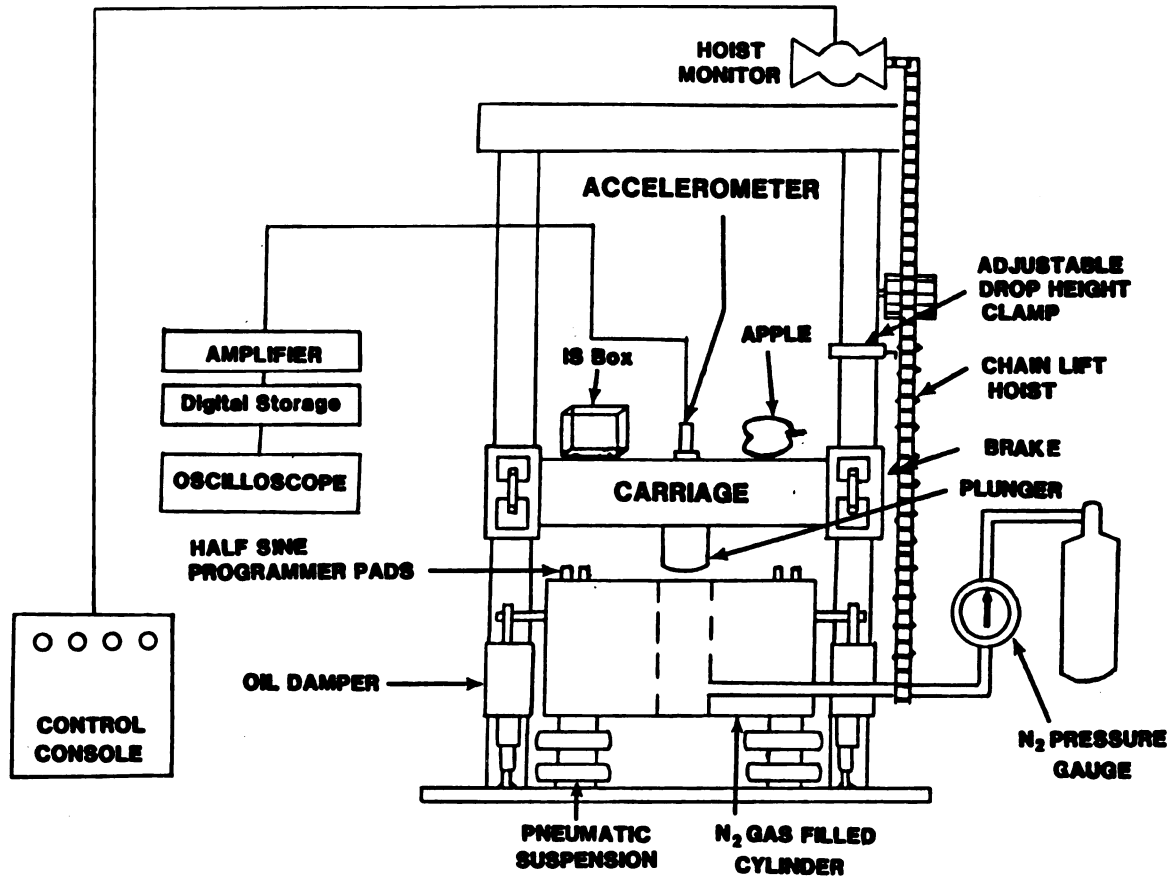


Fig. 3.7 Schematic of an Impact Testing Machine.

used an impact table to study potato bruising in handling and transporting. Using an impact table to establish a damage boundary curve, he concluded that typical handling conditions can result in bruising.

The impact testing as well as the IS calibration were performed by using a Lansmont model No. 23 Impact Testing Machine (hereafter referred to as the impact table) which is a programmable free-fall type machine. The impact of this table onto different types of "programmers" creates various impact shapes. One type of programmer (hard plastic) is used to create high g and short duration impact. Another programmer uses a nitrogen gas-filled cylinder such that when the table is raised to a predetermined drop height and released, a plunger located under the table penetrates the gas filled cylinder, thus generating longer duration and lower amplitude impacts.

3.2. Procedure for Drop Tests

When the impact table is dropped with apples placed on the table they experience acceleration which can be measured and recorded. This impact, which varies in shape and duration can range from 1.5 ms to 15 ms with the corresponding amplitude range of 300 m/s^2 to 9000 m/s^2 depending on the programmer type (impacting surface). A NBS calibrated accelerometer was placed on the table to capture the impact acceleration that was experienced by each

apple. The bruise created by this impact approximates the bruise created by dropping the apple onto a rigid surface from twice the height setting of the impact table (which will be explained next).

First, let us look at the thermodynamic energy balance of an apple when it is dropped onto a rigid immovable surface. Such an apple with mass M when dropped from an initial height of H_i , rebounds to a height H_r and has the following energy balance:

$$Q_{to} + W_{on} = \Delta E_{in}$$

where Q_{to} is the heat added to the apple, W_{on} is the work done on the apple by external forces, and ΔE_{in} is the change in the internal energy.

Assuming that the duration of impact is very short, the heat absorbed is zero and thus the work done is converted into internal energy change which results in cell breakage and bruising. Thus:

$$W_{on} = MG (H_i - H_r).$$

Now by using the simple free-fall velocity relations:

$$v = \sqrt{2GH}$$

$$e_a = v_r/v_i$$

$$H_i = \frac{(v_i)^2}{2G}$$

$$H_r = \frac{(v_r)^2}{2G}$$

which leads to:

$$H_i = \frac{(e_a v_i)^2}{2G}$$

and the final result is that:

$$W_{on} = 0.5 M V_i^2 (1 - e_a^2) \quad [3.8]$$

where:

e_a = coefficient of restitution of the apple

V_i = impact velocity (m/s)

V_r = rebound velocity (m/s)

H_i = impact height (m)

H_r = rebound height (m).

When an apple is placed (strapped down) on the impact table and dropped from an initial height H_i , it will have the same impact velocity V_i as the table just prior to impact.

Walker et al. (1978) have reported that apples have very low natural frequencies, typically in the range of 7 to 22 Hz. On the other hand, the natural frequency of the acceleration wave created by the impact table is in the range of 70 to 700 Hz, which is substantially greater than that of an apple. Because the apple has a low natural

frequency, it responds slower to the acceleration wave than the rebound time on the impact table. Just as the table rebounds from the programmers with V_r , the apple is still traveling down with its initial velocity V_i . Therefore, the apple descending at V_i sees the table rising with V_r , which is equivalent to the apple hitting a stationary object with a net velocity of:

$$\Delta V = V_i + V_r$$

exchanging V_i of equation [3.8] with ΔV for the table,

$$W_{on} = 0.5 M \Delta V^2 (1 - e_a^2) \quad [3.9]$$

It should be noted that e_a in equation [3.9] is the same as e_a on a hard rigid surface, since the apple is contacting the metallic surface of the impact table. The equivalent drop height of the impact table is now given by:

$$H_e = \frac{\Delta V^2}{2G} \quad [3.10]$$

Total velocity change ΔV can be measured directly by integrating the acceleration-time curve for the impact table. This value is then used in equation [3.10] to obtain an equivalent drop height which produces the same bruise for a free fall onto a hard stationary surface.

3.2.1 Half-Sine and Extended Half-Sine Impacts

It should be noted that the impact table can simulate different types of impacting surfaces such as very-hard, hard, semi-hard and soft or cushioned surfaces. As the surface gets softer, the duration of impact gets longer and the peak acceleration gets smaller. For this research only two types of impacting surfaces were considered, the very hard and the hard.

Figure 3.8 displays a half-sine impact, which is very short in duration (less than 2 ms) and high in acceleration. It represents an impact onto a "very-hard" surface such as steel or concrete. This type of impact is desirable, for a worst-case-study, since it creates the most severe bruise and is least desirable.

Table 3.3 shows averages of the various parameters such as duration, maximum acceleration, total velocity change and equivalent drop height for the half-sine impacts.

In order to obtain a more realistic impact that an apple sees when dropped onto a semi-hard surface the extended half-sine was used, as shown in Fig. 3.8. The duration of this type of impact is approximately 6 ms, and it does not produce as much damage as the half-sine for the same drop height. The extended half-sine would represent an impact such as that of an apple on a "hard-surface" like wood. Table 3.3 displays the various parameters for the extended half-sine impact.

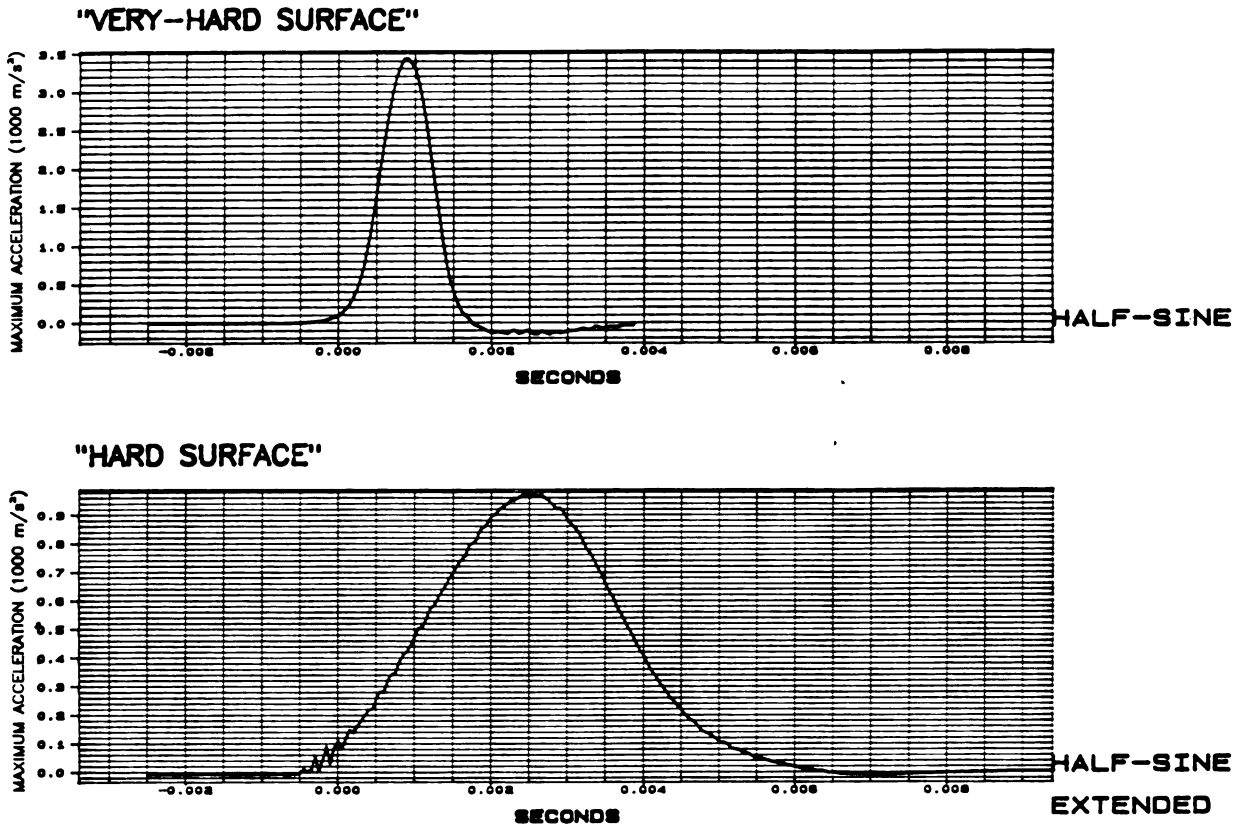


Fig. 3.8 Acceleration VS Time plot for Half-Sine and Extended Half-Sine.

Table 3.3 Duration, Maximum Acceleration, Total Velocity Change and Equivalent Drop Height for Half-Sine and Extended Half-Sine.

	Duration (ms)	Maximum Acceleration (m/s ²)	Total Velocity (m/s)	Equivalent Drop Height (mm)
HALF- SINE	2.0	615	0.93	47.5
	2.0	815	1.26	64.5
	2.0	1168	1.31	86.6
	2.0	1382	1.44	105.1
	2.0	2029	1.77	160.5
	2.0	2450	2.05	206.2
	2.0	2850	2.24	254.6
	2.0	3080	2.47	311.1
EXTENDED HALF- SINE	6.0	305	1.29	85.5
	6.0	355	1.46	109.1
	6.0	410	1.66	132.6
	6.0	621	2.10	226.3
	6.0	672	2.24	255.0
	6.0	774	2.44	304.2
	6.0	880	2.64	356.8
	6.0	963	2.80	398.1

3.3 Procedure for Calibration

As mentioned earlier, a PCB (model No. 301A03) calibrated accelerometer was used during the course of all experiments. I calibrated the PCB accelerometer against a standard which is traceable to the National Bureau Of Standards (see Appendix A.2). The calibration procedure involved the use of impact and shaker tables, and in cases where the accelerometer was not linear a calibration factor was introduced.

3.3.1 Accelerometer

Every accelerometer, including the triaxial that was used inside the IS, was provided with a calibration chart from the manufacturer (see Appendix A.2). These accelerometers were also calibrated against the piezoelectric accelerometer with calibration records traceable to the NBS. The specific calibration data for the NBS unit is also provided in Appendix A.2. The procedure for calibration was to compare the frequency and phase response of each accelerometer with the NBS response. This comparison was done at discrete frequencies of 30, 40, 70, 90, 150, 300, and 500 Hz using a shaker table. The resulting magnitude and phase relations are displayed for all three axes of the triaxial accelerometer (Figs. 3.9 and 3.10). There is no significant difference (at 99 percent confidence) between

the triaxial and the NBS accelerometer, as can be observed from the calibration charts. In cases where the responses were not satisfactory a correction factor could be introduced to account for the error.

3.3.2 Impact Table

The impact table was calibrated for half-sine impacts, and in each case the maximum acceleration was compared with the NBS output acceleration. This procedure verified the repeatability and accuracy of the Lansmont impact table for all conditions used in this study. Table 3.4 shows the simple statistics that result in a maximum coefficient of variation of 3.5 percent for the maximum acceleration at the lowest drop height.

3.3.3 IS Data Acquisition System

The IS data acquisition system was tested for its maximum operable sampling frequency, as well as its amplitude response and linearity.

Sampling frequency verification involved the use of a wave generator as the input source for the A/D. An input frequency of 10 Hz was used with various sampling frequencies. The number of samples in each period was compared with the theoretical values obtained by addition of software execution time and A/D conversion time. The results show that the operational sampling rate exceeds the

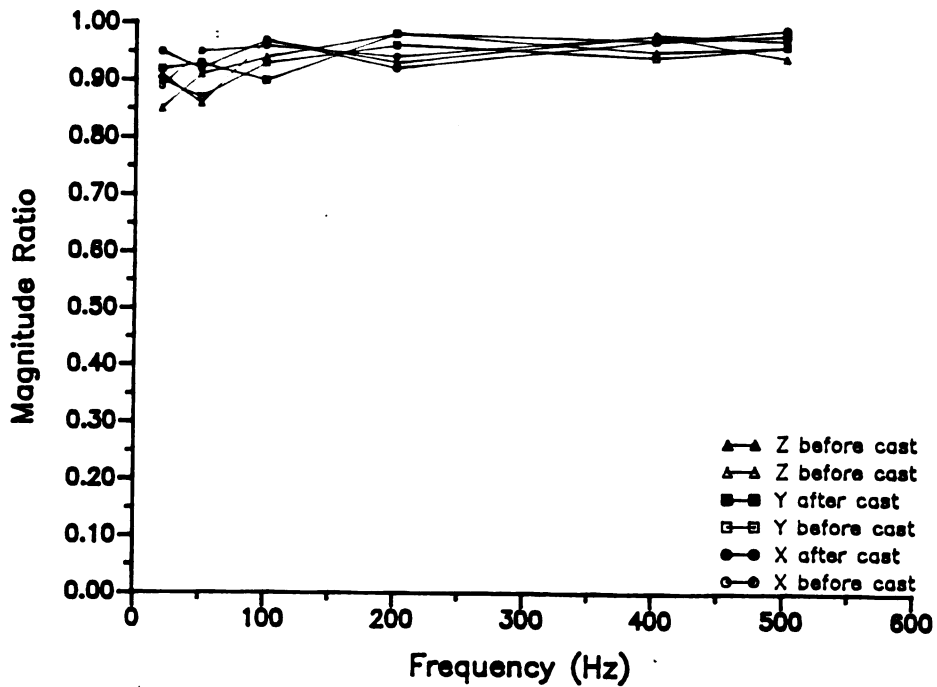


Fig. 3.9 Magnitude Response of the Triaxial Accelerometer Calibration Used in the IS System.

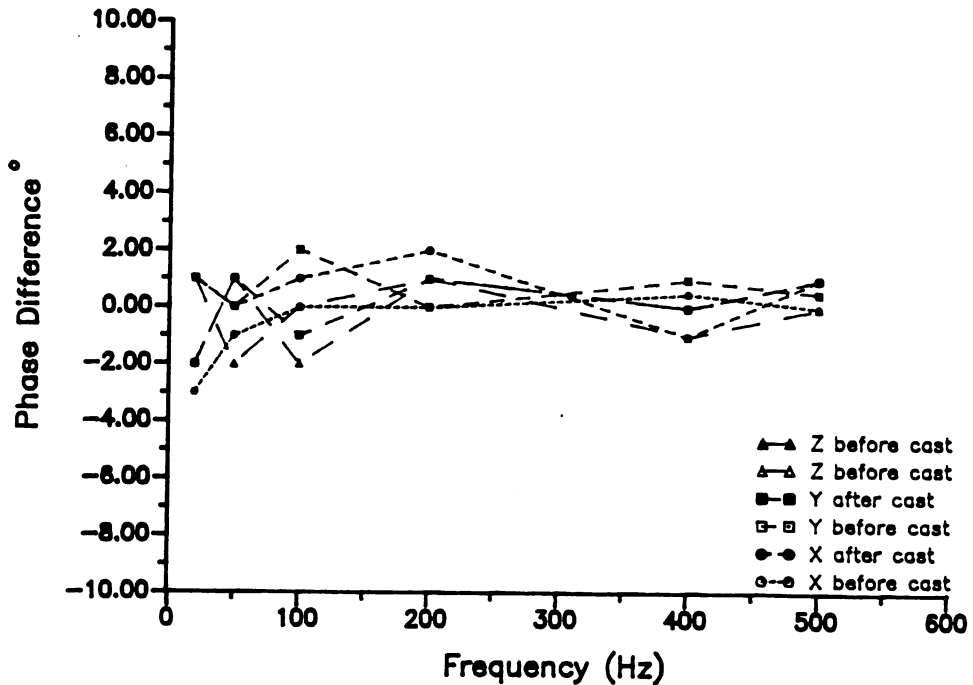


Fig. 3.10 Phase Response of the Triaxial Accelerometer Calibration Used in the IS System.

Table 3.4 Simple Statistics for the Lansmont Impact Table Calibration.

Impact Drop Height (cm)	Total Number of Reps.	Average Maximum Acceleration (g)	Standard Deviation ($\pm g$)	Coefficient of Variation ($\pm g/g$)100
2.0	16	60.46	2.12	3.5
5.0	16	139.47	1.04	0.7
15.0	16	315.58	3.67	1.2

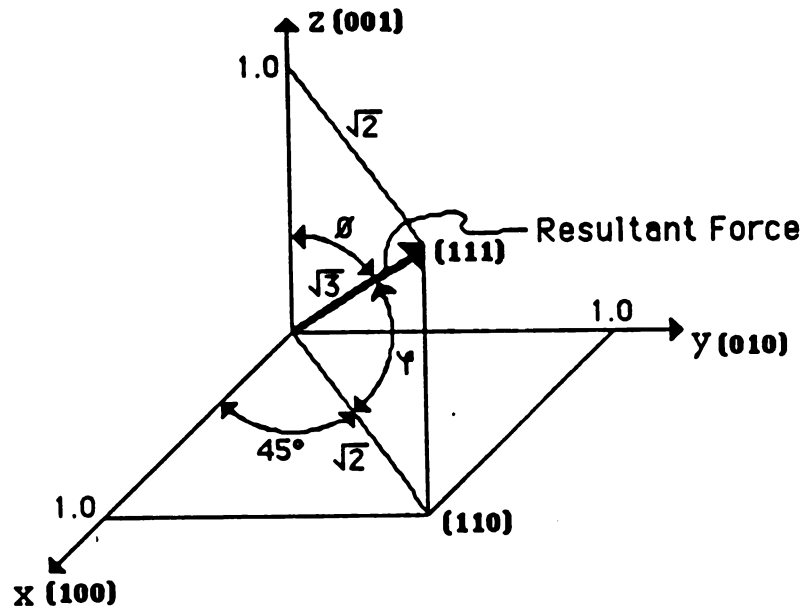


Fig. 3.11 The {111} Position of the Accelerometer Used in IS System Calibration.

theoretical maximum of 4.25 kHz by 18 percent with less than 0.5 percent error.

Amplitude calibration of the IS involved use of the Lansmont impact table to generate extended half-sine impact of varying magnitudes, over the range of 0 to 262 g. Each impact was captured by the IS, as well as a calibrated accelerometer along with an Analogic Data 6000 calibrated digital scope. Six different drop heights were selected in the above range and ten repetitions were performed for each impact. This procedure was repeated for both the single axes and the triaxial resultant vector sum. The vector sum was calibrated for the worst case, which meant positioning the triaxial accelerometer in a {111} direction as shown in Fig. 3.11. These data were transferred to an IBM AT for further statistical analysis. Results of these calibrations were very satisfactory and they are discussed in Chapter 4.

3.4 Experimental Procedure

Two different sets of Ida-Red apples were used for this study. The first set of apples (hereafter referred to as CS apples) were hand picked and carefully placed in trays and boxes on September 24, 1985. They were placed in a conventional cold (CS) storage ($T= 3^{\circ}$ C and 85% RH) until needed. The CS apples were removed from the storage and brought to room temperature at least 2h prior to each experiment. Table 3.5 lists the number of days after harvest, impact type and impact machine height setting for each experiment. The second set of apples (hereafter referred to as CA apples) were picked in October 1985 from a different orchard; they were placed in a controlled atmosphere (CA) storage ($T= 0^{\circ}$ C and 90% RH). They were removed from storage on January 15, 1986. Table 3.6 lists the parameters for the tests using CA apples. It should be noted that the impact machine drop settings listed in Tables 3.5 and 3.6 were selected based on preliminary tests. The selected range of drop heights should cover the maximum allowable bruise diameter outlined by the U.S.D.A. (1964), as shown in Table 3.7. These limits are used throughout the packing industry to classify quality of apples. Observed bruises greater than these limits will decrease the classification of apples, which lowers their market value. Also given in Table 3.7 are the relative percent dollar values for each grade.

In addition to half-sine impacts, each apple from the CS set was also subjected to an extended half-sine impact. As indicated in Tables 3.5 and 3.6 a total of 798 apples were tested in this study. A total of 516 CS apples were tested by the half-sine impact, and 144 CA apples were tested by both half-sine and extended half-sine impacts (once on opposite sides).

3.4.1 Parameter Selection and Measurement

Based on previous studies, and both Hertz and plastic theories, the following parameters, as listed in Fig. 3.12, were selected and measured on each apple before each impact:

1. horizontal apple diameter, AHD
2. vertical apple diameter, AVD
3. apple mass, AM.

After every impact the following readings were also taken on each apple:

4. Magness-Taylor force, MT
5. horizontal bruise diameter, HBD
6. vertical bruise diameter, VBD
7. bruise depth, BD.

Parameters, AHD and AVD were obtained by measuring apple circumference with a graduated band to an accuracy of 1 mm. A digital caliper was used to measure HBD, VBD and BD

Table 3.5 CS Type Apple Impact Test Parameters.

Number of Days from Harvest	Impact Type	Impact Table Drop Height (cm)
28	HALF-SINE	2, 3, 4, 5, 7.5, 9, 10, 15
37	HALF-SINE	//
41	HALF-SINE	//
50	HALF-SINE	//
59	HALF-SINE	//
73	HALF-SINE	//

Table 3.6 CA Type Apple Impact Test Parameters.

Number of Days out of CA Storage	Impact Type	Impact Table Drop Height (cm)
	HALF-SINE	2, 3, 4, 5, 7.5, 9, 10, 15
10	EXTENDED HALF-SINE	4, 5, 6, 10, 12.5, 15, 17.5, 20

Table 3.7 U.S.D.A. Guideline for Apple Bruise and Quality Classification, and Present Dollar Value.

Quality	Extra Fancy	US #1	Utility
Bruise Diameter (mm)	12.7	19.05	22.2
Percent \$ Value	100	70	30

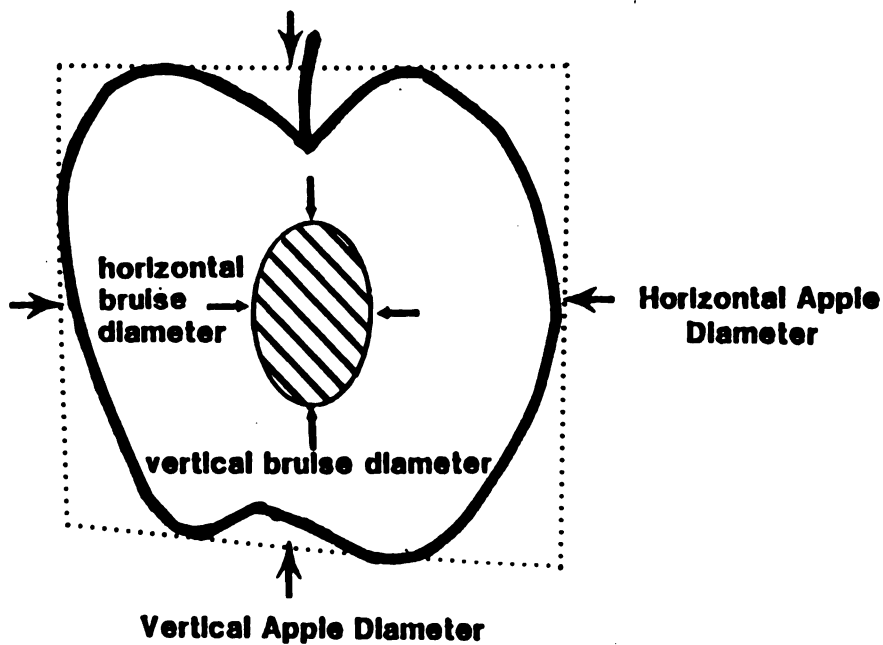


Fig. 3.12 Measured Bruise and Diameter for Ida-Red Apple.

which were based on discoloration of the apple tissue after removal of the skin. The accuracy of the instrument used for bruise measurements was within 0.1 mm, however, the operator's inaccuracy for these measurements was at least 5 percent. Magness-Taylor force was measured with a Chatillon force gage (model HTCM) with an accuracy of 0.1 kg, and apple mass was measured with an accuracy of 1 gram.

The Ida-Red apples experienced impact bruises which were in general not symmetrical. Thus the vertical and horizontal apple diameters and bruise diameters were averaged to obtain:

8. average apple diameter, AAD
9. average bruise diameter, ABD.

For each impact the NBS calibrated accelerometer was mounted on the table to record the impact acceleration trace. The following impact parameters were recorded as well as the actual digitized acceleration trace for every impact:

10. maximum acceleration, MA
11. total velocity change, ΔV .

These measurements were used in equation [3.10] to calculate an equivalent drop height, H_e , for every impact.

3.4.2 Impact Tests

CS and CA apples were initially sized and only apples

within the following size range were used in this research:

68.75 mm (2.71 in.) < Apple Diameter < 78.25 mm (3.08 in.)

The sized apples were selected at random and used in each impact test. Each impact test involved 3 replications for every drop height, thus creating 18 identical bruising tests. As discussed earlier, the impact table is very accurate which permits repeating of test conditions on different days.

4. RESULTS AND DISCUSSION

4.1 IS Calibration and Precision

Calibration procedures explained previously were used to establish a calibration factor for the IS. True maximum accelerations, obtained by the calibrated system, were compared with the IS digitized values for three axes and the triaxial resultant vector. In each case both the true and the IS values were used in a linear regression model to obtain the calibration equations.

The three axes regression analysis resulted in a zero order relation described by equation [4.1]:

$$MA = 2.12255 (ISD) \quad [4.1]$$

where MA is maximum acceleration (m/s^2) and ISD is the IS digitized values.

The actual data points and the derived relation are shown in Fig. 4.1 along with 99 percent (3 Standard Deviations includes 99 percent of the data points) confidence belts for the prediction equation. The worst case residuals resulted in ± 4.35 g within these belts for the IS calibration equation of the three axes.

Regression analysis for the resultant acceleration case

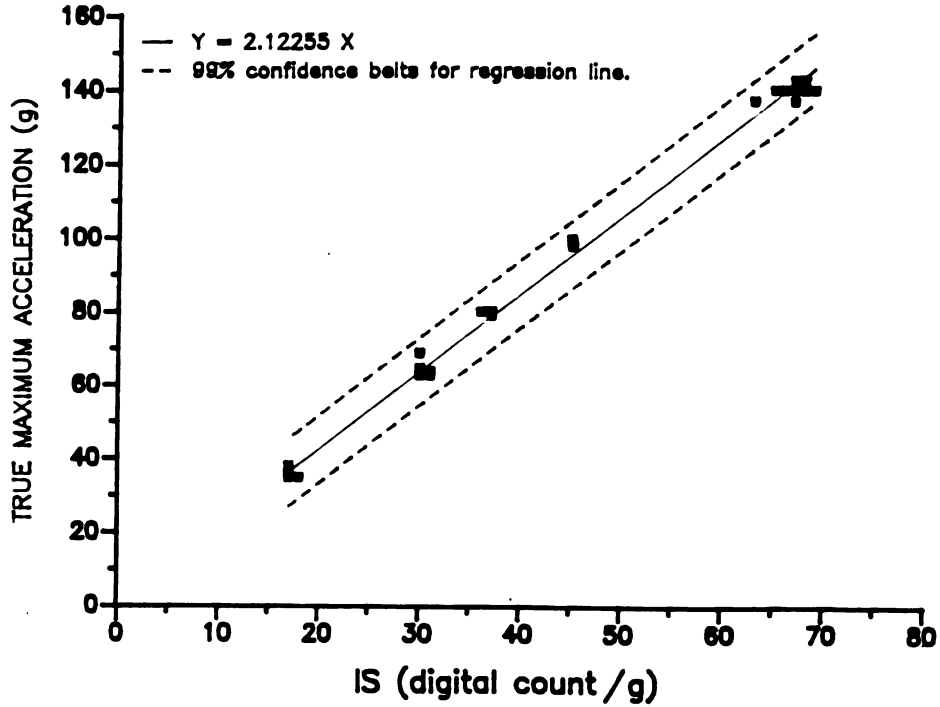


Fig. 4.1 IS Calibration Curve for Single Axes Acceleration.

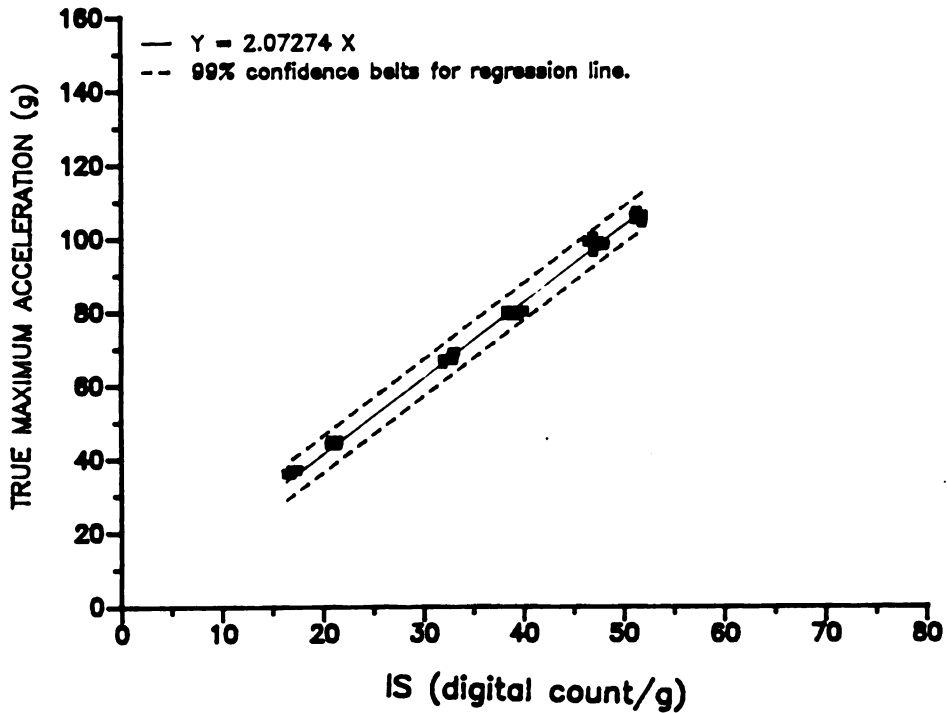


Fig. 4.2 IS Calibration Curve for the {111} Resultant Acceleration.

also resulted in a zero order relation . Equation [4.2] describes this relation, and Fig. 4.2 shows the regression line and 99 percent confidence belts for this case. The worst case residuals resulted in ± 3.2 g for the {111} resultant acceleration within the confidence belts. Both of the single axes and resultant sum results are satisfactory. The vector sum calibration and accuracy indicates great improvements over any previous system (Hallee (1981), reported ± 7.5 percent precision at 97 percent confidence belts).

$$MA = 2.07274 \text{ (ISD)} \quad [4.2]$$

To confirm the accuracy of sampling frequency and to compare the waveform similarity of the impacts recorded by the IS with the calibrated system, the averages of 10 impacts were plotted for both systems in Figs. 4.3 and 4.4. Three types of impacts, with durations of 2, 5 and 9 ms and magnitudes of 140, 60 and 30 g, respectively, were examined. By comparison, there is an excellent correlation between the readings of the two systems. Thus, I conclude that the IS system does not distort the shape of the acceleration curves for impacts with frequencies less than at least one half of the theoretical Nyquist sampling rate of 2.12 kHz.

4.2 Statistical Analysis

During the course of this research a total of 798

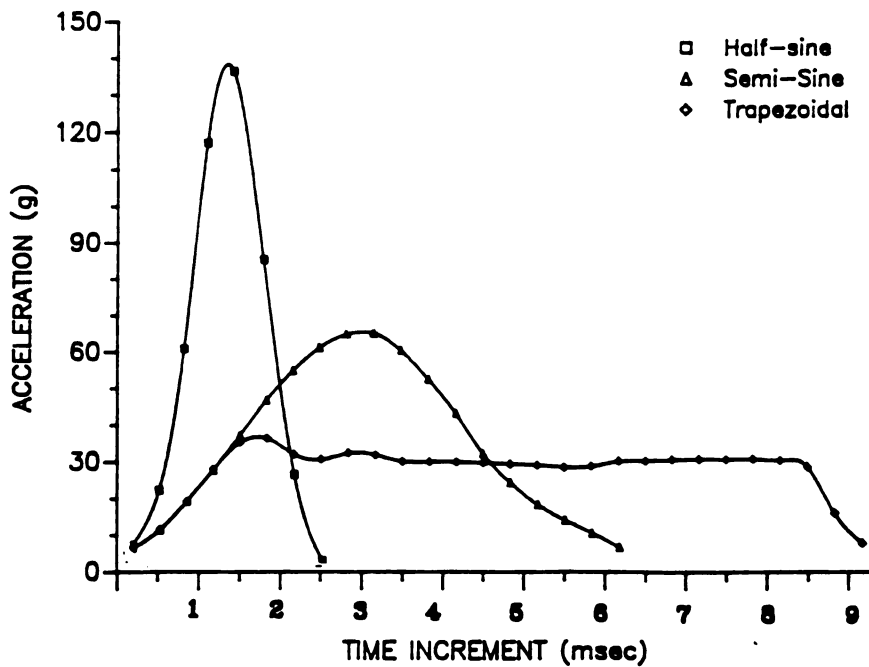


Fig. 4.3 Average of 10 Impacts for 3 Impact Types Collected by IS System at 3.012 kHz Sampling Rate.

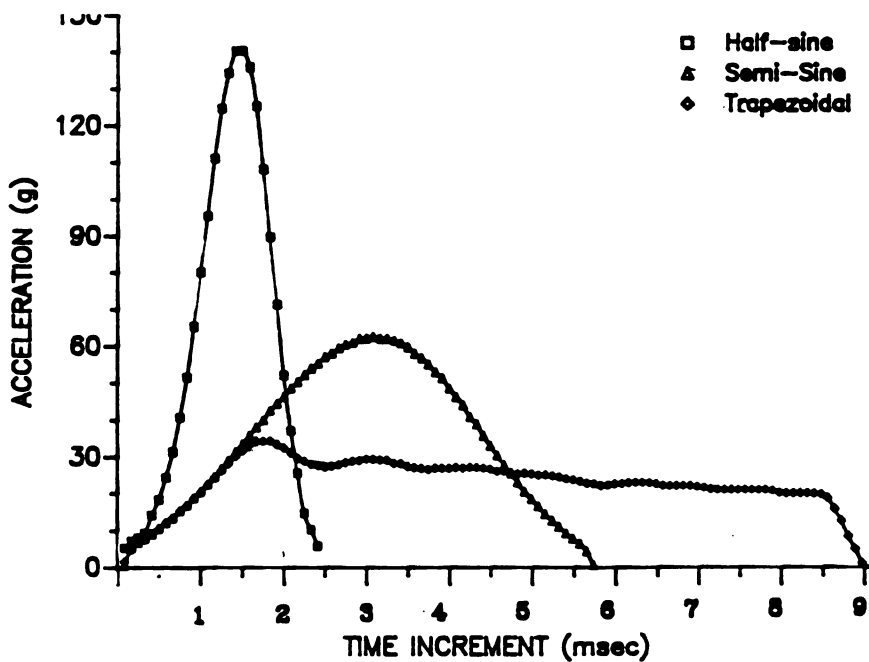


Fig. 4.4 Average of 10 Impacts for 3 Impact Types Collected by Data 6000 as Calibration at 12.048 kHz Sampling Rate.

impact experiments were conducted on Ida-Red apples. This number, which includes the CS apples as well as the CA apples, consists of 654 cases of half-sine and 144 cases of extended half-sine impacts. Both half-sine and extended half-sine impacts were used to establish a general relation to account for the variations in impact duration.

All statistical analyses were performed on an IBM AT by using the statistical packages listed in Appendix C1. These statistics included linear and nonlinear regression analysis as well as analysis of variance. Confidence belts for single predicted values were obtained at the 99 percent level for the prediction lines describing acceleration or bruise diameter.

4.2.1 Apple Physical Properties

Initially, simple statistics were calculated for all 798 cases of data to obtain means and variances for each of the measured physical properties, Table 4.1. To distinguish the CS and CA types of apples and to identify the differences among the two groups, histogram charts of apple diameter, apple mass and Magness-Taylor are provided in Figs. 4.5, 4.6 and 4.7, respectively. These figures show that, on average, the CA type apples have larger mass and diameter. On the other hand, the CA apples have slightly larger Magness-Taylor values than the CS apples, which means that the short CS storage period lowered the firmness of the

Table 4.1 Means and Variances for the Apple Physical Properties and Impact Conditions.

Title: APPLE IMPACT (HALF-SINE) VS BRUISE (Ida-Red) Sep 1985

Function: STAT
Data case no. 1 to 798

Variable Number	N of Cases	Minimum	Maximum	Sum	Mean	Variance

Measured Bruise Diameter (mm)						
1	798	11.000	32.550	16997.975	21.301	18.163
Average Apple Diameter (mm)						
2	798	68.750	78.250	58754.452	73.627	3.672
Apple Mass (Kg)						
3	798	0.137	0.180	128.315	0.161	0.000
Magness-Taylor Force (Kg)						
4	798	3.000	7.938	4119.768	5.163	1.072
Equivalent Drop Height (mm)						
5	798	44.623	410.638	135349.776	169.611	9276.105
Maximum Acceleration (m/s ²)						
7	798	305.437	3368.949	1268799.039	1589.974	816831.005
Total Velocity Change (m/s)						
8	798	0.935	2.838	1394.349	1.747	0.274

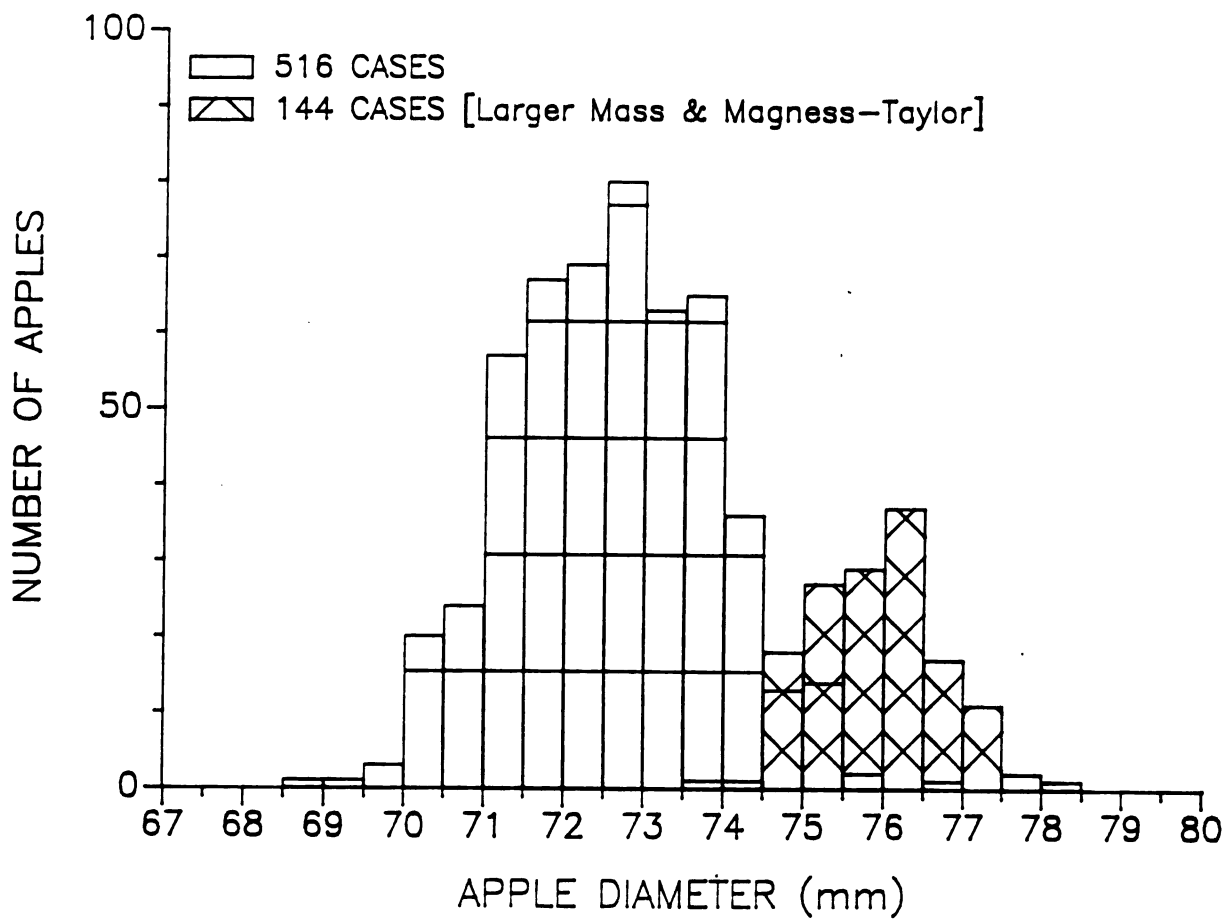


Figure 4.5 Frequency Distribution of Apple Diameters.

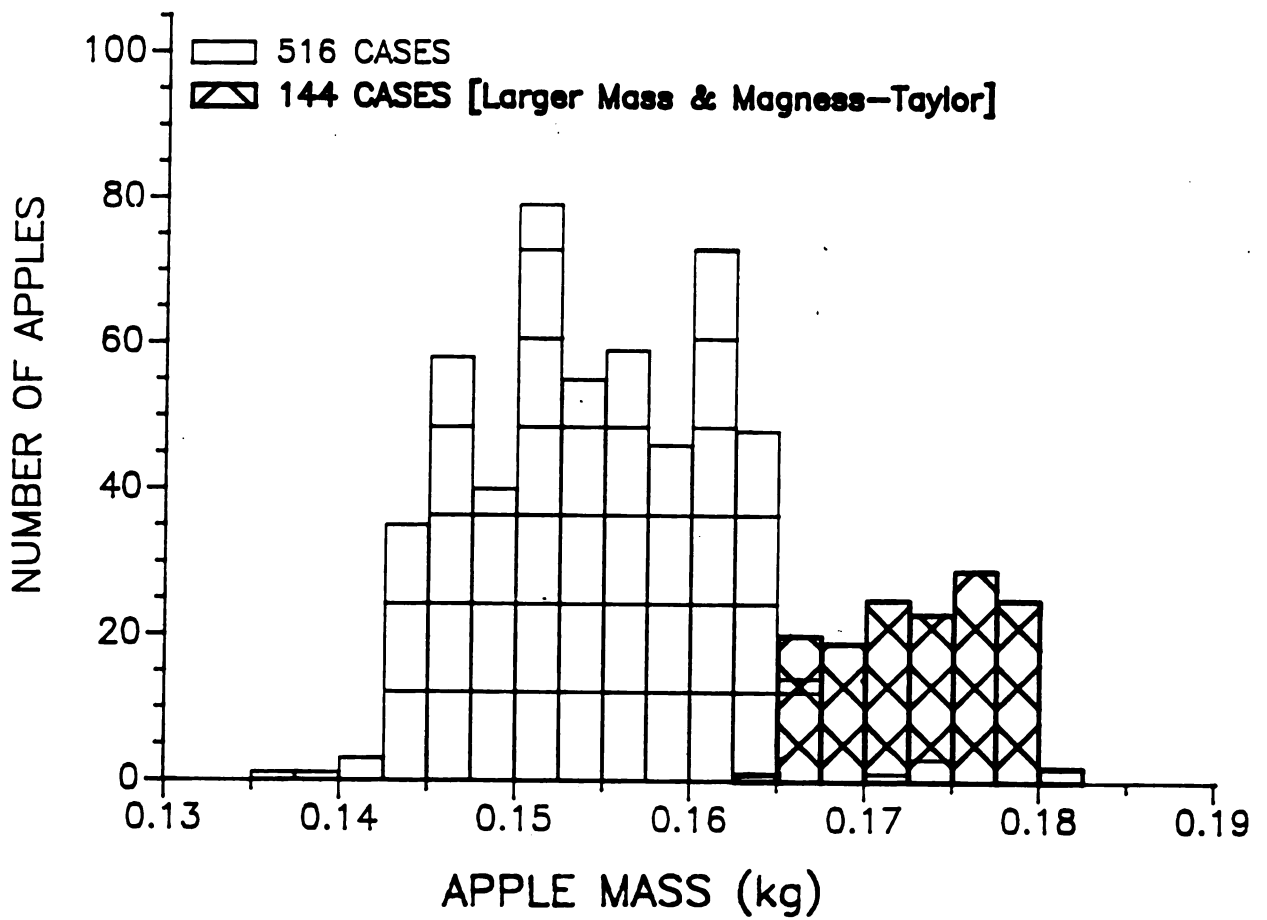


Figure 4.6 Frequency Distribution of Apple Mass.

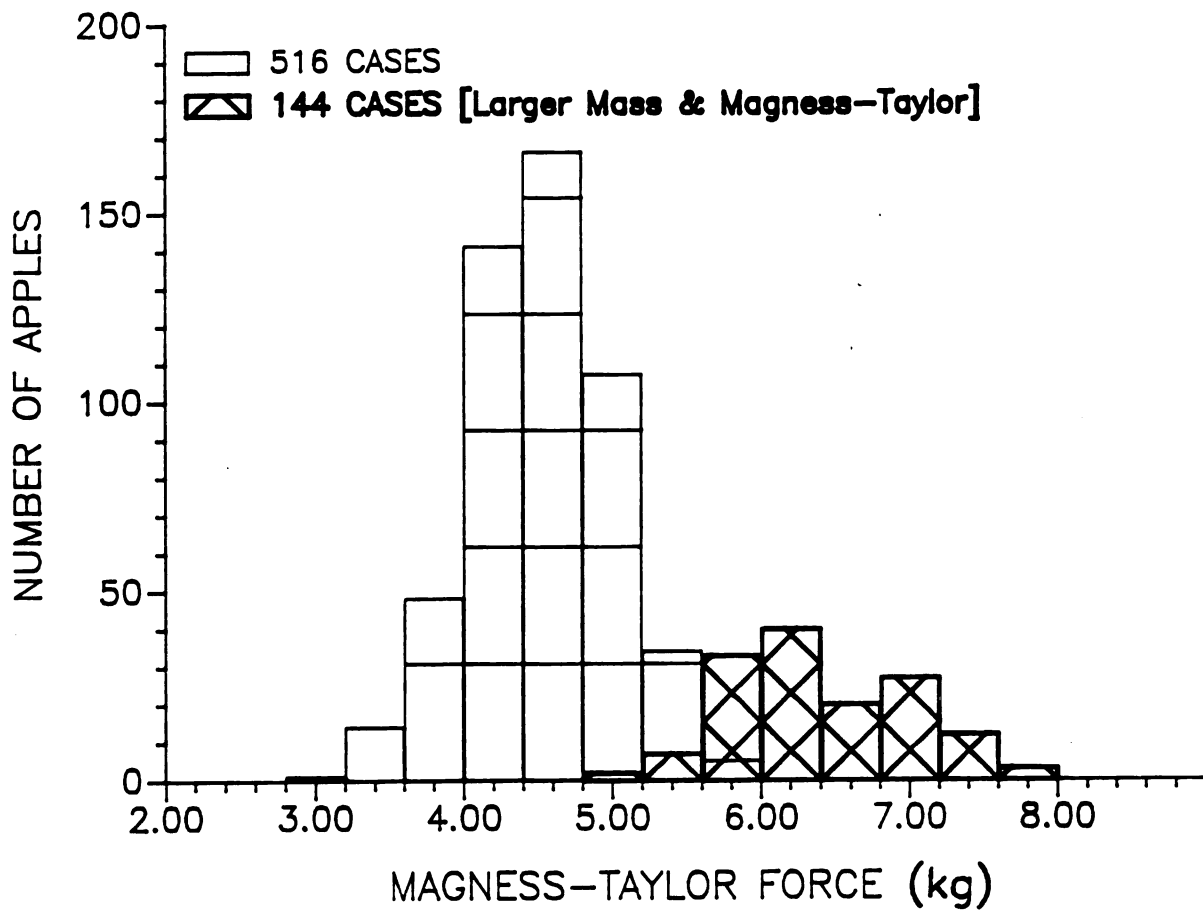


Fig. 4.7 Frequency Distribution of Apple Magness-Taylor.

CS apples. The loss in firmness could result because the CS storage had 3° C higher temperature and 5 percent lower relative humidity than the CA storage. Nelson and Mohsenin (1968) indicate that CS storage humidity and temperature are critical elements in maintaining high apple Magness-Taylor values and bruise resistance .

Since impact experiments were performed on different days, the variations in Magness-Taylor values and resulting apple bruising changes were investigated. Magness-Taylor values, given in Table 4.1, ranged from 3.0 to 7.94 kg. Therefore, all the values were classified in the following four groups, 3.0 to 4.0, 4.0 to 4.5, 4.5 to 5.0 and 5.0 to 6.0 (the 6.0 to 8.0 data were deleted), to check for bruise differences among groups. A one-way analysis of variance indicated that the mean values of bruise diameter were significantly different among the four Magness-Taylor groups.

The measured mean bruise diameter was plotted as a function of equivalent drop height and Magness-Taylor value, Fig. 4.8. From Fig. 4.8 it is apparent that an increase in apple firmness reduces the bruise diameter slightly. Both mean drop height and Magness-Taylor values were then grouped and used in a two-way analysis of variance. The results indicate that both variables caused significant differences in the means of the bruise diameters, with drop height significant at the 0.01 percent level and Magness-Taylor only significant at the 1 percent level. From the above

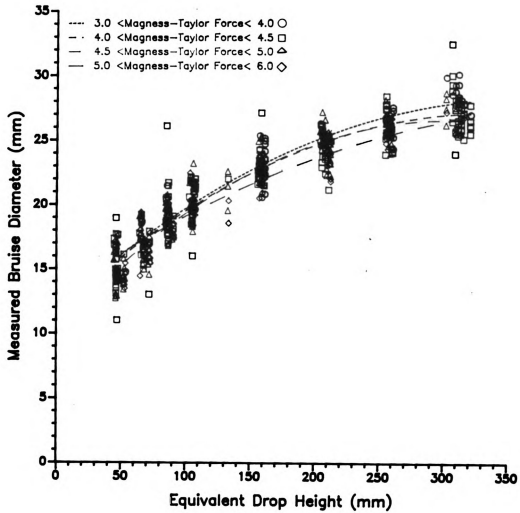


Fig. 4.8 Bruise Diameter Versus Maximum Acceleration for 4 Ranges of Magness-Taylor Force.

analysis it is clear that bruise diameter increases with an increase in drop height and a decrease in Magness-Taylor. This agrees with previous work done by Nelson and Mohsenin (1968), and it also agrees with Hertz theory as well as plastic theory.

An increase in drop height will cause the total impact energy to increase and, in turn, result in additional energy to be absorbed (expressed as increased bruise diameter). This result agrees with previous work on apples by Schoorl and Holt (1980), which states that a strong linear correlation exists between absorbed energy and bruise volume. The complete statistical analysis tables are provided in Appendix C.

4.2.2 Methods of Impact Bruise Prediction

As explained previously, average bruise diameter, bruise depth, maximum acceleration, total velocity change and equivalent drop height were measured and recorded for every impact. Although bruise depth is very important in any bruise study, the bruise diameter seems to be a more interesting parameter. This is due to explicit limits set on bruise diameter by the U.S.D.A. grading guideline and by the less destructive nature of this measurement. Both parameters were considered initially, but after the first test demonstrated that these parameters were highly correlated (correlation coefficient = 0.861), only bruise diameter was considered in the final analyses.

The prediction of apple bruise diameter was approached using various mathematical models that used information on both apple physical properties and impact parameters. For each of the 4 methods outlined below, the predicted bruise diameter is compared with the actual measured bruise diameter. This is accomplished by a comparison of R^2 (coefficient of determination) and the confidence interval limits so that the goodness of each approach is related to the higher value of R^2 and smaller range of confidence interval. The 4 methods for bruise prediction are:

1. Hertz calculated bruise diameter, based on equation [2.17].

2. Hertz calculated bruise diameter, adjusted by ψ (a time varying function that compensates for a time varying modulus of elasticity applied to each measurement case).
3. Plastic calculated bruise diameter, based on equation [2.25].
4. Multiple linear regression analysis (MLRA) predicted bruise diameter, based on a best-fit model (highest R^2).

For further comparison of each method, bruise diameter was also plotted versus maximum acceleration. The choice of the maximum acceleration for plotting does not indicate any accuracy advantages over the other impact parameters (drop height and/or total velocity change). However, the parameters of drop height and total velocity change must be calculated from the acceleration time trace. Figures 4.9 and 4.10 allow conversion from acceleration to other impact parameters such as drop height or total velocity change.

4.3 The Bruise Diameter Versus Hertz Theory

Hertz theory has been used to explain (predict) bruising in hard fruit when the impact follows the elastic behavior and the Hookian laws. But for the case of apple impact, the stress/strain behavior is not solely elastic. This fact limits the use of the Hertz theory for accurate bruise diameter prediction. The Hertz relation [2.17], when used with all the measured parameters, did not accurately predict the actual (measured) bruise diameter as shown in

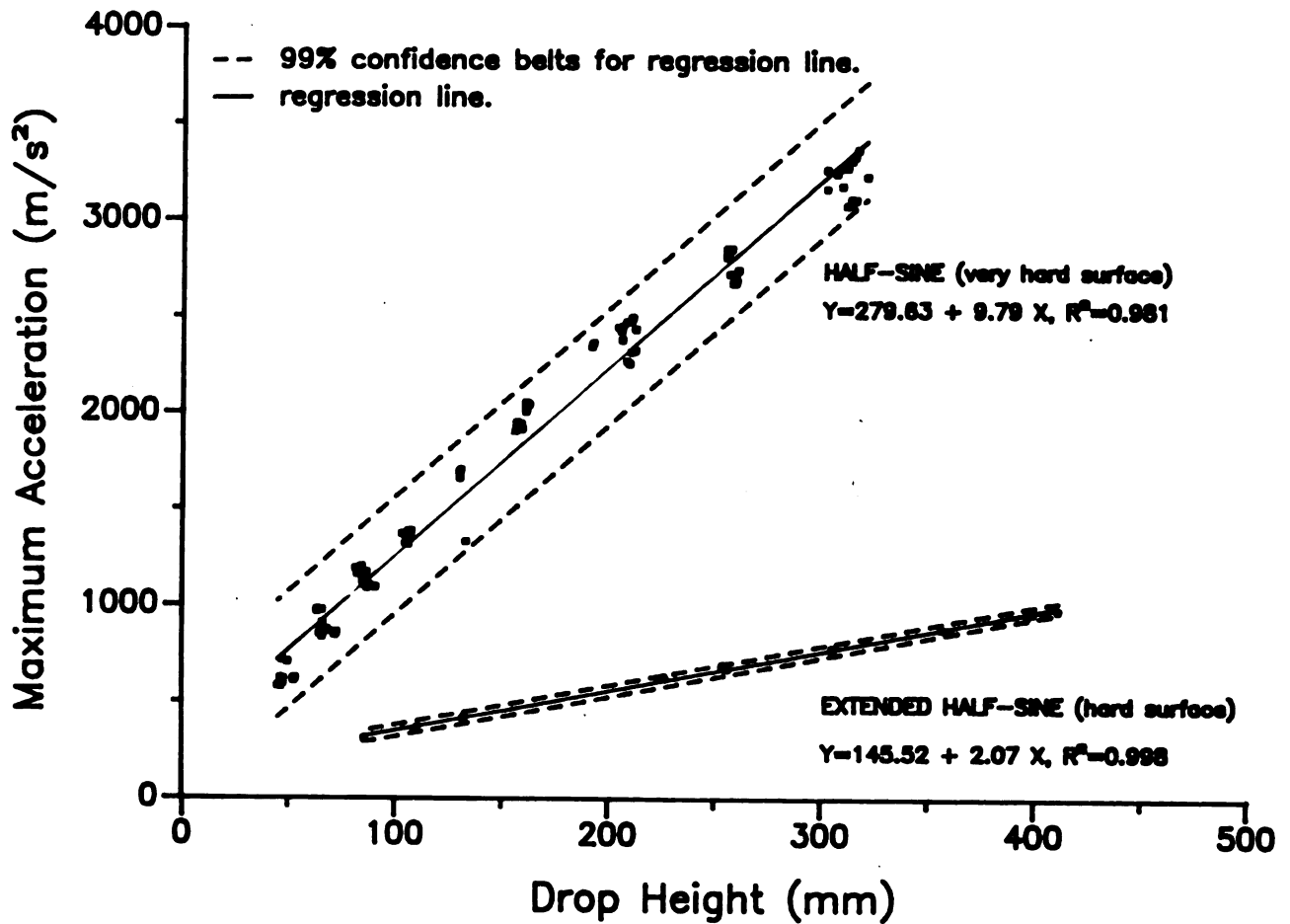


Fig. 4.9

Maximum Acceleration Versus Drop Height Mapped
for Both Half-Sine and Extended Half-Sine Impacts.

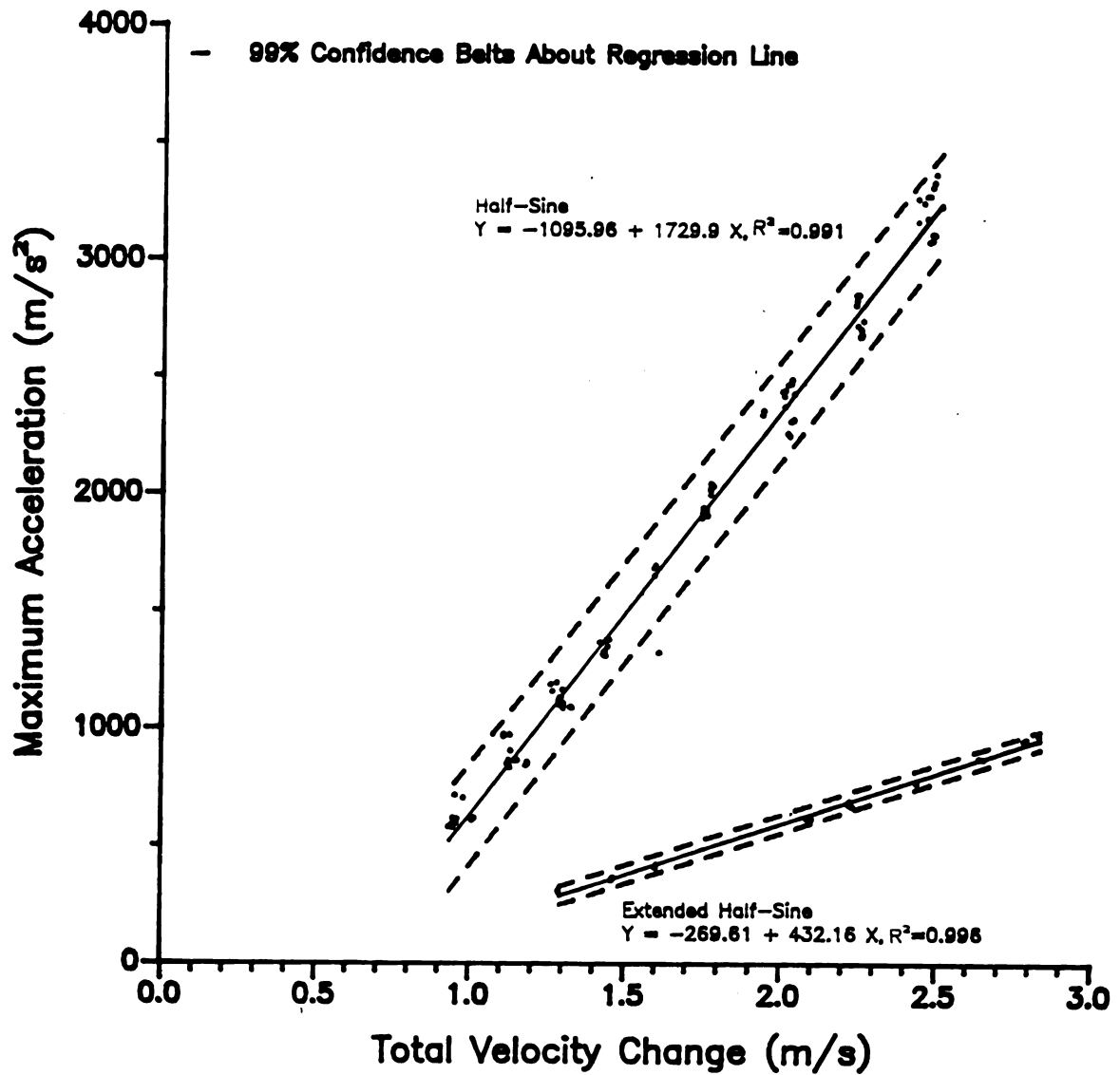


Fig. 4.10 Acceleration Versus Velocity Change Mapped for Both Half-Sine and Extended Half-Sine Impacts.

Fig. 4.11. The regression relation obtained from Fig. 4.11 results in $R^2=0.656$, which verifies the inadequacy of the Hertz calculation. Fig. 4.12 shows the measured and Hertz calculated bruise diameters versus maximum acceleration. This figure indicates that the Hertz method overestimates the bruise diameter by about 35 percent for both "very-hard" and "hard" surfaces.

4.4 The Bruise Diameter Versus Adjusted Hertz Theory

Fruit has been identified as viscoelastic material by Mohsenin (1970). In an attempt to extend the Hertz theory to the viscoelastic case, Hamann (1968) introduced the uniaxial stress-strain relation, which is a function of the rate of loading. Thus, a time dependent modulus of elasticity would be used for apples rather than the constant value. Shahabasi (1979) studied the time dependency of apple modulus of elasticity and the effect of storage condition on the modulus values. Further, the stress-strain relation, varying with the rate of loading, can also lead to a modulus, $\mu(t)$, which varies with impact duration.

In an effort to identify a parameter that will adjust for the time dependent modulus for the apples tested, and to verify if the addition of such a parameter improves the Hertz estimate, the following procedures were performed:

1. a ratio, λ , of measured bruise divided by the Hertz

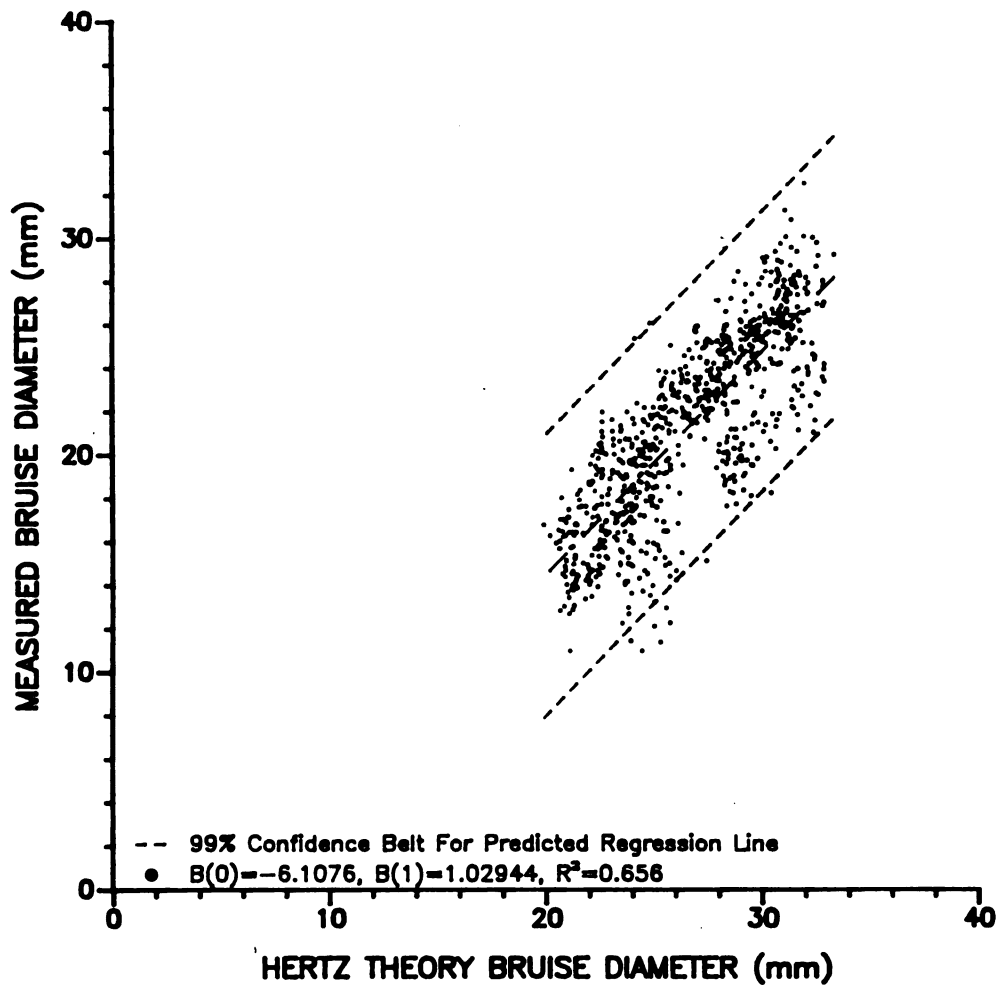


Fig. 4.11 Measured Bruise Versus Hertz Theory Bruise Diameters for All Ida-Red Apples.

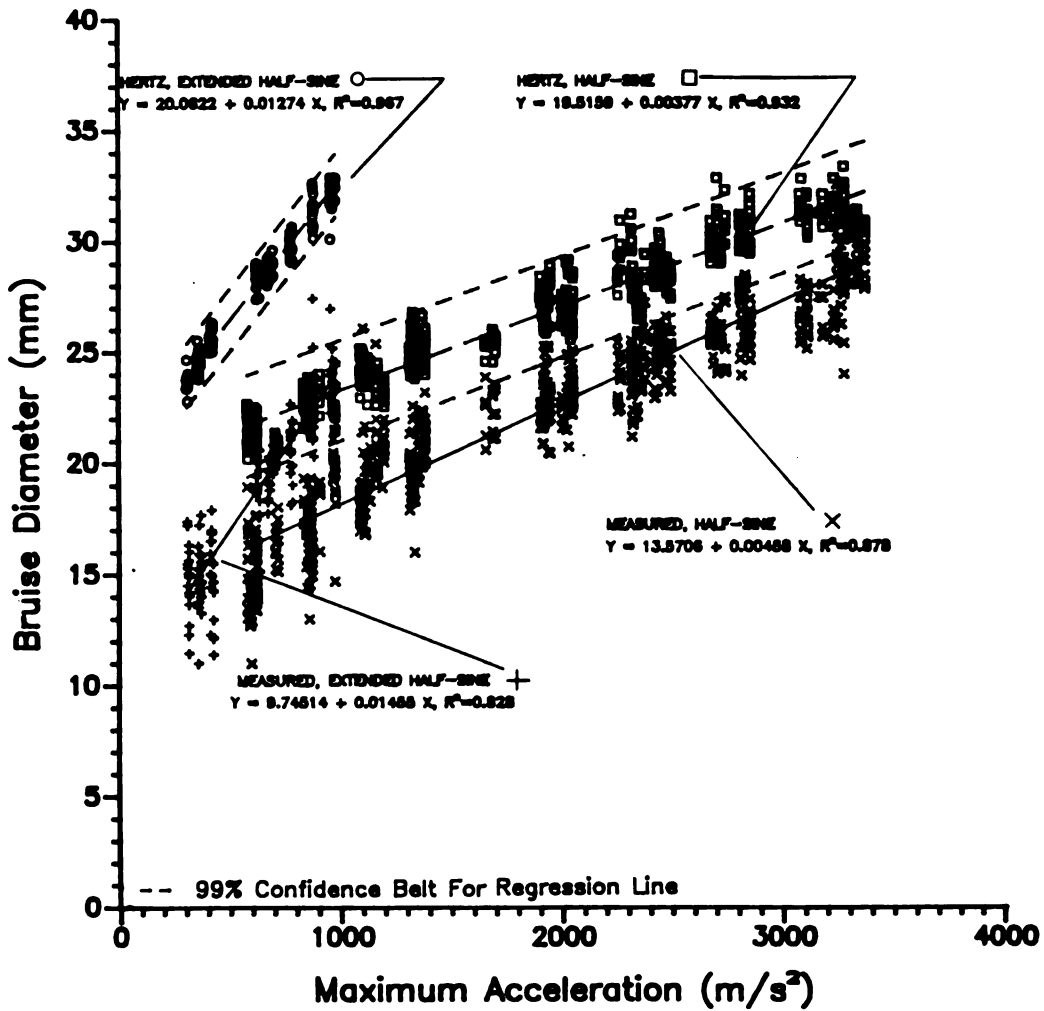


Fig. 4.12

Hertz Theory and Measured Bruise Versus Maximum Acceleration with First Order Regression Lines.

estimated bruise was obtained for every impact.

2. a time function, ψ , given by the ratio of total velocity change over maximum acceleration was obtained for every impact.
3. a regression equation was developed to estimate λ , which turns out to be a nonlinear function in terms of ψ .

With $R^2 = 0.645$ the nonlinear equation for λ is given by:

$$\lambda = \psi / \{43.21\psi^2 + 1.4564\psi - 0.0002846\} \quad [4.3]$$

4. each case, Hertz calculated bruise diameter was then multiplied by the factor λ to obtain an adjusted Hertz bruise diameter.

The adjusted Hertz relation obtained is:

$$DAH = \lambda (D)$$

The adjusted Hertz bruise diameter prediction equation applies to both the half-sine and extended half-sine impacts, and provides very good estimates. In fact, when the adjusted Hertz bruise diameter is plotted against measured bruise diameter as in Fig. 4.13, a coefficient of determination of $R^2 = 0.869$ is obtained. Thus, the Hertz adjustment procedure accounts for 86.9 percent of bruise variation about the mean. At the 99 percent level the confidence belts are ± 4.0 mm, which are also better than for the Hertz model.

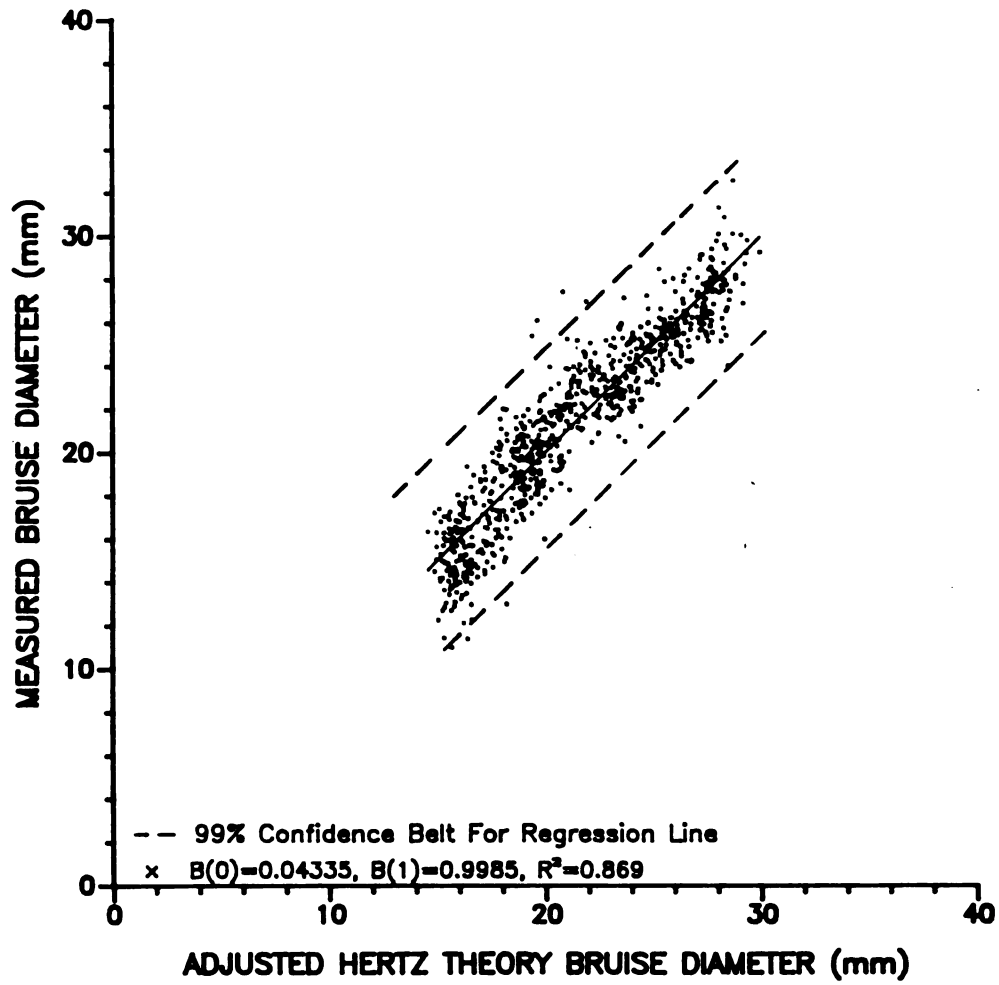


Fig. 4.13 Measured Bruise Versus Adjusted Hertz Bruise Diameters for All Ida-Red Apples.

Figure 4.14 shows the measured and adjusted Hertz bruise diameters versus maximum acceleration along with regression lines for both impacts. The regression lines are best fits through all data points for each impact and they demonstrate the closeness of fit of the adjusted Hertz bruise prediction to the measured bruise. The high coefficients of determination ($R^2 = 0.968$ and 0.975) indicate that the bruise variation about the mean is explained very well for the case of apples impacting hard and very hard surfaces. These graphs can be used to determine the predicted bruise diameter and its variations for "similar apples" and "impact conditions", by plotting the maximum acceleration sensed by the IS. In other cases where drop height or total velocity change are known, or must be estimated, Figs. 4.9 and 4.10 can be used to relate drop height and velocity change to acceleration. Figures 4.9 and 4.10 are actually based on measured maximum accelerations and calculated equivalent drop heights.

4.5 The Bruise Diameter Versus Plastic Theory

Equation [2.25] was obtained by assuming that apples have a yield point which can be determined by means of a stress/strain relation or approximated by a Magness-Taylor force reading. This theory, which relates the elastic and plastic behavior, was also tested for its performance and adequacy.

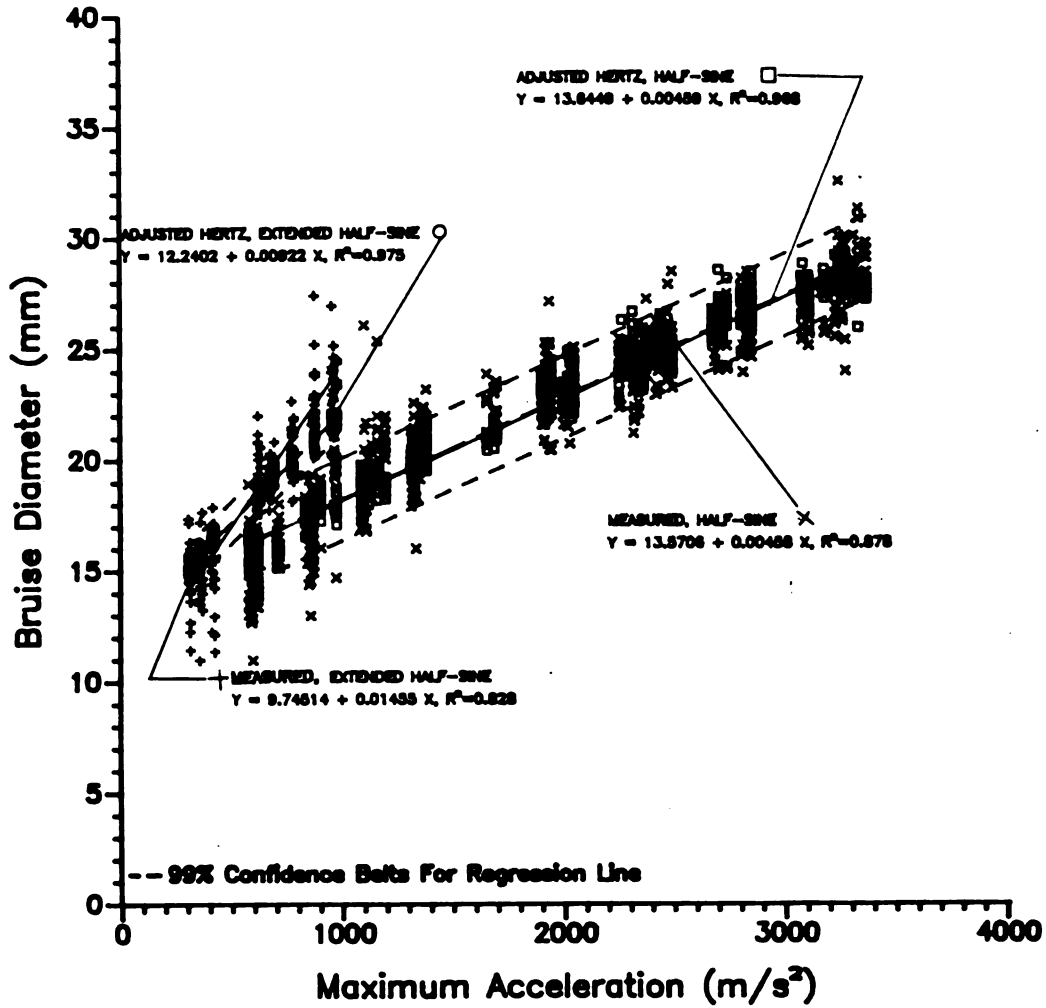


Fig. 4.14 Adjusted Hertz Theory and Measured Bruise Versus Maximum Acceleration with First Order Regression Lines.

When the predicted plastic bruise diameter was calculated and compared with measured values, the predicted bruise diameters were always larger. One reason for this behavior could be that the Magness-Taylor forces were measured with an indenter which had a curved contacting surface rather than a flat one. From Magness-Taylor force, $F = \sigma A$ with known indenter area, F is assumed to correspond to the yield point force. However, if A is larger than the assumed flat area the Magness-Taylor force measurements should be corrected by a constant factor (ratio of the curved area divided by the flat area). From equation [2.25], the increase in F will result in a decrease in bruise diameter which can explain the over estimation of this theory. Therefore, the plastic bruise diameters were corrected by a similar factor which reduced the overestimation. Figure 4.15 shows the measured bruise versus the plastic theory bruise. The coefficient of determination was $R^2 = 0.662$, so the plastic theory can only explain 66.2 percent of the variation about the mean bruise diameter. This demonstrates that the plastic theory is still inadequate. The 99 percent confidence belts about the prediction line were at ± 8.5 mm.

Figure 4.16 shows the maximum acceleration versus bruise diameter for both measured and plastic theory based calculations. However, as observed from Fig. 4.16 this theory is still over estimating the bruise diameter for the

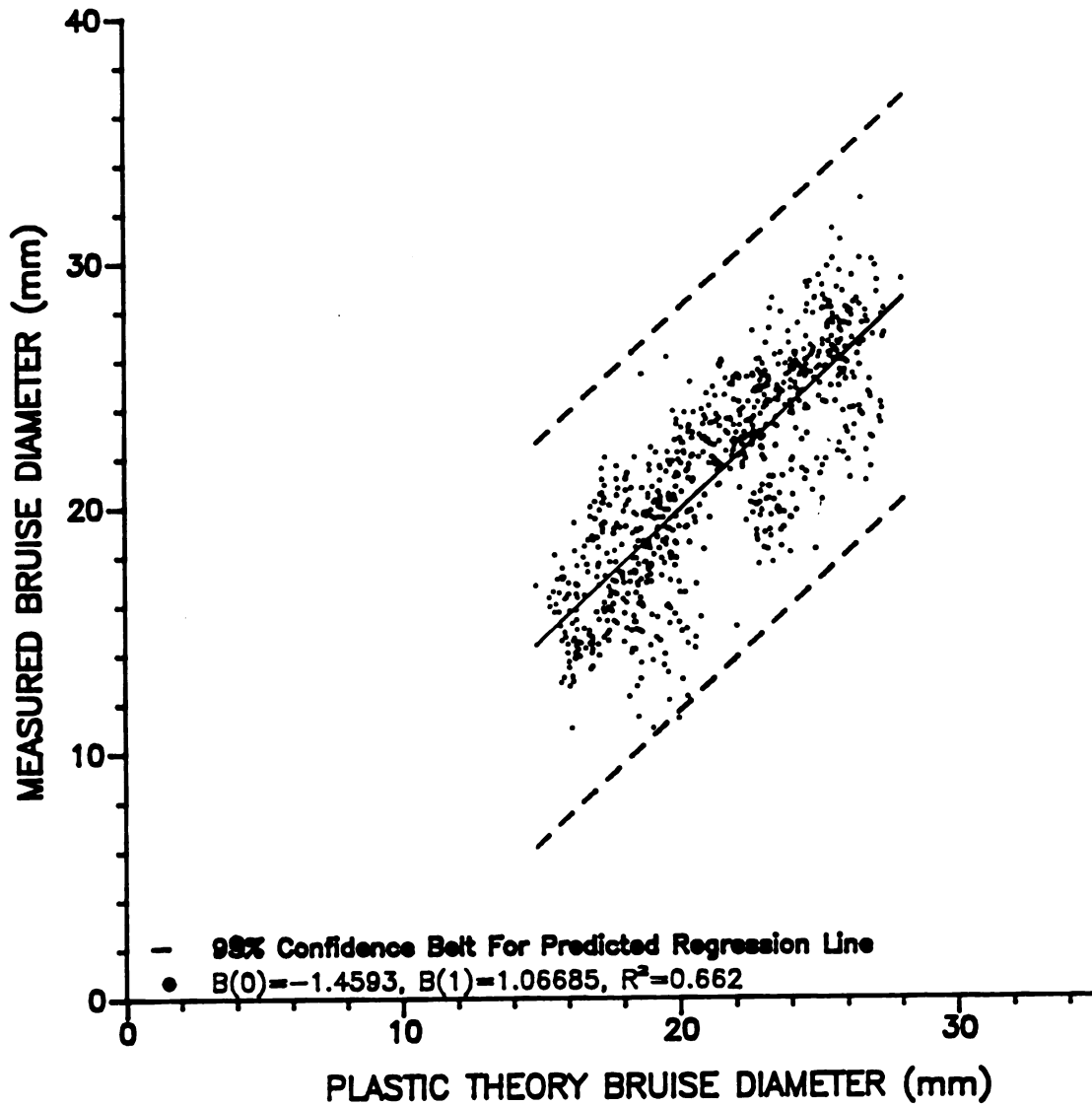


Fig. 4.15

Measured Bruise Versus Plastic Theory Based Bruise Diameters for All Apples.

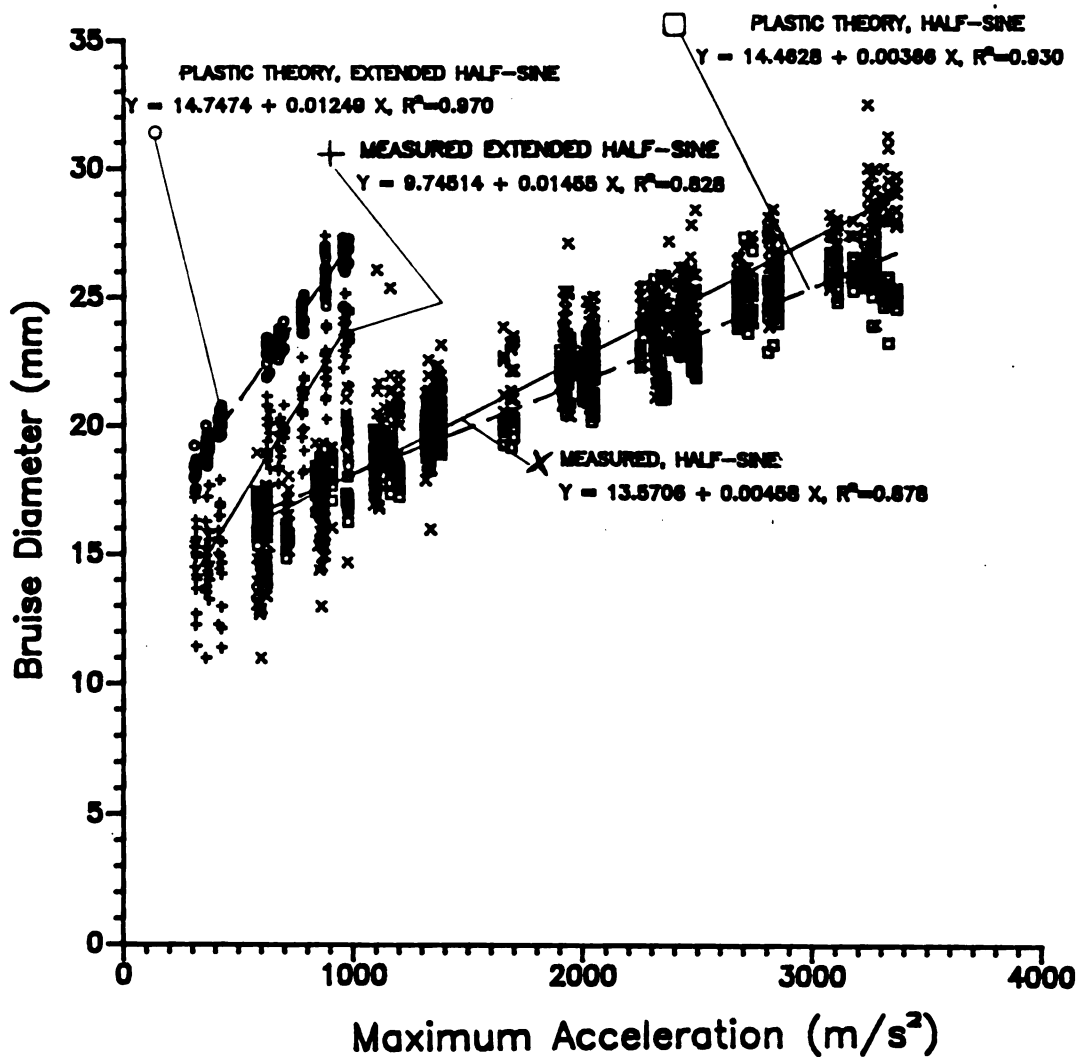


Fig. 4.16 Plastic Theory and Measured Bruise Versus Maximum Acceleration with First Order Regression Lines.

hard-surface by 25 percent and under estimating it for the very hard surface by 10 percent. These results demonstrate the lack of predictability of the plastic method.

4.6 The Bruise Diameter Versus MLRA Model

In an initial step to identify the impact parameters most highly correlated with bruise diameter for multiple linear regression analysis, the correlation coefficient matrix was calculated for all 798 cases (Appendix C.3). This showed that maximum acceleration had the highest correlation, $r = 0.859$, so that maximum acceleration alone can explain 73.8 percent of the bruise diameter variations about the mean ($R^2=0.738$). Rider et al. (1973) demonstrated that maximum acceleration could not solely explain bruising in peaches.

Since this study includes two specific types of impacts on a single variety of apples it provides an opportunity to study the affect of several parameters. In addition to Magness-Taylor, fruit diameter, mass, and drop height other parameters to account for the impact surface and impact duration had high correlation with the bruise diameter (Appendix C.2). When added to a prediction model, these variables should significantly increase the coefficient of determination.

Multiple linear regression analysis (MLRA) was performed on all 798 cases to predict the bruise diameter based on

the above measured parameters. With all parameters present a step-wise linear regression resulted in a "best model" in which average bruise diameter (ABD) was estimated by a linear second-order relation in terms of average apple diameter (AAD), apple Magness-Taylor force (MT), maximum acceleration (MA), and total velocity change (ΔV). This model is represented by the equation:

$$ABD = -15.61 + 0.371(AAD) - 0.223(MT) + 7.62E-3(MA) - 1.2E-6(MA)^2 + 0.795(\Delta V)^2$$

and the final statistics are presented in Table 4.2.

Figure 4.17 shows the measured bruise and MLRA prediction bruise for all apples and types of impact, with a coefficient of determination of, $R^2 = 0.902$. The 99 percent confidence belts are at ± 4.0 mm about the prediction line. This model is very useful and important for the IS, since impact parameters measured directly by the IS along with some apple physical parameters (average diameter and Magness-Taylor force) can predict bruise diameter with high accuracy.

The MLRA model plotted against acceleration in Fig. 4.18 results in the best fit and least deviations when compared to the previous theories. Table 4.2 lists the final statistics which indicate the least contribution to R^2 from the Magness-Taylor force parameter. However, this parameter was left in the model since even the limited range

Table 4.2 Final Statistics for the MLRA Regression Analysis.

Title: APPLE IMPACT (HALF-SINE) VS BRUISE (Ida-Red) Sep 1985
 Function: MULTIPLE LINEAR REGRESSION (MLRA)
 Data case no. 1 to 798

(AAD) Avarage Apple Diameter (mm)
 (MT) Magness-Taylor Force (Kg)
 (MA) Maximum Acceleration (m/s²)
 (MA)² Maximum Acceleration ² (m/s²)²
 ΔV Total Velocity Change ^2 (m/s)²
 (ABD) Measured Average Bruise Diameter (mm)

	Minimum	Maximum	Sum	Mean	Uncorrected Sum of Squares
(AAD)	68.75	78.25	58754.49	73.627	4.321E+6
(MT)	3.00	7.94	4119.77	5.163	22.12E+3
(MA)	05.44	3368.95	1.269E+9	1589.974	2.67E+9
(MA) ²	93.3E+3	11.35E+6	2.67E+9	4.34E+6	17.55E+15
(ΔV) ²	0.88	8.05	2654.48	3.326	11.67E+3
(ABD)	11.00	32.55	16997.98	21.301	376.5E+3

798 cases read 0 missing cases discarded

Correlation Matrix

	2	3	4	5	6	1
2	1.000					
3	0.676	1.000				
4	-0.278	-0.333	1.000			
5	-0.227	-0.295	0.978	1.000		
6	0.094	0.075	0.590	0.624	1.000	
1	-0.075	-0.179	0.888	0.851	0.739	1.000

Variable Number	Regression Coefficient	Standard Error	Std. Partial Regr. Coeff.	Std. Err. of Partial Coef	Student T value	Prob
2	3.7119E-01	3.4382E-02	0.1665E+00	1.5422E-02	10.796	.00
3	-2.2290E-01	6.4694E-02	-.5414E-01	1.5715E-02	-3.445	.00
4	7.6165E-03	2.6479E-04	0.1615E+01	5.6153E-02	28.764	.00
5	-1.2012E-06	7.3456E-08	-.9271E+00	5.6695E-02	-16.352	.00
6	7.9465E-01	3.4455E-02	0.3522E+00	1.5271E-02	23.067	.00

Intercept = -15.61549

Coefficient of Determination (R-Square) = 0.902
 Adjusted R-Square = 0.902
 Multiple R = 0.950
 Standard Err of Est. = 1.337

ANALYSIS OF VARIANCE TABLE

	Sum of Squares	df	Mean Square	F	Signif
Regression	13060.498000	5	2612.09960	1461.42	.000
Residual	1415.595700	792	1.78737		
Total	14476.093800	797			

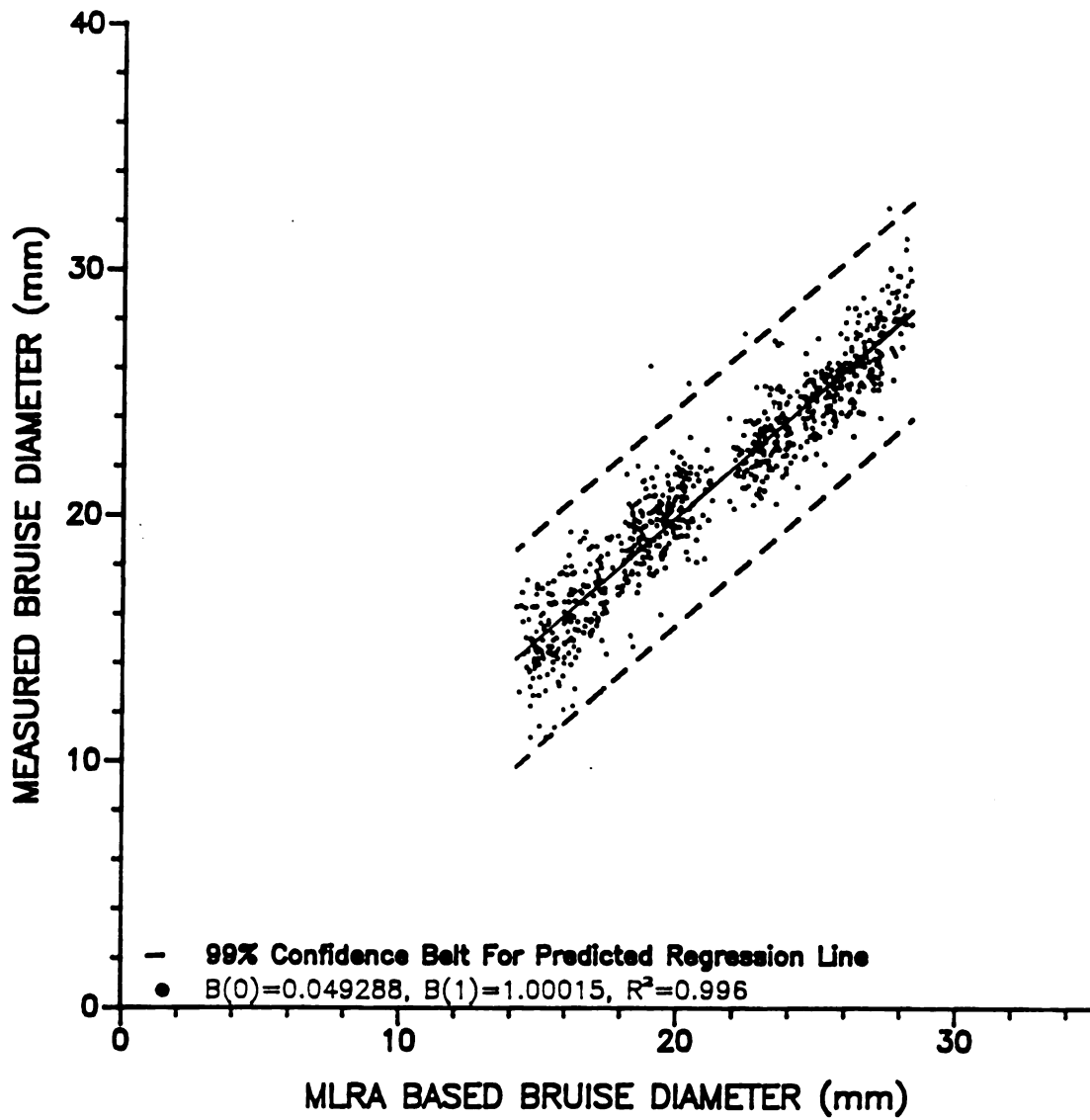


Figure 4.17 Measured Bruise Versus MLRA Prediction Based Bruise Diameters for All Apples.

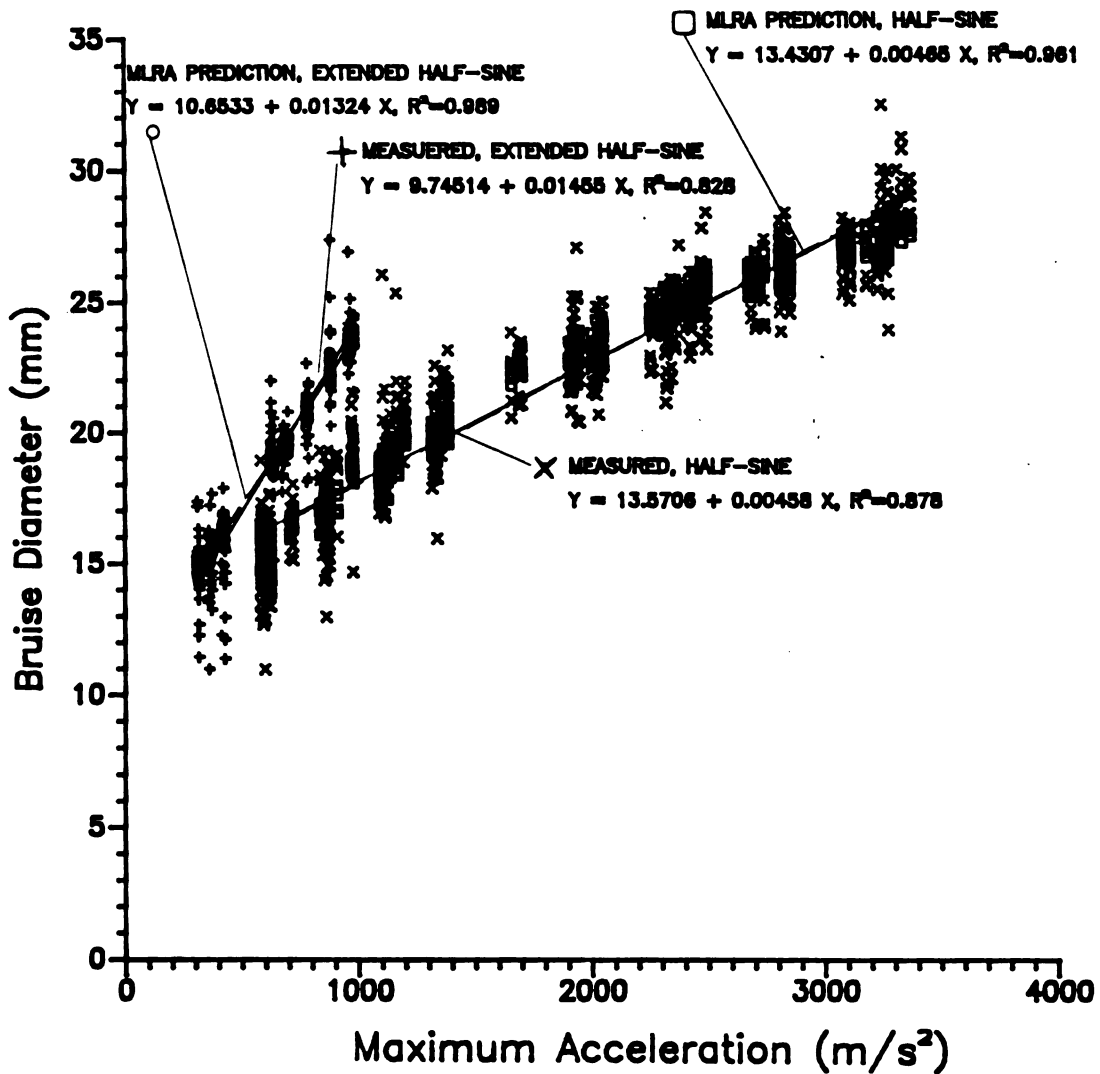


Figure 4.18

MLRA Prediction and Measured Bruise Versus Maximum Acceleration with First Order Regression Lines.

of Magness-Taylor values measured in these tests resulted in significantly different bruise diameters as shown in the analysis of variance. For studies with more extensive variations in Magness-Taylor it is likely that the model will depend critically on this parameter.

4.7 Comparison Among Models

Table 4.3 lists the differences between the four approaches to bruise prediction. A comparison among these models based on closeness of fit to measured data, ranks the MLRA estimate as the best approach followed closely by the adjusted Hertz. The plastic approach does not predict as well as the other two methods, which suggests rejecting the initial assumption that apples have a yield point approximated by the Magness-Taylor force values. It is possible that the Magness-Taylor values used to obtain the yield point stress were not accurately measured. More emphasis should be placed on this measurement, and a more accurate method should be used to obtain the stress-strain deformation before applying the plastic theory.

The MLRA, as well as the adjusted Hertz theory, appear to be very useful methods in bruise diameter prediction. The MLRA is more valuable as mentioned before, since both impact variables (maximum acceleration and total velocity change) can be measured directly by the IS, and its prediction ability is better (higher R^2 , narrower confidence

Table 4.3 Comparison Among All Prediction Methods Based on a First Order Prediction for Bruise Diameter.

Prediction Model	$\beta(0)$	$\beta(1)$	R^2	99 percent Conf. Belt
Hertz Theory	-6.1076	1.02944	0.656	± 7.0
Adjusted Hertz	0.0433	0.99850	0.869	± 4.0
Plastic Theory	-1.4593	1.06685	0.662	± 6.0
MLRA Model	0.0493	0.99792	0.902	± 3.0

$$(\text{Measured Bruise Diameter}) = \beta(0) + \beta(1)(\text{Predicted Bruise})$$

belts). The adjusted Hertz method requires that the equivalent drop height, which becomes a function of the impacting surface, has to be calculated based on the impact information obtained by the IS.

In summary, Table 4.4 lists all the prediction equations used in the Hertz theory, the adjusted Hertz theory, the plastic theory and the MLRA model with their respective parameters.

Table 4.4 Bruise Diameter Prediction Methods and Their Parameters Along with Respective Formulations.

Bruise Prediction Method	Apple Diameter (AAD) D	Apple Mass (AM) W	Magness Taylor (MT) F	Drop Height (EDH) H	Maximum Acceleration (MA)	(MA) ²	(ΔV) ²	$\frac{MA}{\Delta V}$ (ψ _n)
Hertz Theory (D ₁)	X	X	X	X				
Adjusted Hertz (D ₂)	X	X	X	X				X
Plastic Theory (D ₃)	X	X	X	X				
MLRA Model (D ₄)	X		X		X	X	X	X

$$D_1 = 4.624 (W_1 H)^{1/5} \left(\frac{D_1}{2} \right)^{2/5} F_1^{-1/5}$$

$$D_2 = \frac{MA}{\Delta V} D_1$$

$$D_3 = 5.63 \left(\frac{HWD}{F} \right)^{1/4}$$

$$D_4 = -15.615 + 0.3712(AM) - 0.233(MT) + 7.62 \times 10^{-6}(MA) - 1.2 \times 10^{-3}(MA)^2 + 7.616 \times 10^{-3}(\Delta V)^2$$

5. SUMMARY

The primary goals of this research were: 1) to develop and evaluate a data acquisition system in the form of an instrumented box and eventually develop an instrumented sphere (IS) capable of measuring and storing triaxial impact accelerations (accelerations versus time curve along with time of occurrence), and 2) to obtain an accurate bruise size prediction model based on the IS recording and measured parameters for single impact bruises.

Triaxial accelerometers were used as inputs to a microcontroller-based data acquisition system that stores accelerations above a preset threshold level. The sampling frequency is adjustable up to 4.25 kHz and the amplitude can be adjusted for up to $\pm 2550 \text{ m/s}^2$ ($\pm 262 \text{ g}$). This system was calibrated for both single axes and resultant vector sum of triaxial accelerations. The calibration factors are 2.124 and 2.073 (digital count/g), respectively, and the maximum error is $\pm 4.35 \text{ g}$ for 99 percent confidence limits. The stored data and time of occurrence of each impact are retrieved through a serial communication port for further analysis.

An impact table was used to produce two types of

impacts representing a "very-hard" and a "hard-surface". Ida-Red apples were used to establish bruise relations for the IS in terms of a bruise diameter prediction equation based on apple, surface and impact data.

A prediction model was obtained by step-wise multiple linear regression which can predict bruise diameter with $R^2 = 0.902$. Thus, over 90 percent of the bruise diameter variation about the mean can be explained by the model. Critical parameters were identified to predict bruise diameter based on apple diameter, apple Magness-Taylor force, maximum acceleration and total velocity change. This model was compared with both viscoelastic and plastic theory. Standard Hertz theory could only account for 65.6 percent of the bruise diameter variation about the mean. As a result, an adjusted Hertz theory (viscoelastic) was developed which can predict and account for 86.9 percent of the bruise diameter variation about the mean. The plastic theory only accounted for 66 percent of the bruise diameter variation about the mean.

When fully developed, the IS data acquisition system can be used to record maximum acceleration and total velocity change to predict and reduce damage to agricultural products as well as other easily damaged articles. The IS has a high potential for accurate drop height measurements on various surfaces when calibrated properly, and it could easily be adjusted to sense impacts up to $\pm 73000 \text{ m/s}^2$ ($\pm 750 \text{ g}$).

6. CONCLUSIONS

1. A data acquisition system was successfully designed and conceptually tested which can sense, store and output on command the acceleration-time history of a series of impact events in the range of ± 2500 m/s² (± 262 g) for impact conditions in which the total duration is greater than 1.0 ms.
2. Based on measured impact accelerations, 99 percent of the output accelerations that the IS calculated as a resultant vector were within ± 5.5 percent of the measured input values.
3. The frequency and phase response of the cast resin IS resulted in less than 5 percent distortion between the surface-input and center-sensed accelerations.
4. Hertz theory, when adjusted for impact duration, was used to predict bruise diameter and resulted in a coefficient of determination $R^2 = 0.869$, which accounts for 86.9 percent of the bruise variations about the mean for Ida-Red apples.
5. A MLRA bruise diameter prediction model was developed based on apple diameter, Magness-Taylor force,

maximum acceleration and total velocity change. The model explained 90.2 percent of the variation in bruise diameter about the mean diameter ($R^2 = 0.902$) for Ida-Red apples.

6. Apple bruise diameter increased with an increase maximum acceleration, total velocity change, drop height and apple diameter but it decreased with an increase in Magness-Taylor force (apple firmness).
7. The IS data acquisition system appears to meet the design criteria. When further developed it should provide needed insight into bruise prediction and bruise reduction for fruits, vegetables, and damage reduction for non-food articles that are easily damaged during impacts.

7. RECOMMENDATIONS FOR FUTURE RESEARCH

Based on results and experiences of this research, my recommendations for future research include:

1. The apples tested in this research had low Magness-Taylor force readings, as a result of using the Ida-Red variety and poor storage conditions. In order to expand the bruise prediction model more varieties having a broader range of Magness-Taylor force should be tested.

2. The Magness-Taylor force values are not adequate for estimating the modulus of elasticity, which is a critical factor in all of the bruise diameter prediction approaches studied. Thus, other methods should be used to obtain the strain and stress values as well as the rate of loading.

3. The impact table would be more useful if the acceleration and duration could be set for the exact condition that apples would encounter when dropped on typical handling materials. The actual conditions should be determined, and those table settings used.

4. The IS system could predict drop heights if a series of calibration curves were obtained for various surfaces such that impact duration could be used to select appropriate adjustment factors. The prediction of drop height should be pursued.

8. APPENDICES

A.1 Physical Properties Of Casting Material

A.1 Physical Properties Of Casting Material

AD-TECH PLASTIC SYSTEMS CORP.

P O Box 437
815 Shepherd Street
Charlotte, Michigan 48813
Phone: 517/543-7810

PRODUCT BULLETIN

EC-420
WATER WHITE CLEAR EPOXY
CASTING RESIN

DESCRIPTION

EC-420 CLEAR EPOXY CASTING RESIN is a water clear, two part epoxy compound. This compound couples a long pot life with low exotherm to produce a glass-like object with excellent thermal and mechanical shock characteristics.

USES

General purpose clear resin for casting or embedding objects for decoration, electrical or mechanical applications.

HANDLING

Mix Ratio: (by weight).....2R/1H
(by volume).....5R/3H
Viscosity, cps.....500-1000
Pot Life, 1 lb. @ 25°C/77°F.....5-6 hours
Peak Exotherm, 1 lb. @ 25°C/77°F.....78°C/173°F
Cure, 25°C/77°F.....18-24 hours
Plus Post Cure, 65°C/149°F2 hours
Alternate Cure, 25°C/77°F.....3-5 days

PROPERTIES

Hardness Shore D.....D-70
Tensile Strength, psi.....6000
Elongation, (%).....10
Volume Resistivity, ohm - cm..... 2.5×10^{16}
Dielectric Strength, v/mil.....485

A.2 Accelerometer Calibration Charts

A.2 Accelerometer Calibration Charts



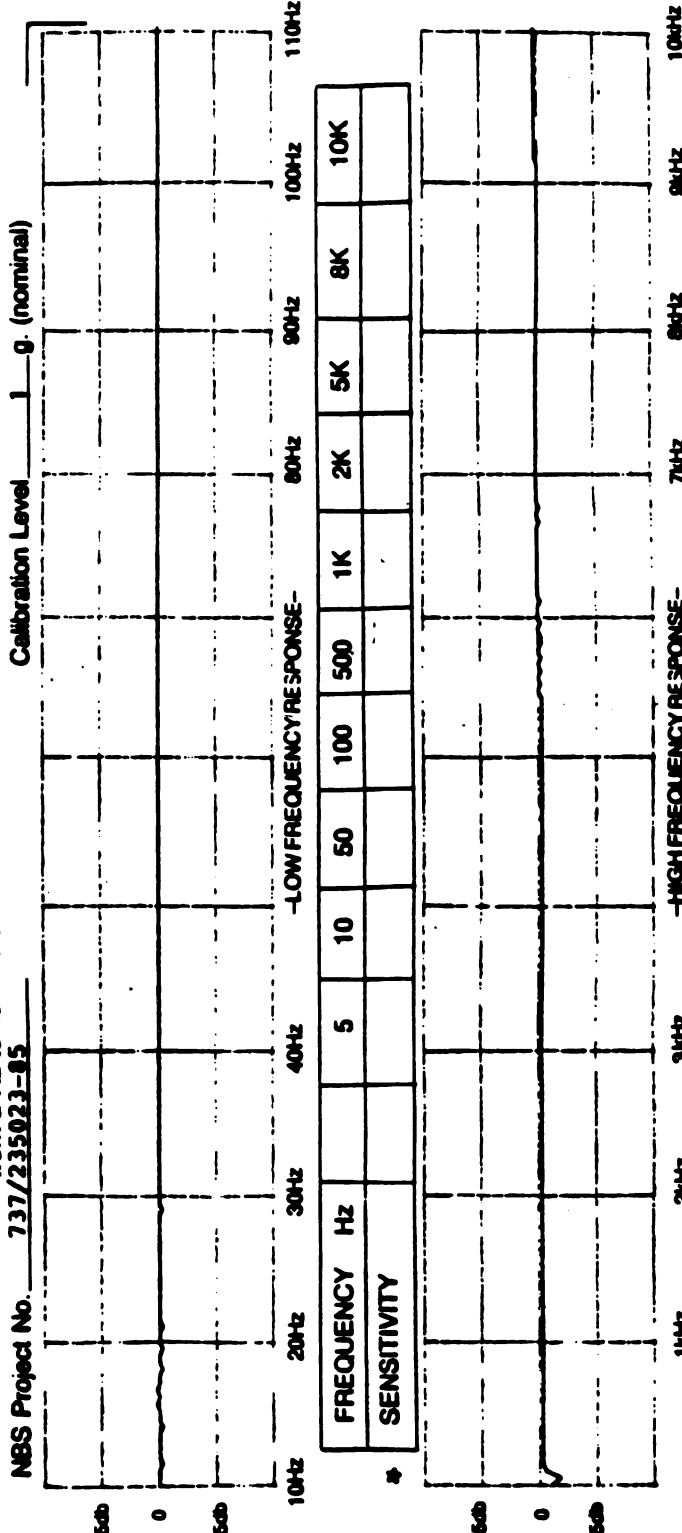
ACCELEROMETER CALIBRATION DATA

Model No. 3112 By WLD
 Serial No. 12 Date 10/2/45

TYPICAL SPECIFICATIONS

Basic Sensitivity 10 μ m/g @100Hz (measured)
 Noise Floor 0.002 mv/rms (typical)
 Resonant Frequency >55 kHz (typical)
 Transverse Sen. 5 % (measured)
 Time Constant — sec.
 Temperature (Max.) 250 °F
 Mounting Torque 5 in./lbs.
 Accelerometer Capacitance — pfd

All Vibra-Metrics Inc. calibration data is traceable to NBS at selected frequencies from 2 Hz to 10 KHz and conforms to MIL-STD 45662 and MIL-Q9858



* Note: Point to point sensitivity used in special NBS certified calibration only

Special Notes: _____



ACCELEROMETER CALIBRATION DATA

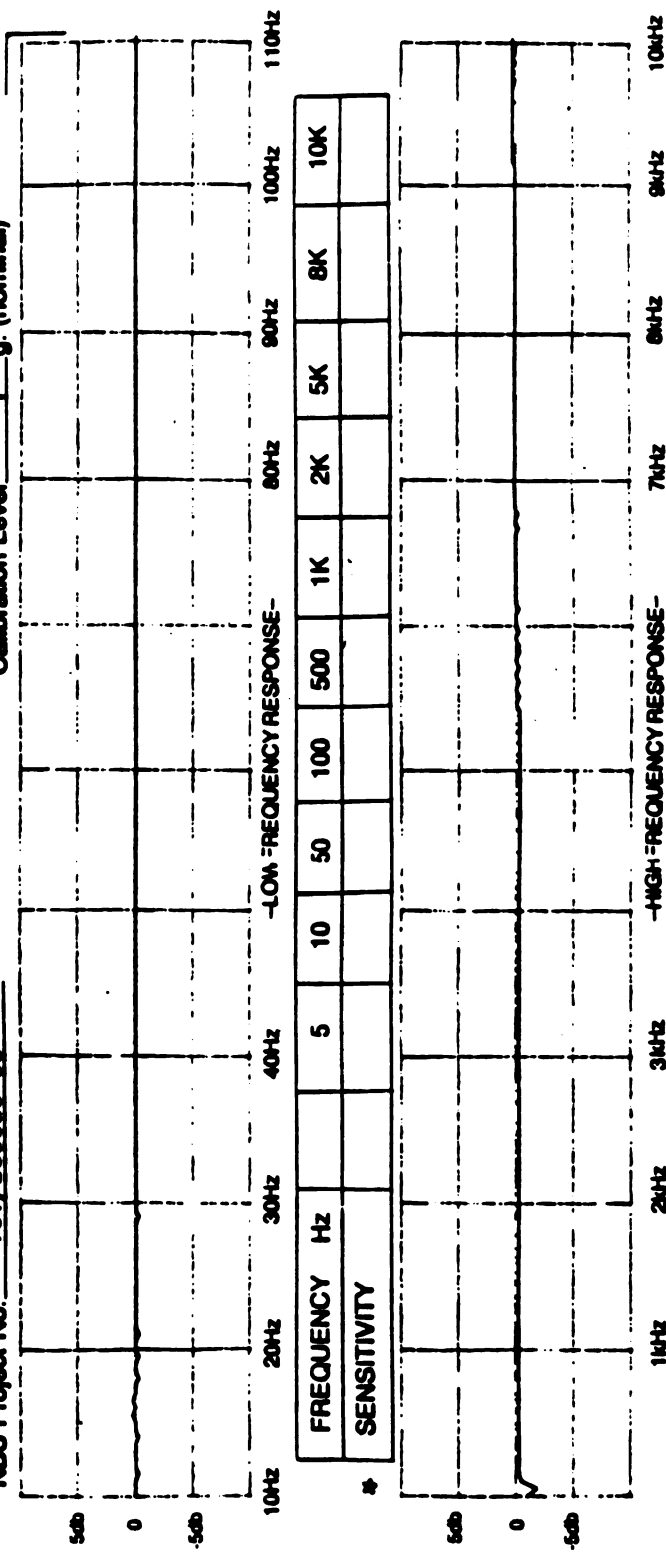
Model No. 3132 By CV AXI
 Serial No. 12 Date 2-2-68

TYPICAL SPECIFICATIONS

Basic Sensitivity 9.9 mv/g @100Hz (measured)
pc/g @ 100Hz (measured)
 Resonant Frequency >6.5 kHz (typical)
 Noise Floor .002 mv/rms (typical)
 Frequency Response 3 Hz to 10 kHz $\pm 5\%$
 Transverse Sen. 5 % (measured)
 Max. Accel. w/o Clipping 250 g
 Time Constant — sec.
 Max. Shock w/o Damage 10,000 g
 Temperature (Max.) 250 °F
 Bias Level 4-6 volts
 Mounting Torque 5 in./lbs.
 Power Supply 8-24 Volts, 0.5-1 ma
 Accelerometer Capacitance — pfd

All Vibra-Metrics Inc. calibration data is traceable to NBS at selected frequencies from 2 Hz to 10 KHz and conforms to MIL-STD 45662 and MIL-Q9858

NBS Project No. 737/235023-85 Calibration Level 1 g. (nominal)



Special Notes: —
 † Note: Point to point sensitivity used in special NBS certified calibration only. enc:ems



ACCELEROMETER CALIBRATION DATA

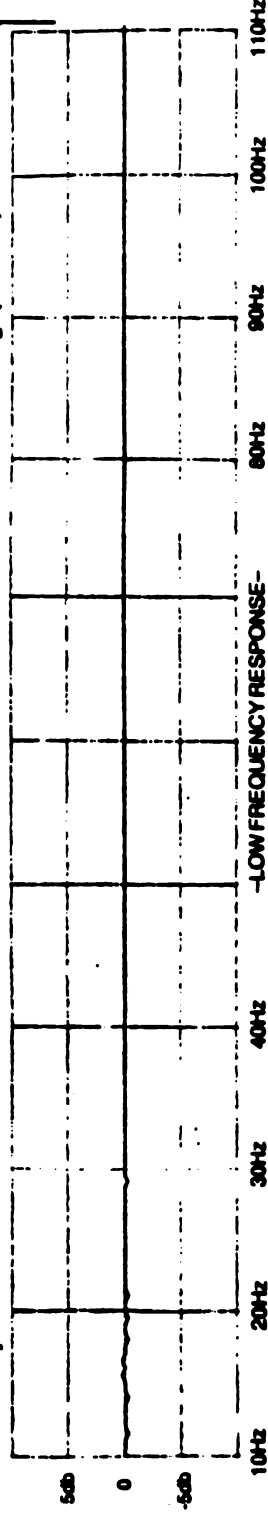
Model No. 3132 By LLD
 Serial No. 12 Date 12/21/5

TYPICAL SPECIFICATIONS

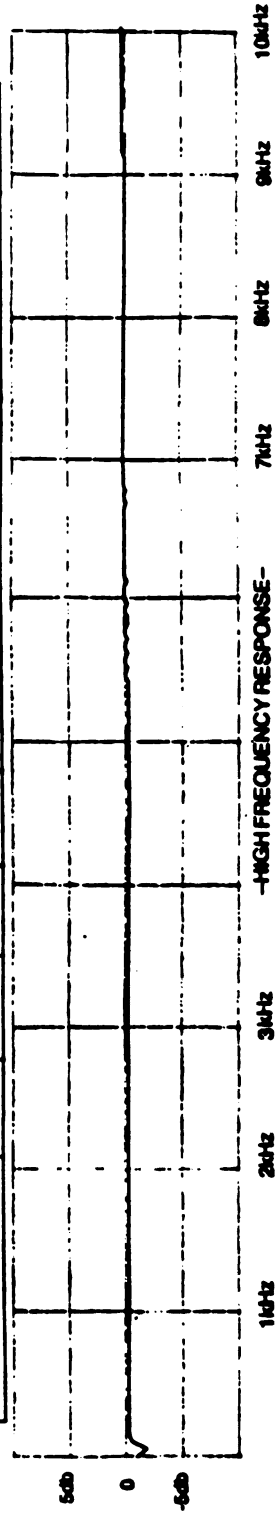
Basic Sensitivity 7.9 mV/g @ 100Hz (measured)
pc/g @ 100Hz (measured)
 Resonant Frequency > 6.5 kHz (typical)
 Noise Floor .002 mV/rms (typical)
 Transverse Sen. 5 % (measured)
 Time Constant — sec.
 Temperature (Max.) 250 °F
 Mounting Torque 5 in./lbs.
 Accelerometer Capacitance — pfd

All Vibra-Metrics Inc. calibration data is traceable to NBS at selected frequencies from 2 Hz to 10 KHz and conforms to MIL-STD 45662 and MIL-C8858

NBS Project No. 737/235023-85 Calibration Level 1 g. (nominal)



FREQUENCY Hz	-LOW FREQUENCY RESPONSE-									
	5	10	50	100	500	1K	2K	5K	8K	10K
SENSITIVITY										



* Note: Point to point sensitivity used in special NBS certified calibration only

Special Notes: _____

PCB

PIEZOTRONICS

394A04 SYSTEM

CALIBRATION DATA

ICP ACCELEROMETER (per ISA-CP 37.2)

Model No. 301A03/402A03

Serial No. 395/902

By *R. J. [Signature]*

Date 3/22/85

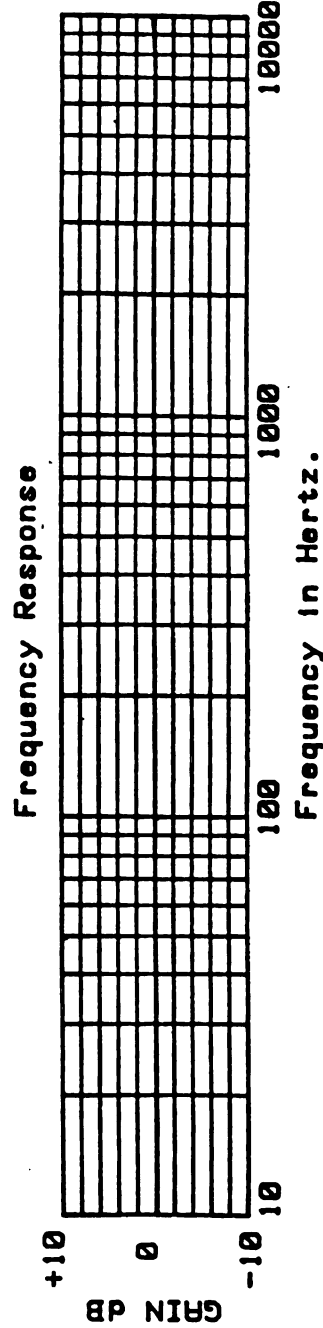
Voltage sensitivity: 10.00 mV/g
 Transverse sensitivity: 1.3 %
 Resolution: 0.01 g
 Output bias level: 12.9 V

Resonant Frequency: 60 kHz
 Time constant: 0.6 s
 Maximum temperature: 150 °F
 Range: 500 ± g

The Calibration procedure of PCB Piezotronics is in compliance with MIL-STD-45662.

Freq. Hz	20	30	50	100	300	500	1000	3000	5000	7000	10000
Deviation %	-0.5	-0.2	0.0	0.0	0.3	0.3	0.5	0.7	1.1	0.3	1.8

Calibration traceable to NBS through project no. 737/234009-85



PCB PIEZOTRONICS, INC. 3425 Malden Avenue Depew, New York 14043-2495

A.3 Microcontroller Specifications

A.3 Microcontroller Specifications

The following tables are copied from INTEL (1986).



MCS²-96
809X-90, 839X-90

PERFORMANCE

ELECTRICAL CHARACTERISTICS ABSOLUTE MAXIMUM RATINGS*

Ambient Temperature Under Bias . . . 0°C to +70°C
Storage Temperature -40°C to +150°C
Voltage from Any Pin to
VSS or ANGND -0.3V to +7.0V
Average Output Current from Any Pin.10 mA
Power Dissipation1.5 Watts

*NOTICE: Stresses above those listed under "Absolute Maximum Ratings" may cause permanent damage to the device. This is a stress rating only and functional operation of the device at these or any other conditions above those indicated in the operational sections of this specification is not implied. Exposure to absolute maximum rating conditions for extended periods may affect device reliability.

OPERATING CONDITIONS

Symbol	Parameter	Min	Max	Units
TA	Ambient Temperature Under Bias	0	+70	C
VCC	Digital Supply Voltage	4.50	5.50	V
VREF	Analog Supply Voltage	4.5 VCC - 0.3	5.5 VCC + 0.3	V V
fOSC	Oscillator Frequency	6.0	12	MHz
VPD	Power-Down Supply Voltage	4.50	5.50	V

V_{DD} should be connected to ANGND through a 0.01 μ F capacitor. ANGND and VSS should be nominally at the same potential.

DC CHARACTERISTICS

Symbol	Parameter	Min	Max	Units	Test Conditions
VIL	Input Low Voltage (Except $\overline{\text{RESET}}$)	-0.3	+0.8	V	
VIL1	Input Low Voltage, $\overline{\text{RESET}}$	-0.3	+0.7	V	
VIH	Input High Voltage (Except $\overline{\text{RESET}}$, NMI, XTAL1)	2.0	VCC + 0.5	V	
VIH1	Input High Voltage, $\overline{\text{RESET}}$ Rising	2.4	VCC + 0.5	V	
VIH2	Input High Voltage, $\overline{\text{RESET}}$ Falling	2.1	VCC + 0.5	V	
VIH3	Input High Voltage, NMI, XTAL1	2.4	VCC + 0.5	V	
VOL	Output Low Voltage		0.45	V	See Note 1.
VOH	Output High Voltage	2.4		V	See Note 2.
ICC	VCC Supply Current		200	mA	All outputs disconnected.
IPD	VPD Supply Current		1	mA	Normal operation and Power-Down.
IREF	VREF Supply Current		8	mA	
ILI	Input Leakage Current to all pins of HSI, P0, P3, P4, and to P2.1.		± 10	μ A	Vin = 0 to VCC See Note 3
IIH	Input High Current to $\overline{\text{EA}}$		100	μ A	VIH = 2.4V
IIL	Input Low Current to all pins of P1, and to P2.6, P2.7.		-100	μ A	VIL = 0.45V
IIL1	Input Low Current to $\overline{\text{RESET}}$		-2	mA	VIL = 0.45V
IIL2	Input Low Current P2.2, P2.3, P2.4, READY		-50	μ A	VIL = 0.45V
Cs	Pin Capacitance (Any Pin to VSS)		10	pF	fTEST = 1 MHz

NOTES:

1. IOL = 0.36 mA for all pins of P1, for P2.6 and P2.7, and for all pins of P3 and P4 when used as ports.
IOL = 2.0 mA for TXD, RXD (in serial port mode 0), PWM, CLKOUT, ALE, $\overline{\text{BHE}}$, RD, WR, and all pins of HSO and P3 and P4 when used as external memory bus (AD0-AD15).
2. IOH = -20 μ A for all pins of P1, for P2.6 and P2.7
IOH = -200 μ A for TXD, RXD (in serial port mode 0), PWM, CLKOUT, ALE, $\overline{\text{BHE}}$, $\overline{\text{WR}}$, and all pins of HSO and P3 and P4 when used as external memory bus (AD0-AD15).
P3 and P4, when used as ports, have open-drain outputs.
3. Analog Conversion not in process.



MCS⁺-96
809X-90, 839X-90

PRELIMINARY

A/D CONVERTER SPECIFICATIONS

A/D Converter operation is verified only on the 8097, 8397, 8095, 8395.

The absolute conversion accuracy is dependent on the accuracy of VREF. The specifications given below assume adherence to the Operating Conditions section of these data sheets. Testing is done at VREF = 5.120 volts.

Resolution ± 0.001 VREF
Accuracy ± 0.004 VREF
Differential nonlinearity. ± 0.002 VREF max
Integral nonlinearity ± 0.004 VREF max
Channel-to-channel matching. ± 1 LSB
Crosstalk (DC to 100 kHz) -60 dB max

AC CHARACTERISTICS (VCC, VPD = 4.5 to 5.5 Volts; T_A = 0°C to 70°C; fosc = 6.0 to 12.0 MHz)

Test Conditions: Load capacitance on output pins = 80 pF
Oscillator Frequency = 12.00 MHz

Timing Requirements (other system components must meet these specs)

Symbol	Parameter	Min	Max	Units
TCLYX	READY Hold after CLKOUT falling edge	0 (1)		nsec
TLLYV	End of ALE to READY Setup	- T _{osc}	2T _{osc} - 60	nsec
TLLYH	End of ALE to READY high	2 T _{osc} + .60	4T _{osc} - 60 (2)	nsec
TYLYH	Non-ready time		1000	nsec
TAVDV	Address Valid to Input Data Valid		5T _{osc} - 90	nsec
TRLDV	RD/Active to Input Data Valid		3T _{osc} - 60	nsec
TRXDZ	Data Hold after RD/inactive (3)	0		nsec
TRXDZ	RD/Inactive to Input Data Float (3)		T _{osc} - 20	nsec

Timing Responses (MCS-96 parts meet these specs)

Symbol	Parameter	Min	Max	Units
FXTAL	Oscillator Frequency	6.00	12.00	MHz
Tosc	Oscillator Period	83	166	nsec
TCHCH	CLKOUT Period (3)	3T _{osc} (4)	3T _{osc} (4)	nsec
TCHCL	CLKOUT High Time	T _{osc} - 20	T _{osc} + 20	nsec
TCLLH	CLKOUT Low to ALE High	- 5	20	nsec
TLLCH	ALE Low to CLKOUT High	T _{osc} - 20	T _{osc} + 40	nsec
TLHLL	ALE Pulse Width	T _{osc} - 25	T _{osc} + 15	nsec
TAVLL	Address Setup to End of ALE	T _{osc} - 50		nsec
TLLRL	End of ALE to RD/ or WR/ active	T _{osc} - 20		nsec
TLLAX	Address hold after End of ALE	T _{osc} - 20		nsec
TWLWH	WR/ Pulse Width	2T _{osc} - 35		nsec
TQVWX	Output Data Setup to End of WR/	2T _{osc} - 60		nsec
TWXQX	Output Data Hold after End of WR/	T _{osc} - 25		nsec
TWXLH	End of WR/ to next ALE	2T _{osc} - 30		nsec
TRLRH	RD/ Pulse Width	3T _{osc} - 30		nsec
TRHLH	End of RD/ to next ALE	T _{osc} - 25		nsec

NOTES:

1. If the 48-pin part is being used then this timing can be generated by assuming that the CLKOUT falling edge has occurred at 2T_{osc} + 60 (TLLCH(max) + TCHCL(max)) after the falling edge of ALE.
2. If more than one wait state is desired, add 3T_{osc} for each additional wait state.
3. This specification is not tested, but is verified by design analysis and/or derived from other tested parameters.
4. CLKOUT is directly generated as a divide by 3 of the oscillator. The period will be 3T_{osc} +/- 10 nsec if T_{osc} is constant and the rise and fall times on XTAL 1 are less than 10 nsec.



Figure 2-5. Instruction Summary

Mnemonic	Operands	Operation (Note 1)	Flags						Notes
			Z	N	C	V	VT	ST	
ADD/ADDB	2	$D \leftarrow D + A$	✓	✓	✓	✓	↑	—	
ADD/ADDB	3	$D \leftarrow B + A$	✓	✓	✓	✓	↑	—	
ADDC/ADDCB	2	$D \leftarrow D + A + C$	↓	✓	✓	✓	↑	—	
SUB/SUBB	2	$D \leftarrow D - A$	✓	✓	✓	✓	↑	—	
SUB/SUBB	3	$D \leftarrow B - A$	✓	✓	✓	✓	↑	—	
SUBC/SUBCB	2	$D \leftarrow D - A + C - 1$	↓	✓	✓	✓	↑	—	
CMP/CMPB	2	$D - A$	✓	✓	✓	✓	↑	—	
MUL/MULU	2	$D, D + 2 \leftarrow D * A$	—	—	—	—	—	?	2
MUL/MULU	3	$D, D + 2 \leftarrow B * A$	—	—	—	—	—	?	2
MULB/MULUB	2	$D, D + 1 \leftarrow D * A$	—	—	—	—	—	?	3
MULB/MULUB	3	$D, D + 1 \leftarrow B * A$	—	—	—	—	—	?	3
DIV/DIVU	2	$D \leftarrow (D, D + 2) / A$ D + 2 remainder	—	—	—	✓	↑	—	2
DIVB/DIVUB	2	$D \leftarrow (D, D + 1) / A$ D + 1 remainder	—	—	—	✓	↑	—	3
AND/ANDB	2	$D \leftarrow D \text{ and } A$	✓	✓	0	0	—	—	
AND/ANDB	3	$D \leftarrow B \text{ and } A$	✓	✓	0	0	—	—	
OR/ORB	2	$D \leftarrow D \text{ or } A$	✓	✓	0	0	—	—	
XOR/XORB	2	$D \leftarrow D \text{ (excl. or) } A$	✓	✓	0	0	—	—	
LD/LDB	2	$D \leftarrow A$	—	—	—	—	—	—	
ST/STB	2	$A \leftarrow D$	—	—	—	—	—	—	
LDBSE	2	$D \leftarrow A; D + 1 \leftarrow \text{SIGN}(A)$	—	—	—	—	—	—	3,4
LDBZE	2	$D \leftarrow A; D + 1 \leftarrow 0$	—	—	—	—	—	—	3,4
PUSH	1	$SP \leftarrow SP - 2; (SP) \leftarrow A$	—	—	—	—	—	—	
POP	1	$A \leftarrow (SP); SP \leftarrow SP + 2$	—	—	—	—	—	—	
PUSHF	0	$SP \leftarrow SP - 2; (SP) \leftarrow \text{PSW};$ $\text{PSW} \leftarrow 0000H$ $I \leftarrow 0$	0	0	0	0	0	0	
POPF	0	$\text{PSW} \leftarrow (SP); SP \leftarrow SP + 2; I \leftarrow \checkmark$	✓	✓	✓	✓	✓	✓	
SJMP	1	$PC \leftarrow PC + 11\text{-bit offset}$	—	—	—	—	—	—	5
LJMP	1	$PC \leftarrow PC + 16\text{-bit offset}$	—	—	—	—	—	—	5
BR(indirect)	1	$PC \leftarrow (A)$	—	—	—	—	—	—	
SCALL	1	$SP \leftarrow SP - 2; (SP) \leftarrow PC;$ $PC \leftarrow PC + 11\text{-bit offset}$	—	—	—	—	—	—	5
LCALL	1	$SP \leftarrow SP - 2; (SP) \leftarrow PC;$ $PC \leftarrow PC + 16\text{-bit offset}$	—	—	—	—	—	—	5
RET	0	$PC \leftarrow (SP); SP \leftarrow SP + 2$	—	—	—	—	—	—	
J(conditional)	1	$PC \leftarrow PC + 8\text{-bit offset}$	—	—	—	—	—	—	5
JC	1	Jump if C = 1	—	—	—	—	—	—	5
JNC	1	Jump if C = 0	—	—	—	—	—	—	5

Note

1. If the mnemonic ends in "B", a byte operation is performed, otherwise a word operation is done. Operands D, B, and A must conform to the alignment rules for the required operand type. D and B are locations in the register file; A can be located anywhere in memory.
2. D, D + 2 are consecutive WORDS in memory. D is DOUBLE-WORD aligned.
3. D, D + 1 are consecutive BYTES in memory; D is WORD aligned.
4. Changes a byte to a word.
5. Offset is a 2's complement number.



Mnemonic	Operands	Operation (Note 1)	Flags						Notes
			Z	N	C	V	VT	ST	
JE	1	Jump if Z = 1	—	—	—	—	—	—	5
JNE	1	Jump if Z = 0	—	—	—	—	—	—	5
JGE	1	Jump if N = 0	—	—	—	—	—	—	5
JLT	1	Jump if N = 1	—	—	—	—	—	—	5
JGT	1	Jump if N = 0 and Z = 0	—	—	—	—	—	—	5
JLE	1	Jump if N = 1 or Z = 1	—	—	—	—	—	—	5
JH	1	Jump if C = 1 and Z = 0	—	—	—	—	—	—	5
JNH	1	Jump if C = 0 or Z = 1	—	—	—	—	—	—	5
JV	1	Jump if V = 1	—	—	—	—	—	—	5
JNV	1	Jump if V = 0	—	—	—	—	—	—	5
JVT	1	Jump if VT = 1; Clear VT	—	—	—	—	0	—	5
JNVT	1	Jump if VT = 0; Clear VT	—	—	—	—	0	—	5
JST	1	Jump if ST = 1	—	—	—	—	—	—	5
JNST	1	Jump if ST = 0	—	—	—	—	—	—	5
JBS	3	Jump if Specified Bit = 1	—	—	—	—	—	—	5.6
JBC	3	Jump if Specified Bit = 0	—	—	—	—	—	—	5.6
DJNZ	1	D ← D - 1; if D ≠ 0 then PC ← PC + 8-bit offset	—	—	—	—	—	—	5
DEC/DECB	1	D ← D - 1	✓	✓	✓	✓	↑	—	
NEG/NEGB	1	D ← 0 - D	✓	✓	✓	✓	↑	—	
INC/INCB	1	D ← D + 1	✓	✓	✓	✓	↑	—	
EXT	1	D ← D; D + 2 ← Sign (D)	✓	✓	0	0	—	—	2
EXTB	1	D ← D; D + 1 ← Sign (D)	✓	✓	0	0	—	—	3
NOT/NOTB	1	D ← Logical Not (D)	✓	✓	0	0	—	—	
CLR/CLRB	1	D ← 0	1	0	0	0	—	—	
SHL/SHLB/SHLL	2	C ← msb — — — — — lsb ← 0	✓	?	✓	✓	↑	—	7
SHR/SHRB/SHRL	2	0 → msb — — — — — lsb → C	✓	0	✓	0	—	✓	7
SHRA/SHRAB/SHRAL	2	msb → msb — — — — — lsb → C	✓	✓	✓	0	—	✓	7
SETC	0	C ← 1	—	—	1	—	—	—	
CLRC	0	C ← 0	—	—	0	—	—	—	
CLRVT	0	VT ← 0	—	—	—	—	0	—	
RST	0	PC ← 2080H	0	0	0	0	0	0	8
DI	0	Disable All Interrupts (I ← 0)	—	—	—	—	—	—	
EI	0	Enable All Interrupts (I ← 1)	—	—	—	—	—	—	
NOP	0	PC ← PC + 1	—	—	—	—	—	—	
SKIP	0	PC ← PC + 2	—	—	—	—	—	—	
NORML	2	Normalize	✓	1	0	—	—	—	7
TRAP	0	SP ← SP - 2; (SP) ← PC PC ← (2010H)	—	—	—	—	—	—	9

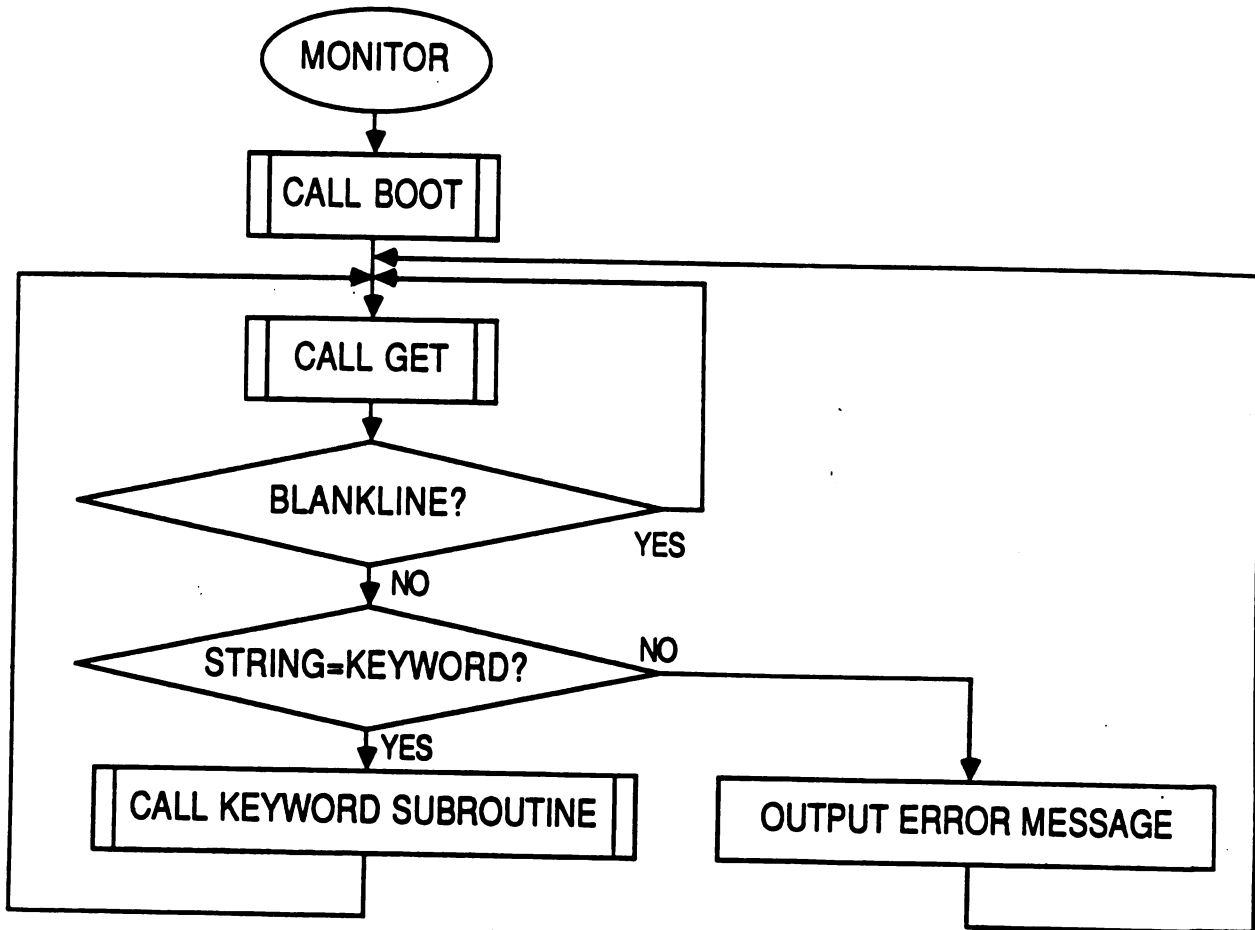
Note

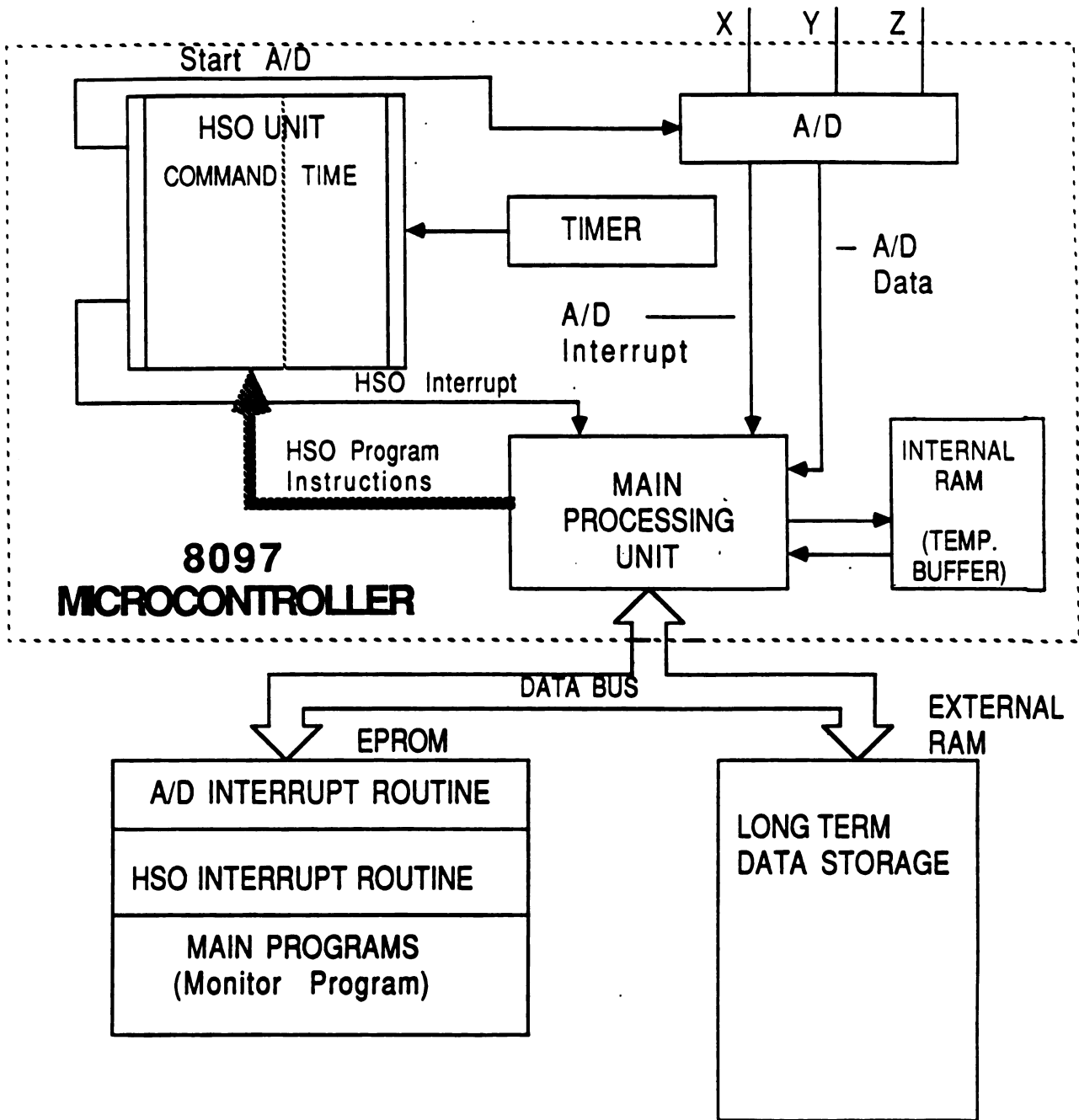
1. If the mnemonic ends in "B", a byte operation is performed, otherwise a word operation is done. Operands D, B and A must conform to the alignment rules for the required operand type. D and B are locations in the register file; A can be located anywhere in memory.
5. Offset is a 2's complement number.
6. Specified bit is one of the 2048 bits in the register file.
7. The "L" (Long) suffix indicates double-word operation.
8. Initiates a Reset by pulling RESET low. Software should re-initialize all the necessary registers with code starting at 2080H.
9. The assembler will not accept this mnemonic.

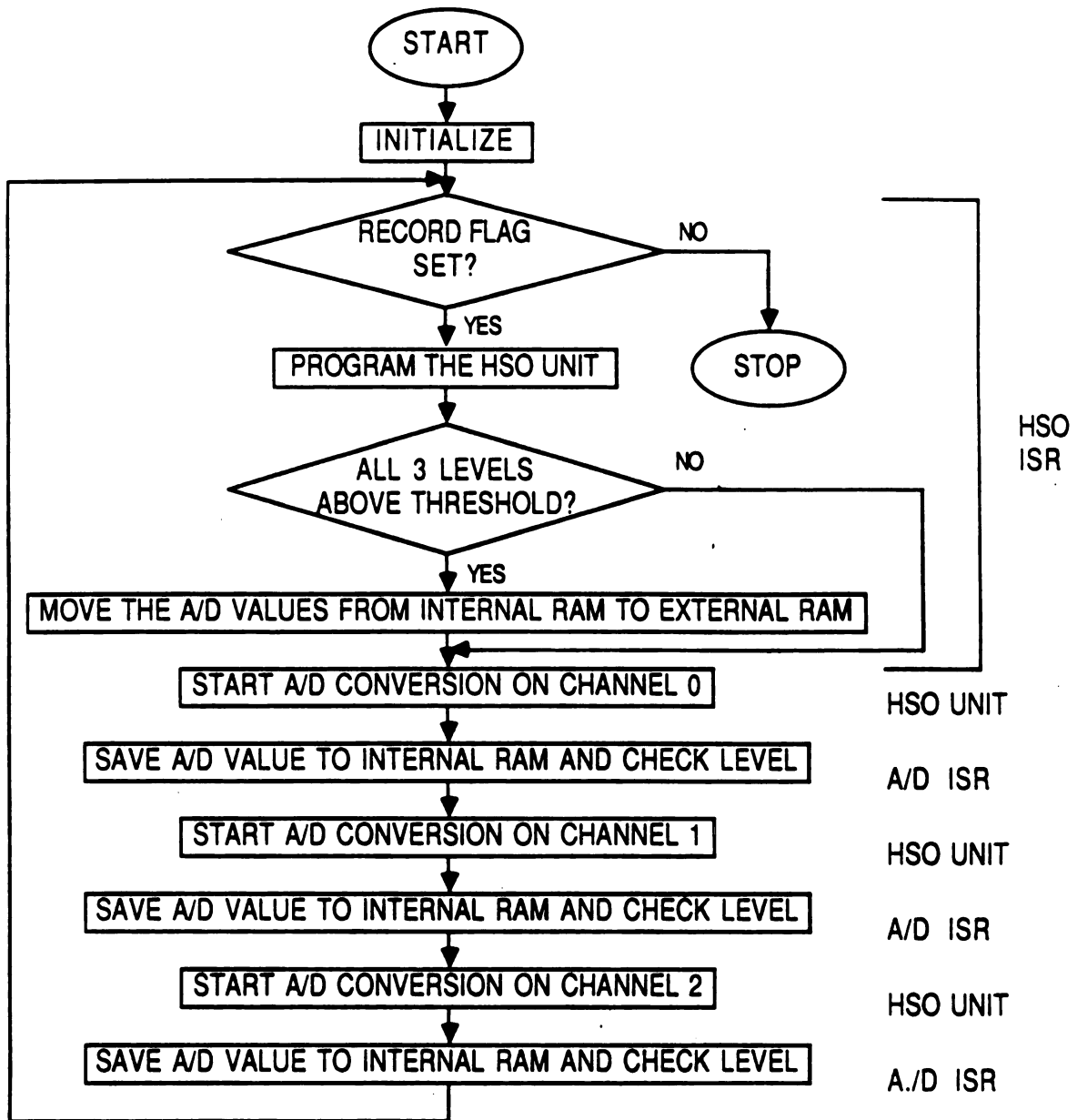
B.1 Software Block-Diagrams

B.1 Software Block-Diagrams.

The following software block diagrams are copied from KLUG et al. (1986).







Note: The RECORD Flag is changed external to this flow chart.

C. Data and Statistical Analysis

Title: APPLE IMPACT (HALF-SINE) VS BRUISE (Ida-Red) Sep 1985

Data case no. 1 to 798

Average Apple Diameter (mm)
 Apple Mass (Kg)
 Magness-Taylor Force (Kg)
 Equivalent Drop Height (mm)
 Maximum Acceleration (m/s²)
 Total Velocity Change (m/s)
 Measured Bruise Diameter (mm)

	Minimum	Maximum	Sum	Mean	Uncorrected Sum of Squares
2	68.75	78.25	58754.49	73.627	4328839.50
3	0.14	0.18	128.31	0.161	20.72
4	3.00	7.94	4119.77	5.163	22122.94
5	44.62	410.64	135349.73	169.611	30349932.00
6	305.44	3368.95	1268798.88	1589.974	2668369700.00
7	0.94	2.84	1394.35	1.747	2654.48
1	11.00	32.55	16997.98	21.301	376545.44

798 cases read

0 missing cases discarded

Correlation Matrix

	2	3	4	5	7	8	1
2	1.000						
3	0.942	1.000					
4	0.676	0.727	1.000				
5	0.095	0.076	0.075	1.000			
6	-0.278	-0.295	-0.333	0.590	1.000		
7	0.084	0.066	0.072	0.991	0.629	1.000	
1	-0.075	-0.115	-0.179	0.739	0.888	0.770	1.000

Determinant of matrix is= 3.576057E-04

Data file BRUISE DIAMETER GROUPED BY DROP HEIGHT
 Title: APPLE IMPACT (HALF-SINE) VS BRUISE (Ida-Red) Sep 1985

Function: ANOVA-1
 Data case no. 1 to 798
 Without selection

One way ANOVA grouped over EQUIVALENT DROP HEIGHT (mm)
 Drop Grouping
 with values from 1 to 8

Variable 1
 Measured Bruise Diameter (mm)

A N A L Y S I S O F V A R I A N C E T A B L E

	Degrees of Freedom	Sum of Squares	Error Mean Square	F-value	Prob.
Between	7	8974.1048	1282.01	184.08	.000
Within	790	5502.0349	6.96		
Total	797	14476.1398			

Coefficient of Variation= 12.39%

Var. 5	V A R I A B L E Number	Sum	Average	No. 1 SD	SE
1	60.00	931.750	15.53	1.58	0.34
2	78.00	1334.750	17.11	2.16	0.30
3	108.00	1965.745	18.20	2.53	0.25
4	84.00	1593.700	18.97	2.61	0.29
5	132.00	2868.555	21.73	3.00	0.23
6	120.00	2864.755	23.87	2.24	0.24
7	84.00	2066.190	24.60	2.87	0.29
8	132.00	3372.530	25.55	3.14	0.23
Total	798.00	16997.975	21.30	4.26	0.15
Within				2.64	

Bartlett's Test

Chi-square = 48.84089
 Number of Degrees of Freedom = 7
 Approximate Significance = 0

Data file BRUISE DIAMETER GROUPED BY MAGNESS-TAYLOR
 Title: APPLE IMPACT (HALF-SINE) VS BRUISE (Ida-Red) Sep 1985

Function: ANOVA-1
 Data case no. 1 to 798
 Without selection

One way ANOVA grouped over MAGNESS-TAYLOR FORCE
 MT Grouping
 with values from 1 to 6

Variable 1
 Measured Bruise Diameter (mm)

A N A L Y S I S O F V A R I A N C E T A B L E

	Degrees of Freedom	Sum of Squares	Error Mean Square	F-value	Prob.
Between	5	737.4839	147.50	8.50	.000
Within	792	13738.6559	17.35		
Total	797	14476.1398			

Coefficient of Variation= 19.55%

Var. 4	V A R I A B L E No. 1	Number	Sum	Average	SD	SE
1		94.00	2222.000	23.64	3.71	0.43
2		202.00	4348.550	21.53	4.40	0.29
3		152.00	3156.650	20.77	4.35	0.34
4		149.00	3173.670	21.30	4.22	0.34
5		153.00	3112.160	20.34	4.06	0.34
6		48.00	984.945	20.52	3.47	0.60
Total		798.00	16997.975	21.30	4.26	0.15
Within					4.16	

Bartlett's Test

Chi-square = 7.196449
 Number of Degrees of Freedom = 5
 Approximate Significance = .2064

Data file DROP HEIGHT GROUPING (mm)

Title: APPLE IMPACT (HALF-SINE) VS BRUISE (Ida-Red) Sep 1985

Function: GROUPT

Data case no. 1 to 798

Without selection

Var. 3 High limit	Var. 5 Group	Freq
50	1	60
70	2	78
90	3	108
110	4	84
170	5	132
230	6	120
290	7	84
450	8	132

Data file MAGNESS-TAYLOR GROUPING (kg)

Title: APPLE IMPACT (HALF-SINE) VS BRUISE (Ida-Red) Sep 1985

Function: GROUPT

Data case no. 1 to 798

Without selection

Var. 2 High limit	Var. 4 Group	Freq
4	1	94
4.5	2	202
5	3	152
6	4	149
7	5	153
8	6	48

=====

1Step 1 Variable Entered 4

M u l t i p l e R e g r e s s i o n A n a l y s i s

Multiple R	.888	F Change	2960.275
R Square	.788	R Square Change	.788
Adjusted R Square	.788	Sum of Squares Change	11408.48
Std. Err. of Est.	1.96312	Percent of SS Change	78.81

Date: 10/16/86

Time: 15:57:04

	Regression Coefficient	Std. Err. Reg. Coeff.	Beta Weight	Std. Err. Beta Weight	Student T value	Sig.
B(4)	.41861860E-02	.7694007E-04	.8877	.0163	54.41	.00
B(0)	14.644800					

A n a l y s i s O f V a r i a n c e

	Sum of Squares	Degrees of Freedom	Error Mean Square	F-test	Sig.
Regression	11408.4700	1	11408.470		
Residual	3067.66200	796	3.8538460	2960.27	.000
Total	14476.1500	798 cases from file:		E:MLRA.ASC	

A N A L Y S I S O F R E S I D U A L S

Number of positive residuals:	376
Largest positive residual:	9.12383
Number of negative residuals:	422
Largest negative residual:	-6.14309
Number of sign runs:	246
Significance of sign runs test:	.0000
Average absolute residual:	1.45002
Residual sum of squares:	3067.66
Residual mean square:	3.85385
Residual standard deviation:	1.96312
Durbin-Watson statistic:	.690840
Auto-correlation coefficient:	.653

1Step 2 Variable Entered 6

M u l t i p l e R e g r e s s i o n A n a l y s i s

```
-----
Multiple R           .927                F Change      -538.611
R Square            .859                R Square Change .071
Adjusted R Square   .859                Sum of Squares Change 1026.544
Std. Err. of Est.   1.60233            Percent of SS Change 7.09
-----
```

Date: 10/16/86

Time: 15:57:08

```
-----
Regression   Std. Err.   Beta   Std. Err. Student
Coefficient   Reg. Coeff.   Weight Beta Weight T value Sig.
B( 4)   .32681390E-02 .7779270E-04 .6931   .0165   42.01 .00
B( 6)   .74428220   .3722205E-01 .3299   .0165   20.00 .00
B( 0)   13.628680
-----
```

A n a l y s i s O f V a r i a n c e

```
-----
                Degrees of   Error
                Sum of Squares Freedom Mean Square   F-test Sig.
Regression      12435.0500         2      6217.5230
Residual         2041.1170        795      2.5674430   2421.66 .000
-----
Total            14476.1500        798 cases from file: E:MLRA.ASC
-----
```

A N A L Y S I S O F R E S I D U A L S

```
=====
Number of positive residuals:      411
Largest positive residual:         7.62845

Number of negative residuals:      387
Largest negative residual:         -5.54599

Number of sign runs:               266
Significance of sign runs test:    .0000

Average absolute residual:         1.23301
Residual sum of squares:           2041.12

Residual mean square:              2.56744
Residual standard deviation:       1.60232

Durbin-Watson statistic:           1.03657
Auto-correlation coefficient:       .481
=====
```

1Step 3 Variable Entered 5

M u l t i p l e R e g r e s s i o n A n a l y s i s

Multiple R	.941	F Change	-361.614
R Square	.886	R Square Change	.027
Adjusted R Square	.886	Sum of Squares Change	393.0315
Std. Err. of Est.	1.44072	Percent of SS Change	2.72

Date: 10/16/86

Time: 15:57:12

	Regression Coefficient	Std. Err. Reg. Coeff.	Beta Weight	Std. Err. Beta Weight	Student T value	Sig.
B(4)	.69395640E-02	.2758261E-03	1.4716	.0585	25.16	.00
B(6)	.87756310	.3484138E-01	.3889	.0154	25.19	.00
B(5)	-.10771110E-05	.7827581E-07	-.8313	.0604	-13.76	.00
B(0)	10.949530					

A n a l y s i s O f V a r i a n c e

	Sum of Squares	Degrees of Freedom	Error Mean Square	F-test	Sig.
Regression	12828.0600	3	4276.0200		
Residual	1648.10100	794	2.0756930	2060.05	.000
Total	14476.1500	798 cases from file:	E:MLRA.ASC		

A N A L Y S I S O F R E S I D U A L S

```

=====
Number of positive residuals:      397
Largest positive residual:        7.34702

Number of negative residuals:      401
Largest negative residual:        -4.57447

Number of sign runs:              280
Significance of sign runs test:    .0000

Average absolute residual:        1.11785
Residual sum of squares:          1648.10

Residual mean square:             2.07569
Residual standard deviation:      1.44073

Durbin-Watson statistic:          1.27524
Auto-correlation coefficient:      .362

```

1Step 4 Variable Entered 2

M u l t i p l e R e g r e s s i o n A n a l y s i s

Multiple R	.949	F Change	-260.794
R Square	.901	R Square Change	.015
Adjusted R Square	.900	Sum of Squares Change	211.3551
Std. Err. of Est.	1.34602	Percent of SS Change	1.46

Date: 10/16/86

Time: 15:57:17

	Regression Coefficient	Std. Err. Reg. Coeff.	Beta Weight	Std. Err. Beta Weight	Student T value	Sig.
B(4)	.76594280E-02	.2661750E-03	1.6243	.0564	28.78	.00
B(6)	.77166250	.3399583E-01	.3420	.0151	22.70	.00
B(5)	-.11931410E-05	.7391544E-07	-.9209	.0570	-16.14	.00
B(2)	.29970570	.2774859E-01	.1344	.0124	10.80	.00
B(0)	-11.521270					

A n a l y s i s O f V a r i a n c e

	Sum of Squares	Degrees of Freedom	Error Mean Square	F-test	Sig.
Regression	13039.4200	4	3259.8550		
Residual	1436.74600	793	1.8117860	1799.26	.000
Total	14476.1500	798 cases from file: E:MLRA.ASC			

A N A L Y S I S O F R E S I D U A L S

Number of positive residuals:	401
Largest positive residual:	7.31315
Number of negative residuals:	397
Largest negative residual:	-4.47964
Number of sign runs:	294
Significance of sign runs test:	.0000
Average absolute residual:	1.02722
Residual sum of squares:	1436.75
Residual mean square:	1.81179
Residual standard deviation:	1.34603
Durbin-Watson statistic:	1.32425
Auto-correlation coefficient:	.338

Data and Statistical Analysis

Data file IMAN

Title: APPLE IMPACT (HALF-SINE) VS BRUISE (Ida-Red) Sep 1985

Data case no. 1 to 798

LIST OF VARIABLES

VAR	TYPE	NAME/DESCRIPTION
1	numeric	Measured Bruise Diameter (mm)
2	numeric	Avarage Apple Diameter (mm)
3	numeric	Apple Mass (Kg)
4	numeric	Magness-Taylor Force (Kg)
5	numeric	Equivalent Drop Height (mm)
6	numeric	Maximum Acceleration (m/s^2)
7	numeric	Total Velocity Change (m/s)
8	numeric	HERTZ Bruise Diameter (mm)
9	numeric	Adjusted Hertz Bruise Diameter (mm)
10	numeric	Plastic Theory Bruise Diameter (mm)
11	numeric	MLRA Pridicted Bruise Diameter (mm)

CASE NO.	1	2	3	4	5	6	7	8	9	10	11
1	14.6	73.8	.161	4.2	47.5	615.6	0.965	22.1	16.4	15.0	15.8
2	15.0	71.0	.146	4.2	47.5	615.6	0.965	21.3	15.9	14.6	14.8
3	17.6	74.0	.164	4.5	47.5	615.6	0.965	21.9	16.3	14.9	15.8
4	17.6	75.0	.164	5.0	47.5	615.6	0.965	21.5	16.0	14.6	16.1
5	17.0	72.0	.150	5.0	47.5	615.6	0.965	20.8	15.5	14.2	15.0
6	14.1	71.5	.146	4.3	47.5	615.6	0.965	21.3	15.8	14.5	14.9
7	16.3	71.5	.145	4.5	46.0	621.2	0.950	20.9	15.6	14.3	14.9
8	14.4	70.3	.143	4.3	46.0	621.2	0.950	20.9	15.6	14.3	14.5
9	16.5	73.0	.151	4.7	46.0	621.2	0.950	21.1	15.8	14.4	15.4
10	15.7	74.3	.163	4.0	46.0	621.2	0.950	22.3	16.7	15.1	16.0
11	16.3	70.5	.145	4.5	46.0	621.2	0.950	20.8	15.6	14.3	14.5
12	16.5	74.0	.160	5.5	46.0	621.2	0.950	20.8	15.5	14.1	15.6
13	16.8	73.3	.157	4.5	46.1	617.5	0.951	21.5	16.0	14.6	15.5
14	17.7	75.3	.167	4.1	46.1	617.5	0.951	22.4	16.7	15.2	16.4
15	16.8	71.5	.150	4.2	46.1	617.5	0.951	21.4	16.0	14.6	14.9
16	16.3	71.0	.147	4.1	46.1	617.5	0.951	21.3	15.9	14.6	14.8
17	14.5	72.5	.152	3.8	46.1	617.5	0.951	22.0	16.4	15.0	15.4
18	16.5	73.8	.160	4.7	46.1	617.5	0.951	21.4	16.0	14.6	15.7
19	14.4	74.8	.164	5.6	64.3	851.7	1.123	22.3	17.2	15.1	17.5
20	17.2	72.8	.158	5.3	64.3	851.7	1.123	22.2	17.1	15.1	16.8
21	19.1	72.0	.152	4.8	64.3	851.7	1.123	22.3	17.2	15.3	16.6
22	17.8	72.0	.151	4.5	64.3	851.7	1.123	22.6	17.4	15.4	16.7
23	17.5	73.8	.157	5.3	64.3	851.7	1.123	22.3	17.2	15.1	17.2
24	18.0	71.3	.154	5.7	64.3	851.7	1.123	21.6	16.6	14.8	16.2
25	18.1	73.5	.159	5.0	65.0	867.7	1.129	22.6	17.5	15.4	17.3
26	19.4	71.0	.146	5.9	65.0	867.7	1.129	21.2	16.4	14.5	16.1
27	18.8	73.5	.156	5.6	65.0	867.7	1.129	22.0	17.0	15.0	17.1
28	17.7	71.0	.152	5.5	65.0	867.7	1.129	21.7	16.7	14.8	16.2
29	18.6	72.5	.152	5.3	65.0	867.7	1.129	22.0	17.0	15.0	16.8
30	18.4	73.8	.159	5.4	65.0	867.7	1.129	22.3	17.2	15.1	17.3
31	16.0	72.0	.149	4.4	65.6	907.0	1.135	22.7	17.7	15.5	17.1
32	18.8	72.0	.148	5.0	65.6	907.0	1.135	22.1	17.3	15.1	16.9
33	19.1	73.8	.164	4.7	65.6	907.0	1.135	23.1	18.0	15.7	17.6
34	19.2	74.3	.160	4.4	65.6	907.0	1.135	23.4	18.2	15.9	17.9
35	18.9	74.5	.164	4.3	65.6	907.0	1.135	23.6	18.4	16.0	18.0
36	18.6	74.3	.159	3.8	65.6	907.0	1.135	24.0	18.7	16.3	18.0
37	19.8	71.8	.146	4.4	86.3	1168.2	1.301	23.9	19.1	16.3	18.6
38	20.6	73.8	.161	4.5	86.3	1168.2	1.301	24.5	19.6	16.7	19.4
39	20.0	71.5	.149	5.2	86.3	1168.2	1.301	23.2	18.5	15.9	18.4
40	21.5	72.3	.154	4.5	86.3	1168.2	1.301	24.1	19.3	16.5	18.8
41	19.6	72.5	.153	4.6	86.3	1168.2	1.301	24.0	19.2	16.4	18.9
42	19.5	71.0	.145	4.0	86.3	1168.2	1.301	24.2	19.4	16.6	18.4
43	19.1	71.3	.144	4.4	85.8	1134.5	1.297	23.7	18.9	16.2	18.3
44	19.5	72.3	.145	3.8	85.8	1134.5	1.297	24.6	19.6	16.8	18.8
45	19.6	71.5	.145	4.1	85.8	1134.5	1.297	24.1	19.2	16.5	18.4
46	19.8	71.8	.151	4.3	85.8	1134.5	1.297	24.1	19.2	16.5	18.5
47	20.8	73.0	.154	4.8	85.8	1134.5	1.297	23.9	19.0	16.3	18.8
48	19.0	71.3	.145	3.9	85.8	1134.5	1.297	24.3	19.4	16.7	18.4
49	18.3	71.3	.149	4.2	84.9	1134.5	1.290	24.1	19.2	16.5	18.3
50	18.8	72.8	.154	4.2	84.9	1102.6	1.290	24.4	19.3	16.7	18.7
51	21.4	72.8	.157	4.0	84.9	1102.6	1.290	24.8	19.6	16.9	18.8

52	26.1	73.5	.160	4.1	84.9	1102.6	1.290	24.8	19.6	16.9	19.0
53	20.5	71.5	.146	4.2	84.9	1102.6	1.290	24.0	19.0	16.4	18.2
54	20.5	74.8	.163	4.2	84.9	1102.6	1.290	25.0	19.8	16.9	19.4
55	22.0	73.0	.153	4.1	107.3	1382.6	1.450	25.7	20.9	17.5	20.5
56	20.0	71.0	.144	4.8	107.3	1382.6	1.450	24.4	19.8	16.7	19.6
57	21.2	72.0	.151	4.5	107.3	1382.6	1.450	25.0	20.3	17.1	20.0
58	21.3	70.8	.144	4.1	107.3	1382.6	1.450	25.1	20.4	17.2	19.6
59	22.0	74.0	.163	4.2	107.3	1382.6	1.450	26.1	21.2	17.7	20.8
60	21.5	73.0	.154	5.2	107.3	1382.6	1.450	24.6	20.0	16.7	20.2
61	23.2	73.3	.161	4.6	105.9	1382.6	1.441	25.4	20.6	17.3	20.4
62	20.8	72.3	.148	5.2	105.9	1382.6	1.441	24.2	19.7	16.5	19.9
63	20.3	71.5	.150	5.4	105.9	1382.6	1.441	24.0	19.5	16.4	19.6
64	21.8	73.3	.157	4.5	105.9	1382.6	1.441	25.4	20.6	17.3	20.5
65	21.0	72.5	.161	4.2	105.9	1382.6	1.441	25.7	20.9	17.6	20.2
66	21.6	72.5	.150	5.0	105.9	1382.6	1.441	24.5	19.9	16.7	20.1
67	19.8	71.3	.149	4.7	106.7	1353.2	1.446	24.6	19.9	16.9	19.5
68	21.5	73.3	.153	4.2	106.7	1353.2	1.446	25.6	20.7	17.4	20.4
69	19.1	72.5	.156	5.3	106.7	1353.2	1.446	24.4	19.8	16.7	19.9
70	21.0	71.8	.148	4.9	106.7	1353.2	1.446	24.5	19.8	16.7	19.7
71	19.5	72.3	.155	4.0	106.7	1353.2	1.446	25.8	20.8	17.6	20.1
72	20.8	72.8	.151	4.5	106.7	1353.2	1.446	25.1	20.3	17.1	20.1
73	20.8	71.3	.143	4.0	160.6	2029.8	1.775	27.4	23.4	18.7	23.0
74	24.7	73.5	.156	3.4	160.6	2029.8	1.775	29.1	24.9	19.8	23.9
75	24.1	73.3	.153	3.7	160.6	2029.8	1.775	28.5	24.4	19.4	23.8
76	24.9	74.0	.161	3.9	160.6	2029.8	1.775	28.6	24.5	19.4	24.0
77	22.3	71.0	.144	4.4	160.6	2029.8	1.775	26.9	23.0	18.4	22.8
78	23.0	72.0	.149	4.6	160.6	2029.8	1.775	27.0	23.1	18.4	23.1
79	23.5	71.8	.144	4.3	160.6	2049.5	1.775	27.1	23.2	18.5	23.1
80	22.8	73.5	.151	3.8	160.6	2049.5	1.775	28.3	24.3	19.3	23.9
81	24.0	73.8	.162	4.6	160.6	2049.5	1.775	27.7	23.7	18.8	23.8
82	22.6	70.3	.143	4.1	160.6	2049.5	1.775	27.1	23.2	18.6	22.6
83	25.1	73.0	.152	3.6	160.6	2049.5	1.775	28.6	24.5	19.5	23.7
84	23.5	71.0	.145	3.8	160.6	2049.5	1.775	27.7	23.8	19.0	23.0
85	22.3	68.8	.143	4.0	160.6	2020.0	1.775	27.0	23.1	18.6	22.0
86	23.5	71.8	.148	4.9	160.6	2020.0	1.775	26.6	22.7	18.1	22.9
87	21.5	70.8	.139	4.1	160.6	2020.0	1.775	27.0	23.1	18.5	22.7
88	24.9	75.0	.160	3.7	160.6	2020.0	1.775	29.0	24.8	19.7	24.4
89	22.8	69.0	.137	4.7	160.6	2020.0	1.775	26.0	22.2	17.9	21.9
90	22.8	73.0	.150	4.1	160.6	2020.0	1.775	27.8	23.7	18.9	23.6
91	25.8	74.0	.164	4.7	204.0	2441.7	2.000	29.0	25.3	19.7	25.4
92	26.3	73.5	.157	4.0	204.0	2441.7	2.000	29.6	25.9	20.2	25.4
93	26.0	73.0	.158	3.5	204.0	2441.7	2.000	30.4	26.5	20.7	25.3
94	24.5	71.0	.145	3.5	204.0	2441.7	2.000	29.5	25.8	20.2	24.6
95	25.1	72.8	.160	4.8	204.0	2441.7	2.000	28.6	24.9	19.5	24.9
96	26.3	74.3	.163	3.8	204.0	2441.7	2.000	30.3	26.5	20.6	25.7
97	23.6	71.8	.149	4.3	208.1	2471.1	2.020	28.7	25.1	19.6	24.8
98	25.4	70.8	.147	3.9	208.1	2471.1	2.020	29.1	25.4	19.9	24.5
99	26.7	71.3	.151	4.6	208.1	2471.1	2.020	28.4	24.8	19.4	24.5
100	25.3	73.3	.153	4.2	208.1	2471.1	2.020	29.3	25.6	19.9	25.4
101	24.5	73.3	.156	4.5	208.1	2471.1	2.020	29.0	25.3	19.7	25.3
102	24.8	71.3	.150	3.9	208.1	2471.1	2.020	29.3	25.6	20.0	24.7
103	25.0	72.5	.153	4.7	206.0	2446.6	2.010	28.4	24.8	19.4	24.9
104	25.5	72.8	.150	3.6	206.0	2446.6	2.010	29.9	26.1	20.4	25.2
105	24.9	71.3	.145	4.6	206.0	2446.6	2.010	28.1	24.5	19.2	24.5

106	24.7	71.5	.152	4.3	206.0	2446.6	2.010	28.8	25.1	19.7	24.6
107	25.0	71.8	.148	4.0	206.0	2446.6	2.010	29.1	25.4	19.9	24.8
108	25.6	74.0	.164	4.3	206.0	2446.6	2.010	29.6	25.8	20.1	25.6
109	26.9	73.3	.155	4.0	257.1	2853.5	2.246	30.9	27.4	21.0	26.7
110	26.4	72.5	.156	3.9	257.1	2853.5	2.246	31.0	27.4	21.1	26.4
111	24.7	72.8	.158	4.9	257.1	2853.5	2.246	29.7	26.3	20.3	26.3
112	26.5	72.5	.157	3.7	257.1	2853.5	2.246	31.4	27.8	21.4	26.4
113	26.7	74.5	.164	3.6	257.1	2853.5	2.246	32.2	28.5	21.8	27.2
114	26.0	71.8	.144	4.2	257.1	2853.5	2.246	29.9	26.5	20.5	26.0
115	26.7	73.5	.164	4.3	254.9	2853.5	2.236	30.8	27.3	21.0	26.6
116	25.5	70.5	.144	4.1	254.9	2853.5	2.236	29.8	26.4	20.4	25.6
117	25.1	73.5	.161	5.3	254.9	2853.5	2.236	29.4	26.1	20.0	26.4
118	26.3	73.5	.155	4.7	254.9	2853.5	2.236	29.9	26.5	20.4	26.6
119	27.4	74.8	.165	3.9	254.9	2853.5	2.236	31.7	28.1	21.5	27.2
120	26.8	72.0	.147	3.9	254.9	2853.5	2.236	30.5	27.0	20.8	26.2
121	24.0	70.5	.146	4.2	254.9	2814.3	2.236	29.7	26.2	20.4	25.5
122	25.2	72.0	.147	4.1	254.9	2814.3	2.236	30.2	26.6	20.6	26.1
123	26.5	73.0	.154	3.9	254.9	2814.3	2.236	30.9	27.3	21.1	26.5
124	26.3	71.5	.150	3.8	254.9	2814.3	2.236	30.7	27.1	21.0	26.0
125	27.3	71.5	.145	3.7	254.9	2814.3	2.236	30.6	27.0	21.0	26.0
126	26.9	72.5	.156	4.6	254.9	2814.3	2.236	29.9	26.4	20.4	26.2
127	26.5	71.3	.148	4.4	306.4	3245.8	2.451	30.8	27.7	21.1	26.7
128	32.5	73.3	.158	4.1	306.4	3245.8	2.451	32.0	28.7	21.8	27.5
129	28.5	71.8	.154	4.0	306.4	3245.8	2.451	31.7	28.5	21.7	27.0
130	30.1	73.5	.160	4.2	306.4	3245.8	2.451	32.0	28.7	21.7	27.6
131	28.9	70.8	.143	4.1	306.4	3245.8	2.451	30.9	27.8	21.2	26.6
132	29.4	73.3	.157	4.3	306.4	3245.8	2.451	31.6	28.4	21.5	27.5
133	27.6	71.3	.150	4.5	308.9	3275.2	2.461	30.8	27.7	21.1	26.7
134	25.4	71.8	.149	4.0	308.9	3275.2	2.461	31.6	28.4	21.6	27.0
135	28.2	75.0	.162	4.4	308.9	3275.2	2.461	32.0	28.8	21.7	28.1
136	29.2	74.0	.161	3.9	308.9	3275.2	2.461	32.6	29.4	22.2	27.9
137	28.7	73.0	.159	3.8	308.9	3275.2	2.461	32.5	29.3	22.2	27.5
138	24.0	72.5	.155	4.2	308.9	3275.2	2.461	31.6	28.5	21.6	27.2
139	29.3	71.8	.146	3.0	311.4	3275.2	2.471	33.3	30.0	22.8	27.3
140	28.0	72.0	.153	4.2	311.4	3275.2	2.471	31.5	28.3	21.5	27.1
141	27.8	72.8	.159	4.4	311.4	3275.2	2.471	31.6	28.4	21.5	27.3
142	30.0	73.3	.161	4.0	311.4	3275.2	2.471	32.4	29.1	22.0	27.6
143	28.1	72.5	.154	4.4	311.4	3275.2	2.471	31.3	28.2	21.4	27.2
144	28.3	70.8	.147	3.9	311.4	3275.2	2.471	31.5	28.3	21.6	26.7
145	19.0	76.5	.173	4.2	46.1	577.6	0.951	22.6	16.7	15.2	16.5
146	15.7	75.8	.174	4.4	46.1	577.6	0.951	22.3	16.5	15.1	16.2
147	13.9	75.8	.174	4.3	46.1	577.6	0.951	22.4	16.5	15.2	16.2
148	14.9	74.8	.167	3.8	46.1	577.6	0.951	22.7	16.7	15.4	16.0
149	13.5	75.0	.170	4.4	46.1	577.6	0.951	22.1	16.3	15.0	15.9
150	13.0	72.0	.153	4.9	46.1	577.6	0.951	20.9	15.4	14.2	14.7
151	14.8	75.0	.165	4.4	46.1	590.3	0.951	22.0	16.3	14.9	16.0
152	13.7	71.5	.148	4.5	46.1	590.3	0.951	21.0	15.6	14.4	14.7
153	13.1	74.5	.147	4.5	46.1	590.3	0.951	21.3	15.8	14.5	15.8
154	14.3	75.0	.164	4.5	46.1	590.3	0.951	21.9	16.2	14.8	16.0
155	12.7	72.5	.150	4.6	46.1	590.3	0.951	21.1	15.6	14.4	15.1
156	12.9	70.5	.143	4.6	46.1	590.3	0.951	20.7	15.3	14.2	14.3
157	11.0	71.5	.149	4.5	47.1	596.8	0.961	21.1	15.7	14.5	14.8
158	14.4	74.0	.163	4.9	47.1	596.8	0.961	21.4	15.9	14.6	15.6
159	12.9	73.0	.151	4.6	47.1	596.8	0.961	21.3	15.8	14.5	15.3

160	14.9	72.0	.148	4.8	47.1	596.8	0.961	20.9	15.5	14.3	14.9
161	14.2	74.0	.162	4.2	47.1	596.8	0.961	22.1	16.4	15.0	15.8
162	14.0	73.5	.158	4.1	47.1	596.8	0.961	22.0	16.3	15.0	15.6
163	16.0	73.0	.158	3.9	68.2	866.9	1.156	23.9	18.4	16.3	17.4
164	16.3	73.5	.155	4.5	68.2	866.9	1.156	23.2	17.8	15.8	17.4
165	16.9	73.0	.160	4.1	68.2	866.9	1.156	23.7	18.2	16.1	17.3
166	15.0	70.5	.148	4.6	68.2	866.9	1.156	22.5	17.3	15.4	16.3
167	15.8	72.5	.152	5.0	68.2	866.9	1.156	22.5	17.3	15.3	16.9
168	17.1	75.0	.165	4.9	68.2	866.9	1.156	23.3	17.9	15.8	17.9
169	15.0	73.0	.158	4.2	67.5	873.3	1.150	23.5	18.1	16.0	17.3
170	15.3	72.0	.149	4.4	67.5	873.3	1.150	22.9	17.6	15.6	16.9
171	16.5	73.5	.165	5.0	67.5	873.3	1.150	22.9	17.7	15.6	17.3
172	16.8	72.5	.151	4.8	67.5	873.3	1.150	22.6	17.4	15.4	17.0
173	15.8	73.0	.157	4.9	67.5	873.3	1.150	22.7	17.5	15.5	17.2
174	16.1	73.5	.154	4.3	67.5	873.3	1.150	23.3	18.0	15.9	17.5
175	15.7	72.5	.152	5.0	67.2	864.8	1.148	22.4	17.3	15.3	16.9
176	16.9	73.5	.155	4.4	67.2	864.8	1.148	23.2	17.9	15.8	17.4
177	15.4	72.5	.155	4.7	67.2	864.8	1.148	22.8	17.5	15.6	17.0
178	15.9	73.5	.163	5.5	67.2	864.8	1.148	22.4	17.3	15.3	17.2
179	16.5	73.5	.159	4.1	67.2	864.8	1.148	23.7	18.2	16.1	17.5
180	17.2	71.5	.143	4.6	67.2	864.8	1.148	22.4	17.2	15.3	16.6
181	19.2	73.0	.162	4.3	86.7	1099.3	1.304	24.7	19.5	16.8	18.8
182	18.1	72.0	.152	3.8	86.7	1099.3	1.304	24.9	19.6	17.0	18.5
183	19.0	73.5	.160	4.0	86.7	1099.3	1.304	25.1	19.8	17.1	19.0
184	17.2	72.5	.156	4.2	86.7	1099.3	1.304	24.6	19.4	16.8	18.6
185	18.6	71.5	.145	4.6	86.7	1099.3	1.304	23.6	18.6	16.2	18.2
186	17.1	71.0	.150	4.4	86.7	1099.3	1.304	23.9	18.9	16.4	18.0
187	19.1	72.5	.153	3.9	86.6	1087.5	1.303	24.8	19.5	16.9	18.6
188	18.0	71.0	.144	4.0	86.6	1087.5	1.303	24.2	19.0	16.6	18.1
189	18.6	72.0	.153	4.5	86.6	1087.5	1.303	24.1	18.9	16.4	18.3
190	18.5	73.5	.163	4.0	86.6	1087.5	1.303	25.2	19.8	17.1	19.0
191	17.0	71.0	.148	4.2	86.6	1087.5	1.303	24.1	19.0	16.5	18.0
192	17.5	71.5	.150	4.3	86.6	1087.5	1.303	24.1	19.0	16.5	18.2
193	18.5	72.0	.146	4.3	86.1	1100.2	1.299	24.0	19.0	16.4	18.4
194	18.5	72.0	.155	4.5	86.1	1100.2	1.299	24.1	19.0	16.5	18.4
195	18.0	72.5	.152	3.8	86.1	1100.2	1.299	24.9	19.7	17.0	18.7
196	17.8	72.0	.151	4.5	86.1	1100.2	1.299	24.0	18.9	16.4	18.4
197	19.0	74.0	.161	5.3	86.1	1100.2	1.299	23.8	18.8	16.1	18.9
198	17.6	72.5	.149	4.3	86.1	1100.2	1.299	24.2	19.1	16.5	18.6
199	20.1	72.5	.159	5.2	104.5	1320.9	1.432	24.5	19.8	16.7	19.7
200	19.3	72.0	.152	3.8	104.5	1320.9	1.432	25.8	20.8	17.6	19.9
201	18.5	71.5	.146	4.5	104.5	1320.9	1.432	24.7	19.9	16.9	19.5
202	18.3	73.5	.158	3.8	104.5	1320.9	1.432	26.2	21.1	17.8	20.4
203	19.1	72.5	.148	4.0	104.5	1320.9	1.432	25.5	20.5	17.4	20.0
204	19.6	72.5	.155	4.5	104.5	1320.9	1.432	25.1	20.2	17.1	19.9
205	19.2	73.5	.161	4.4	105.4	1335.6	1.438	25.6	20.7	17.4	20.4
206	18.4	70.0	.143	5.1	105.4	1335.6	1.438	23.8	19.2	16.4	18.9
207	19.8	73.5	.157	4.3	105.4	1335.6	1.438	25.6	20.7	17.4	20.4
208	19.8	74.0	.161	4.4	105.4	1335.6	1.438	25.7	20.7	17.4	20.5
209	16.0	71.0	.148	4.5	105.4	1335.6	1.438	24.7	20.0	16.9	19.4
210	18.3	70.0	.144	4.6	105.4	1335.6	1.438	24.3	19.6	16.7	19.0
211	19.5	72.5	.156	5.2	104.9	1330.7	1.435	24.5	19.7	16.7	19.8
212	18.7	71.5	.146	4.5	104.9	1330.7	1.435	24.7	19.9	16.9	19.6
213	19.9	73.0	.156	4.1	104.9	1330.7	1.435	25.7	20.7	17.5	20.2

214	19.2	73.0	.153	4.4	104.9	1330.7	1.435	25.3	20.4	17.2	20.1
215	20.0	75.0	.165	4.2	104.9	1330.7	1.435	26.2	21.1	17.7	20.9
216	18.5	73.5	.164	4.4	104.9	1330.7	1.435	25.7	20.7	17.5	20.3
217	22.1	72.5	.155	4.3	155.9	1902.4	1.748	27.5	23.1	18.7	22.9
218	22.6	72.5	.155	4.5	155.9	1902.4	1.748	27.2	22.9	18.6	22.9
219	21.6	72.0	.152	4.1	155.9	1902.4	1.748	27.5	23.2	18.8	22.8
220	22.8	72.0	.150	4.0	155.9	1902.4	1.748	27.6	23.2	18.9	22.8
221	22.0	74.0	.164	4.0	155.9	1902.4	1.748	28.4	23.9	19.3	23.5
222	22.7	71.5	.148	3.7	155.9	1902.4	1.748	27.9	23.5	19.1	22.7
223	22.2	72.0	.153	4.1	156.6	1934.7	1.752	27.6	23.3	18.8	22.9
224	22.7	72.0	.150	3.8	156.6	1934.7	1.752	27.9	23.6	19.1	22.9
225	21.9	73.0	.147	3.5	156.6	1934.7	1.752	28.4	24.0	19.4	23.4
226	23.7	72.5	.154	3.9	156.6	1934.7	1.752	28.0	23.7	19.1	23.1
227	22.8	75.0	.154	4.4	156.6	1934.7	1.752	27.7	23.4	18.8	23.9
228	22.5	72.5	.164	4.2	156.6	1934.7	1.752	27.9	23.6	19.0	23.0
229	20.5	72.0	.148	5.2	156.6	1946.5	1.752	26.1	22.2	17.9	22.7
230	23.5	75.0	.164	4.4	156.6	1946.5	1.752	28.0	23.8	19.0	24.0
231	22.0	71.5	.148	4.1	156.6	1946.5	1.752	27.3	23.2	18.7	22.7
232	23.3	74.5	.162	3.9	156.6	1946.5	1.752	28.6	24.2	19.4	23.9
233	22.5	74.0	.160	3.6	156.6	1946.5	1.752	28.9	24.5	19.6	23.8
234	23.0	73.5	.154	3.8	156.6	1946.5	1.752	28.3	24.0	19.2	23.5
235	23.2	72.5	.154	4.0	210.9	2317.2	2.034	29.6	25.2	20.2	24.9
236	24.0	72.5	.156	5.3	210.9	2317.2	2.034	28.0	23.9	19.1	24.6
237	23.0	72.5	.158	5.4	210.9	2317.2	2.034	28.0	23.9	19.1	24.6
238	24.6	72.5	.158	5.3	210.9	2317.2	2.034	28.1	24.0	19.2	24.6
239	25.3	74.5	.162	4.1	210.9	2317.2	2.034	30.0	25.7	20.4	25.6
240	21.2	71.0	.146	4.3	210.9	2317.2	2.034	28.6	24.4	19.6	24.3
241	22.5	71.0	.144	4.1	208.1	2264.2	2.020	28.7	24.4	19.7	24.2
242	24.1	74.0	.160	4.5	208.1	2264.2	2.020	29.2	24.9	19.9	25.2
243	23.8	72.0	.158	4.1	208.1	2264.2	2.020	29.4	25.0	20.1	24.5
244	24.7	73.0	.154	3.8	208.1	2264.2	2.020	29.9	25.4	20.3	25.0
245	24.9	74.0	.160	3.4	208.1	2264.2	2.020	30.9	26.3	21.0	25.4
246	23.9	73.0	.162	4.3	208.1	2264.2	2.020	29.4	25.0	20.0	24.9
247	24.9	74.0	.166	3.4	210.1	2314.2	2.030	31.2	26.7	21.2	25.6
248	25.5	73.0	.156	5.2	210.1	2314.2	2.030	28.2	24.1	19.2	24.8
249	25.3	72.5	.158	4.0	210.1	2314.2	2.030	29.7	25.4	20.2	24.9
250	24.5	72.5	.158	5.0	210.1	2314.2	2.030	28.4	24.3	19.4	24.7
251	25.0	74.5	.160	3.7	210.1	2314.2	2.030	30.6	26.1	20.7	25.7
252	23.8	70.0	.144	4.5	210.1	2314.2	2.030	28.1	24.0	19.3	23.8
253	27.0	74.0	.164	3.2	258.7	2705.5	2.252	32.9	28.6	22.3	27.0
254	26.3	73.5	.156	4.1	258.7	2705.5	2.252	30.9	26.8	21.0	26.6
255	25.3	73.5	.160	4.0	258.7	2705.5	2.252	31.2	27.1	21.2	26.6
256	24.3	70.5	.156	3.8	258.7	2705.5	2.252	30.8	26.8	21.2	25.6
257	24.0	71.0	.144	4.6	258.7	2705.5	2.252	29.3	25.4	20.1	25.6
258	26.0	74.0	.156	3.8	258.7	2705.5	2.252	31.4	27.3	21.4	26.9
259	25.5	74.0	.162	5.1	257.8	2675.1	2.249	29.8	25.8	20.3	26.5
260	26.5	73.0	.158	4.3	257.8	2675.1	2.249	30.6	26.5	20.8	26.3
261	25.8	71.5	.154	4.8	257.8	2675.1	2.249	29.5	25.5	20.2	25.7
262	25.8	71.5	.150	4.4	257.8	2675.1	2.249	29.9	25.9	20.4	25.7
263	26.0	72.5	.154	3.9	257.8	2675.1	2.249	30.9	26.8	21.1	26.2
264	25.6	71.0	.150	4.1	257.8	2675.1	2.249	30.2	26.2	20.7	25.6
265	27.3	72.5	.158	3.9	260.3	2742.7	2.259	31.1	27.1	21.2	26.3
266	25.2	74.0	.164	3.5	260.3	2742.7	2.259	32.3	28.2	22.0	27.0
267	27.5	72.5	.152	4.0	260.3	2742.7	2.259	30.7	26.8	21.0	26.3

268	24.1	72.0	.150	4.5	260.3	2742.7	2.259	29.9	26.0	20.4	26.0
269	24.3	72.0	.148	4.0	260.3	2742.7	2.259	30.5	26.6	20.8	26.1
270	24.2	73.5	.162	4.4	260.3	2742.7	2.259	30.7	26.8	20.9	26.6
271	28.0	73.5	.166	3.9	313.3	3085.9	2.479	32.8	28.9	22.3	27.8
272	26.8	72.0	.154	4.5	313.3	3085.9	2.479	31.2	27.4	21.3	27.1
273	27.5	72.5	.156	4.5	313.3	3085.9	2.479	31.3	27.5	21.4	27.3
274	26.0	71.5	.152	4.4	313.3	3085.9	2.479	31.1	27.4	21.3	26.9
275	25.5	74.0	.164	5.0	313.3	3085.9	2.479	31.2	27.5	21.2	27.7
276	26.9	73.5	.160	4.5	313.3	3085.9	2.479	31.7	27.8	21.5	27.6
277	27.1	72.0	.150	4.4	315.3	3109.5	2.487	31.2	27.4	21.3	27.1
278	27.7	71.5	.150	3.8	315.3	3109.5	2.487	32.0	28.2	21.9	27.1
279	28.0	73.5	.164	4.3	315.3	3109.5	2.487	32.1	28.3	21.9	27.7
280	25.1	72.0	.150	4.3	315.3	3109.5	2.487	31.3	27.6	21.4	27.1
281	26.7	74.0	.164	5.1	315.3	3109.5	2.487	31.2	27.4	21.2	27.7
282	27.2	71.0	.144	4.2	315.3	3109.5	2.487	31.0	27.3	21.3	26.8
283	26.5	73.5	.156	4.3	320.6	3230.1	2.507	31.9	28.4	21.7	27.8
284	26.9	74.0	.164	4.0	320.6	3230.1	2.507	32.8	29.2	22.3	28.0
285	27.8	75.0	.164	4.1	320.6	3230.1	2.507	32.8	29.2	22.2	28.4
286	25.5	71.0	.142	4.1	320.6	3230.1	2.507	31.2	27.8	21.4	26.9
287	26.1	70.5	.144	4.5	320.6	3230.1	2.507	30.6	27.2	21.0	26.6
288	26.2	71.5	.152	4.1	320.6	3230.1	2.507	31.7	28.2	21.7	27.1
289	14.9	73.7	.166	4.3	45.8	594.9	0.948	21.9	16.3	14.9	15.6
290	14.7	72.1	.156	4.9	45.8	594.9	0.948	20.9	15.5	14.3	14.9
291	14.5	72.3	.153	5.0	45.8	594.9	0.948	20.8	15.4	14.2	14.9
292	16.4	73.5	.163	4.4	45.8	594.9	0.948	21.7	16.1	14.8	15.5
293	14.6	72.1	.152	4.4	45.8	594.9	0.948	21.3	15.8	14.5	15.0
294	16.9	70.5	.144	4.3	45.8	594.9	0.948	20.9	15.5	14.4	14.4
295	15.8	73.9	.165	5.0	44.6	580.8	0.935	21.2	15.7	14.4	15.4
296	17.0	73.4	.157	5.3	44.6	580.8	0.935	20.7	15.3	14.1	15.2
297	17.3	73.9	.164	4.2	44.6	580.8	0.935	21.9	16.2	14.9	15.6
298	16.8	73.5	.155	4.4	44.6	580.8	0.935	21.4	15.9	14.6	15.4
299	16.3	70.6	.143	5.0	44.6	580.8	0.935	20.2	15.0	13.9	14.2
300	15.7	71.1	.147	4.7	44.6	580.8	0.935	20.6	15.3	14.1	14.4
301	17.3	73.0	.161	4.2	65.4	839.4	1.133	23.4	18.0	16.0	17.1
302	18.2	73.7	.164	4.9	65.4	834.1	1.133	22.9	17.5	15.6	17.2
303	17.3	73.7	.161	4.5	65.4	834.1	1.133	23.2	17.8	15.8	17.3
304	17.3	72.9	.160	4.0	65.4	834.1	1.133	23.6	18.1	16.1	17.1
305	18.4	71.1	.148	5.5	65.4	834.1	1.133	21.6	16.5	14.8	16.1
306	19.3	72.4	.150	4.8	65.4	834.1	1.133	22.4	17.2	15.3	16.7
307	20.1	74.4	.161	4.6	84.5	1122.8	1.288	24.4	19.4	16.6	19.3
308	20.4	74.2	.166	4.5	84.5	1122.8	1.288	24.6	19.6	16.7	19.3
309	18.6	74.8	.164	4.4	84.5	1122.8	1.288	24.8	19.7	16.8	19.5
310	19.7	71.5	.147	4.6	84.5	1122.8	1.288	23.6	18.7	16.1	18.2
311	19.1	69.7	.145	5.3	84.5	1122.8	1.288	22.6	18.0	15.6	17.4
312	19.8	71.1	.145	4.6	84.5	1122.8	1.288	23.5	18.7	16.1	18.1
313	21.8	72.6	.158	3.6	103.8	1367.9	1.427	26.4	21.4	18.0	20.3
314	21.8	72.9	.159	4.9	103.8	1367.9	1.427	24.8	20.2	16.9	20.1
315	21.9	72.9	.158	4.7	103.8	1367.9	1.427	25.0	20.4	17.0	20.2
316	22.1	72.8	.158	4.3	103.8	1367.9	1.427	25.4	20.7	17.3	20.2
317	21.9	72.3	.152	4.3	103.8	1367.9	1.427	25.2	20.5	17.2	20.0
318	21.7	71.6	.151	3.9	103.8	1367.9	1.427	25.6	20.8	17.5	19.9
319	21.7	73.7	.164	3.6	102.9	1369.9	1.421	26.7	21.7	18.1	20.7
320	19.8	72.5	.155	4.7	102.9	1369.9	1.421	24.8	20.2	16.9	20.0
321	20.6	72.6	.160	4.4	102.9	1369.9	1.421	25.3	20.6	17.3	20.1

322	22.4	73.2	.163	5.7	102.9	1369.9	1.421	24.2	19.7	16.5	20.0
323	21.7	72.5	.154	4.6	102.9	1369.9	1.421	24.9	20.3	17.0	20.1
324	20.3	71.6	.154	5.1	102.9	1369.9	1.421	24.3	19.8	16.6	19.6
325	25.3	74.3	.162	4.8	158.3	1937.7	1.762	27.5	23.2	18.6	23.6
326	23.3	72.4	.150	4.2	158.3	1937.7	1.762	27.5	23.2	18.7	23.0
327	22.9	72.0	.147	3.8	158.3	1937.7	1.762	27.9	23.5	19.0	23.0
328	20.5	73.5	.150	3.9	158.3	1937.7	1.762	28.1	23.7	19.1	23.5
329	25.2	73.5	.159	5.0	158.3	1937.7	1.762	27.0	22.8	18.4	23.3
330	27.1	73.4	.157	4.1	158.3	1937.7	1.762	28.0	23.7	19.1	23.4
331	22.7	72.6	.153	4.3	156.4	1923.0	1.751	27.4	23.2	18.7	23.0
332	23.0	71.9	.145	4.3	156.4	1923.0	1.751	27.0	22.8	18.5	22.7
333	23.0	72.3	.145	4.4	156.4	1923.0	1.751	27.0	22.8	18.4	22.9
334	23.3	70.5	.143	4.0	156.4	1923.0	1.751	27.1	22.9	18.6	22.3
335	24.3	72.5	.153	4.0	156.4	1923.0	1.751	27.8	23.5	19.0	23.1
336	25.0	73.4	.156	4.6	156.4	1923.0	1.751	27.3	23.0	18.6	23.2
337	24.3	72.9	.160	4.5	156.9	1918.1	1.754	27.5	23.2	18.7	23.1
338	23.8	72.0	.151	4.9	156.9	1918.1	1.754	26.6	22.4	18.2	22.7
339	25.3	72.6	.157	4.0	156.9	1918.1	1.754	28.0	23.6	19.1	23.1
340	22.8	70.4	.144	5.0	156.9	1918.1	1.754	26.0	21.9	17.8	22.0
341	22.6	70.6	.145	4.5	156.9	1918.1	1.754	26.6	22.4	18.2	22.2
342	21.8	70.4	.149	4.8	156.9	1918.1	1.754	26.4	22.2	18.1	22.1
343	23.0	70.4	.143	4.5	205.4	2422.1	2.007	28.0	24.3	19.2	24.1
344	24.4	73.8	.160	4.7	205.4	2422.1	2.007	28.9	25.1	19.6	25.3
345	23.4	72.3	.151	4.4	205.4	2422.1	2.007	28.7	25.0	19.6	24.8
346	25.5	71.6	.145	4.4	205.4	2422.1	2.007	28.4	24.7	19.4	24.6
347	25.6	72.9	.158	4.1	205.4	2422.1	2.007	29.5	25.6	20.1	25.1
348	26.3	75.3	.165	4.4	205.4	2422.1	2.007	29.7	25.8	20.1	26.0
349	25.8	71.8	.145	4.5	205.8	2377.0	2.009	28.3	24.4	19.3	24.5
350	24.9	71.9	.153	4.7	205.8	2377.0	2.009	28.3	24.5	19.4	24.5
351	23.8	73.4	.161	4.3	205.8	2377.0	2.009	29.4	25.4	20.0	25.2
352	25.5	71.8	.150	3.8	205.8	2377.0	2.009	29.4	25.4	20.1	24.7
353	24.3	73.8	.164	4.4	205.8	2377.0	2.009	29.4	25.4	20.0	25.3
354	27.3	73.0	.155	4.7	205.8	2377.0	2.009	28.6	24.7	19.5	25.0
355	27.5	71.4	.148	4.5	254.9	2809.4	2.236	29.6	26.1	20.2	25.8
356	28.2	73.3	.159	4.7	254.9	2809.4	2.236	30.0	26.5	20.4	26.4
357	27.4	73.0	.153	4.0	254.9	2809.4	2.236	30.7	27.1	20.9	26.5
358	27.6	74.3	.159	4.0	254.9	2809.4	2.236	31.2	27.5	21.2	27.0
359	27.8	74.0	.163	4.2	254.9	2809.4	2.236	31.0	27.3	21.1	26.8
360	24.7	71.4	.142	5.5	254.9	2809.4	2.236	28.2	24.8	19.3	25.5
361	25.7	70.9	.147	4.4	255.5	2833.0	2.239	29.6	26.2	20.3	25.6
362	25.6	75.1	.167	4.6	255.5	2833.0	2.239	30.8	27.2	20.8	27.1
363	25.9	72.4	.156	4.9	255.5	2833.0	2.239	29.6	26.1	20.2	26.1
364	28.5	71.8	.148	4.1	255.5	2833.0	2.239	30.2	26.7	20.6	26.0
365	27.9	71.8	.151	4.4	255.5	2833.0	2.239	29.9	26.4	20.4	26.0
366	25.3	69.6	.142	5.1	255.5	2833.0	2.239	28.3	25.0	19.5	25.0
367	26.3	73.0	.154	5.0	301.8	3263.4	2.433	30.5	27.5	20.7	27.2
368	27.1	71.9	.145	5.6	301.8	3263.4	2.433	29.2	26.4	20.0	26.6
369	27.5	73.8	.158	4.6	301.8	3165.4	2.433	31.3	27.9	21.2	27.5
370	28.8	73.8	.164	4.7	301.8	3263.4	2.433	31.4	28.3	21.3	27.5
371	29.8	74.3	.162	3.9	301.8	3263.4	2.433	32.6	29.4	22.1	27.9
372	28.3	73.0	.160	4.9	301.8	3263.4	2.433	30.8	27.8	21.0	27.2
373	13.8	71.7	.154	5.0	52.2	609.5	1.012	21.3	15.7	14.6	14.9
374	13.4	72.5	.158	5.5	52.2	609.5	1.012	21.1	15.5	14.4	15.1
375	13.9	70.7	.146	4.7	52.2	609.5	1.012	21.2	15.6	14.5	14.6

376	14.5	72.3	.154	4.9	52.2	609.5	1.012	21.4	15.8	14.6	15.1
377	16.1	74.3	.164	4.3	52.2	609.5	1.012	22.5	16.6	15.3	16.0
378	14.4	71.8	.152	4.7	52.2	609.5	1.012	21.5	15.8	14.7	15.0
379	14.5	72.1	.154	5.2	52.8	619.9	1.018	21.2	15.7	14.5	15.1
380	14.2	71.8	.150	4.8	52.8	619.9	1.018	21.4	15.8	14.6	15.0
381	13.9	71.9	.156	5.0	52.8	619.9	1.018	21.4	15.8	14.6	15.0
382	15.1	73.7	.160	5.0	52.8	619.9	1.018	21.7	16.0	14.8	15.7
383	15.4	72.5	.158	5.2	52.8	619.9	1.018	21.4	15.8	14.6	15.2
384	14.7	72.7	.154	4.0	52.8	619.9	1.018	22.4	16.6	15.3	15.6
385	13.9	71.5	.158	4.9	52.2	619.9	1.012	21.5	15.9	14.7	14.9
386	14.4	73.0	.160	4.6	52.2	619.9	1.012	22.0	16.2	15.0	15.5
387	14.1	71.6	.152	5.3	52.2	619.9	1.012	21.0	15.5	14.3	14.8
388	13.4	71.1	.164	4.6	52.2	619.9	1.012	21.8	16.1	15.0	14.8
389	14.4	73.6	.164	4.8	52.2	619.9	1.012	22.0	16.2	14.9	15.7
390	15.8	70.7	.148	4.7	52.2	619.9	1.012	21.3	15.7	14.6	14.6
391	16.5	71.3	.148	4.7	72.1	852.8	1.189	22.8	17.3	15.6	16.6
392	15.4	71.0	.144	5.2	72.1	852.8	1.189	22.1	16.9	15.2	16.3
393	16.5	70.8	.146	4.8	72.1	852.8	1.189	22.6	17.2	15.5	16.4
394	15.9	70.8	.148	4.9	72.1	852.8	1.189	22.5	17.1	15.4	16.3
395	17.9	73.2	.160	4.5	72.1	852.8	1.189	23.6	17.9	16.0	17.3
396	17.0	73.4	.162	4.3	72.1	852.8	1.189	23.9	18.2	16.2	17.4
397	15.4	71.3	.146	4.9	71.4	844.4	1.184	22.5	17.1	15.4	16.5
398	17.0	71.1	.148	4.1	71.4	844.4	1.184	23.3	17.7	16.0	16.5
399	17.4	73.8	.162	5.1	71.4	844.4	1.184	23.1	17.6	15.7	17.3
400	17.0	73.7	.160	5.3	71.4	844.4	1.184	22.8	17.4	15.5	17.2
401	17.0	70.8	.146	4.5	71.4	844.4	1.184	22.8	17.3	15.6	16.3
402	16.8	70.8	.146	5.2	71.4	844.4	1.184	22.1	16.8	15.2	16.2
403	13.0	73.3	.162	4.3	72.0	859.7	1.188	23.8	18.2	16.2	17.4
404	15.5	72.7	.162	4.5	72.0	859.7	1.188	23.5	18.0	16.1	17.1
405	14.6	71.1	.144	4.8	72.0	859.7	1.188	22.5	17.2	15.4	16.5
406	16.5	73.2	.160	4.7	72.0	859.7	1.188	23.4	17.8	15.9	17.3
407	15.8	72.0	.154	5.1	72.0	859.7	1.188	22.6	17.3	15.5	16.7
408	17.8	73.1	.164	5.3	72.0	859.7	1.188	22.9	17.5	15.6	17.1
409	17.5	71.5	.154	4.7	90.4	1090.4	1.332	24.0	18.8	16.4	18.2
410	17.4	72.1	.156	5.3	90.4	1090.4	1.332	23.6	18.5	16.1	18.2
411	19.1	72.9	.158	4.2	90.4	1090.4	1.332	24.9	19.5	17.0	18.8
412	18.5	70.0	.144	5.3	90.4	1090.4	1.332	22.9	18.0	15.8	17.5
413	17.5	71.3	.148	4.5	90.4	1090.4	1.332	24.0	18.8	16.4	18.1
414	18.1	73.0	.160	4.2	90.4	1090.4	1.332	25.0	19.6	17.0	18.8
415	18.4	72.0	.154	5.2	89.8	1095.3	1.327	23.6	18.5	16.1	18.2
416	17.9	73.6	.156	4.4	89.8	1095.3	1.327	24.7	19.3	16.8	19.0
417	17.9	70.1	.144	4.7	89.8	1095.3	1.327	23.5	18.4	16.1	17.7
418	17.6	73.8	.164	4.2	89.8	1095.3	1.327	25.2	19.8	17.1	19.2
419	17.3	71.8	.148	5.0	89.8	1095.3	1.327	23.5	18.5	16.1	18.2
420	17.6	72.3	.154	5.1	89.8	1095.3	1.327	23.7	18.6	16.2	18.4
421	19.0	69.6	.144	4.5	86.7	1111.0	1.304	23.5	18.5	16.1	17.5
422	21.7	71.2	.152	4.4	86.7	1111.0	1.304	24.0	19.0	16.5	18.2
423	19.6	72.1	.154	4.7	86.7	1111.0	1.304	23.9	18.9	16.3	18.4
424	16.8	70.6	.150	4.7	86.7	1111.0	1.304	23.6	18.6	16.2	17.9
425	16.9	72.5	.156	4.7	86.7	1111.0	1.304	24.0	19.0	16.4	18.6
426	17.8	71.0	.144	4.3	86.7	1111.0	1.304	23.9	18.9	16.3	18.1
427	20.0	71.8	.150	4.9	105.8	1314.0	1.441	24.5	19.7	16.7	19.5
428	20.3	74.3	.164	5.0	105.8	1314.0	1.441	25.2	20.2	17.1	20.4
429	21.4	73.4	.162	4.8	105.8	1314.0	1.441	25.2	20.3	17.1	20.2

430	20.3	70.6	.146	4.7	105.8	1314.0	1.441	24.4	19.6	16.7	19.1
431	20.5	72.0	.154	4.8	105.8	1314.0	1.441	24.8	19.9	16.9	19.6
432	17.9	71.8	.156	4.7	105.8	1314.0	1.441	24.9	20.0	17.0	19.5
433	18.8	70.9	.146	4.8	105.1	1316.9	1.436	24.3	19.6	16.7	19.2
434	20.3	73.3	.158	4.7	105.1	1316.9	1.436	25.1	20.2	17.1	20.1
435	19.8	72.4	.154	5.6	105.1	1316.9	1.436	24.0	19.3	16.4	19.6
436	19.8	72.6	.158	5.9	105.1	1316.9	1.436	23.9	19.2	16.3	19.6
437	20.3	73.4	.160	5.0	105.1	1316.9	1.436	24.9	20.0	16.9	20.1
438	20.5	72.1	.156	4.6	105.1	1316.9	1.436	25.0	20.1	17.1	19.7
439	20.3	71.6	.150	5.7	132.7	1327.7	1.613	24.8	19.5	17.0	19.7
440	21.5	74.8	.162	4.6	132.7	1327.7	1.613	26.8	21.0	18.2	21.2
441	22.0	72.6	.150	4.3	132.7	1327.7	1.613	26.4	20.7	18.0	20.4
442	22.6	71.3	.144	5.0	132.7	1327.7	1.613	25.2	19.8	17.3	19.8
443	18.5	70.3	.146	5.2	132.7	1327.7	1.613	25.0	19.6	17.1	19.4
444	19.5	72.7	.162	4.7	132.7	1327.7	1.613	26.4	20.7	18.0	20.4
445	22.7	71.0	.146	5.1	160.8	2001.4	1.776	26.2	22.3	17.9	22.5
446	22.8	74.5	.164	5.0	160.8	2001.4	1.776	27.4	23.3	18.6	23.9
447	22.5	72.5	.150	4.2	160.8	2001.4	1.776	27.6	23.5	18.8	23.3
448	23.0	73.1	.156	4.6	160.8	2001.4	1.776	27.4	23.3	18.6	23.4
449	21.6	72.5	.154	4.9	160.8	2001.4	1.776	26.9	22.9	18.3	23.1
450	22.0	71.1	.152	5.1	160.8	2001.4	1.776	26.4	22.5	18.1	22.6
451	21.6	71.0	.158	4.9	158.5	1915.1	1.763	26.7	22.5	18.3	22.3
452	23.9	72.2	.158	4.4	158.5	1915.1	1.763	27.5	23.1	18.8	22.9
453	23.5	72.6	.156	4.8	158.5	1915.1	1.763	27.0	22.7	18.4	22.9
454	21.9	73.8	.156	5.3	158.5	1915.1	1.763	26.6	22.4	18.1	23.2
455	20.9	72.2	.146	4.7	158.5	1915.1	1.763	26.7	22.5	18.2	22.8
456	21.7	70.0	.146	4.5	158.5	1915.1	1.763	26.6	22.4	18.3	22.0
457	21.8	71.1	.150	4.8	158.9	1912.2	1.765	26.6	22.4	18.2	22.4
458	21.7	71.8	.154	5.0	158.9	1912.2	1.765	26.6	22.4	18.2	22.6
459	22.6	73.8	.162	4.8	158.9	1912.2	1.765	27.4	23.1	18.6	23.4
460	20.9	72.8	.158	5.2	158.9	1912.2	1.765	26.7	22.4	18.2	22.9
461	22.3	73.1	.158	4.7	158.9	1912.2	1.765	27.3	22.9	18.6	23.1
462	22.5	70.1	.146	4.1	158.9	1912.2	1.765	27.1	22.8	18.6	22.1
463	24.8	71.5	.150	5.0	212.1	2430.9	2.040	28.0	24.3	19.1	24.5
464	24.9	73.6	.160	5.3	212.1	2430.9	2.040	28.4	24.6	19.3	25.2
465	24.0	71.1	.150	4.7	212.1	2430.9	2.040	28.3	24.5	19.4	24.5
466	23.3	71.8	.158	4.6	212.1	2430.9	2.040	28.8	25.0	19.7	24.7
467	25.0	73.3	.162	4.3	212.1	2430.9	2.040	29.6	25.6	20.1	25.4
468	24.3	72.0	.154	4.7	212.1	2430.9	2.040	28.6	24.8	19.5	24.8
469	23.0	71.3	.150	5.3	209.3	2251.5	2.026	27.6	23.4	18.9	24.0
470	25.5	72.8	.152	4.1	209.3	2251.5	2.026	29.3	24.9	20.0	24.8
471	24.3	73.3	.160	5.0	209.3	2251.5	2.026	28.6	24.2	19.4	24.8
472	22.4	72.5	.156	5.0	209.3	2251.5	2.026	28.3	24.0	19.3	24.5
473	22.8	72.0	.152	4.8	209.3	2251.5	2.026	28.3	24.0	19.3	24.4
474	25.1	71.5	.144	4.6	209.3	2251.5	2.026	28.2	23.9	19.3	24.2
475	21.8	70.3	.148	5.3	211.9	2322.1	2.039	27.4	23.4	18.8	23.8
476	24.3	72.1	.162	4.7	211.9	2322.1	2.039	28.9	24.7	19.7	24.6
477	24.2	71.4	.160	5.0	211.9	2322.1	2.039	28.3	24.2	19.4	24.3
478	22.0	70.3	.146	5.1	211.9	2322.1	2.039	27.5	23.5	18.9	23.8
479	22.4	72.1	.154	5.0	211.9	2322.1	2.039	28.2	24.1	19.3	24.5
480	23.5	70.3	.146	4.9	211.9	2322.1	2.039	27.8	23.7	19.1	23.9
481	26.1	73.2	.160	4.7	259.4	2686.8	2.255	30.2	26.1	20.5	26.3
482	26.6	72.3	.156	5.2	259.4	2686.8	2.255	29.3	25.4	20.0	25.9
483	26.0	71.3	.152	4.5	259.4	2686.8	2.255	29.8	25.8	20.4	25.7

484	24.5	72.8	.154	4.3	259.4	2686.8	2.255	30.4	26.3	20.7	26.3
485	24.8	71.8	.158	5.0	259.4	2686.8	2.255	29.5	25.6	20.2	25.8
486	25.4	72.3	.156	4.7	259.4	2686.8	2.255	29.9	25.9	20.4	26.0
487	25.8	73.3	.164	5.2	258.9	2676.1	2.253	29.7	25.7	20.2	26.3
488	25.8	70.3	.146	4.8	258.9	2676.1	2.253	29.0	25.1	19.9	25.2
489	25.8	73.6	.160	5.3	258.9	2676.1	2.253	29.5	25.5	20.1	26.3
490	26.1	71.8	.158	5.0	258.9	2676.1	2.253	29.5	25.5	20.2	25.8
491	25.4	73.8	.164	5.0	258.9	2676.1	2.253	30.0	26.0	20.4	26.5
492	26.5	73.1	.160	4.7	258.9	2676.1	2.253	30.1	26.1	20.5	26.3
493	25.6	70.2	.146	4.6	256.2	2722.1	2.242	29.2	25.4	20.0	25.2
494	26.0	71.7	.152	4.9	256.2	2722.1	2.242	29.3	25.5	20.0	25.7
495	24.3	73.8	.162	5.1	256.2	2722.1	2.242	29.8	26.0	20.2	26.5
496	25.6	71.8	.150	4.5	256.2	2722.1	2.242	29.7	25.9	20.3	25.9
497	26.3	73.0	.154	5.4	256.2	2722.1	2.242	29.0	25.3	19.8	26.1
498	25.5	71.4	.152	4.3	256.2	2722.1	2.242	30.0	26.2	20.5	25.8
499	27.5	72.2	.156	3.9	311.1	3079.1	2.470	32.1	28.3	21.9	27.2
500	25.4	72.5	.154	4.4	311.1	3079.1	2.470	31.3	27.5	21.3	27.2
501	26.6	72.6	.150	4.4	311.1	3079.1	2.470	31.1	27.4	21.2	27.3
502	26.0	71.6	.148	4.4	311.1	3079.1	2.470	30.9	27.1	21.1	26.9
503	26.5	72.2	.152	4.2	311.1	3079.1	2.470	31.5	27.7	21.5	27.2
504	28.3	73.8	.162	4.5	311.1	3079.1	2.470	31.8	27.9	21.6	27.7
505	27.5	74.4	.162	4.3	308.9	3181.1	2.461	32.1	28.6	21.8	28.0
506	25.7	72.2	.158	5.0	308.9	3181.1	2.461	30.6	27.3	20.9	27.0
507	28.0	72.8	.164	4.6	308.9	3181.1	2.461	31.5	28.0	21.4	27.3
508	27.5	73.0	.160	4.7	308.9	3181.1	2.461	31.2	27.8	21.3	27.3
509	25.8	71.3	.164	4.2	308.9	3181.1	2.461	31.8	28.3	21.7	26.8
510	26.1	72.6	.156	4.6	308.9	3181.1	2.461	31.1	27.7	21.2	27.2
511	26.3	71.3	.152	4.5	313.3	3112.4	2.479	30.9	27.3	21.2	26.8
512	27.9	71.8	.150	4.2	313.3	3112.4	2.479	31.4	27.7	21.5	27.1
513	28.1	72.3	.158	5.0	313.3	3112.4	2.479	30.7	27.1	21.0	27.1
514	26.4	72.1	.148	5.1	313.3	3112.4	2.479	30.2	26.6	20.6	27.0
515	25.8	72.3	.148	4.2	313.3	3112.4	2.479	31.4	27.7	21.4	27.3
516	25.7	71.3	.146	4.8	313.3	3112.4	2.479	30.3	26.7	20.7	26.8
517	17.5	77.3	.179	6.3	46.7	716.8	0.957	21.1	16.2	14.2	17.2
518	16.5	75.0	.176	6.6	46.7	716.8	0.957	20.6	15.8	14.0	16.3
519	17.1	77.0	.175	6.2	46.7	716.8	0.957	21.0	16.2	14.2	17.1
520	15.1	76.5	.178	6.3	46.7	716.8	0.957	21.0	16.1	14.2	16.9
521	15.7	75.3	.173	6.4	46.7	716.8	0.957	20.7	15.9	14.0	16.4
522	18.0	76.5	.174	6.6	46.7	716.8	0.957	20.7	15.9	14.0	16.9
523	16.8	75.3	.168	7.9	49.4	705.2	0.984	19.9	15.2	13.5	16.1
524	15.9	75.0	.172	7.0	49.4	705.2	0.984	20.5	15.6	13.9	16.2
525	17.1	76.0	.178	6.4	49.4	705.2	0.984	21.1	16.1	14.2	16.7
526	16.0	74.0	.167	6.3	49.4	705.2	0.984	20.7	15.7	14.0	16.0
527	16.5	76.0	.176	6.1	49.4	705.2	0.984	21.3	16.2	14.4	16.8
528	15.3	75.5	.170	5.7	49.4	705.2	0.984	21.4	16.3	14.5	16.7
529	20.0	77.0	.178	6.8	65.4	974.4	1.132	22.2	17.6	14.9	18.7
530	21.5	77.5	.175	6.1	65.4	974.4	1.132	22.6	17.9	15.2	19.1
531	14.7	76.0	.177	6.6	65.4	974.4	1.132	22.2	17.6	15.0	18.4
532	20.1	76.5	.176	6.0	65.4	974.4	1.132	22.6	17.9	15.3	18.7
533	19.8	76.8	.175	5.1	65.4	974.4	1.132	23.4	18.5	15.8	19.0
534	20.1	75.5	.175	5.9	65.4	974.4	1.132	22.5	17.8	15.2	18.4
535	19.9	75.8	.175	5.9	63.1	976.8	1.112	22.4	17.9	15.2	18.5
536	18.8	76.0	.177	6.3	63.1	976.8	1.112	22.2	17.7	15.0	18.4
537	19.5	76.3	.174	6.1	63.1	976.8	1.112	22.3	17.8	15.1	18.6

538	18.7	77.3	.179	6.8	63.1	976.8	1.112	22.1	17.6	14.9	18.8
539	19.6	75.5	.175	6.3	63.1	976.8	1.112	22.1	17.6	14.9	18.3
540	18.2	75.5	.174	7.3	63.1	976.8	1.112	21.5	17.1	14.5	18.1
541	20.4	75.5	.176	5.7	63.0	967.6	1.112	22.6	18.0	15.3	18.4
542	19.4	75.8	.177	5.7	63.0	967.6	1.112	22.7	18.0	15.3	18.5
543	20.5	76.0	.176	5.9	63.0	967.6	1.112	22.5	17.9	15.2	18.5
544	20.2	76.8	.179	6.3	63.0	967.6	1.112	22.3	17.7	15.0	18.7
545	21.1	77.0	.176	5.9	63.0	967.6	1.112	22.6	18.0	15.2	18.9
546	19.3	76.8	.180	6.0	63.0	967.6	1.112	22.6	17.9	15.2	18.7
547	21.4	75.8	.176	6.1	82.0	1161.4	1.268	23.5	18.9	15.9	19.6
548	19.3	76.0	.179	6.8	82.0	1161.4	1.268	23.1	18.6	15.6	19.6
549	25.4	77.5	.178	5.7	82.0	1161.4	1.268	24.1	19.4	16.2	20.4
550	20.8	76.0	.178	7.5	82.0	1161.4	1.268	22.6	18.2	15.3	19.4
551	20.5	76.8	.179	6.9	82.0	1161.4	1.268	23.1	18.6	15.6	19.8
552	22.0	75.3	.175	7.3	82.0	1161.4	1.268	22.6	18.2	15.3	19.2
553	21.1	76.0	.175	6.8	83.8	1198.8	1.282	23.1	18.7	15.6	19.8
554	21.6	75.5	.176	6.8	83.8	1198.8	1.282	23.1	18.6	15.6	19.6
555	20.0	75.5	.177	7.3	83.8	1198.8	1.282	22.8	18.4	15.4	19.5
556	20.6	76.0	.176	6.3	83.8	1198.8	1.282	23.4	18.9	15.8	19.9
557	22.0	76.0	.178	6.0	83.8	1198.8	1.282	23.8	19.2	16.1	20.0
558	20.5	76.3	.180	7.9	83.8	1198.8	1.282	22.6	18.2	15.2	19.6
559	20.8	75.8	.177	6.6	81.2	1190.3	1.262	23.1	18.7	15.6	19.7
560	18.9	76.0	.179	6.9	81.2	1190.3	1.262	23.0	18.6	15.5	19.7
561	21.2	77.3	.178	6.3	81.2	1190.3	1.262	23.5	19.0	15.8	20.3
562	20.3	76.5	.175	6.0	81.2	1190.3	1.262	23.6	19.1	15.9	20.1
563	21.1	77.0	.178	6.3	81.2	1190.3	1.262	23.5	19.0	15.8	20.2
564	20.8	77.3	.179	6.1	81.2	1190.3	1.262	23.7	19.2	16.0	20.3
565	23.9	76.3	.169	6.6	129.9	1655.4	1.596	25.2	21.0	17.0	22.6
566	22.6	75.0	.166	5.9	129.9	1655.4	1.596	25.5	21.2	17.3	22.2
567	20.6	74.5	.166	7.0	129.9	1655.4	1.596	24.6	20.4	16.7	21.8
568	22.7	76.0	.172	6.6	129.9	1655.4	1.596	25.3	21.0	17.1	22.5
569	21.3	76.0	.173	6.4	129.9	1655.4	1.596	25.4	21.1	17.2	22.5
570	22.8	74.8	.169	6.1	129.9	1655.4	1.596	25.4	21.1	17.2	22.1
571	22.2	75.0	.171	6.3	130.3	1698.9	1.598	25.3	21.2	17.2	22.3
572	21.1	74.8	.166	5.7	130.3	1698.9	1.598	25.7	21.5	17.4	22.4
573	22.2	74.8	.167	5.9	130.3	1698.9	1.598	25.6	21.4	17.3	22.3
574	23.4	76.3	.173	6.6	130.3	1698.9	1.598	25.4	21.2	17.1	22.7
575	22.2	75.8	.179	7.3	130.3	1698.9	1.598	25.0	20.9	16.9	22.4
576	23.5	78.3	.180	7.0	130.3	1698.9	1.598	25.5	21.3	17.1	23.4
577	23.3	76.5	.177	6.1	129.7	1687.2	1.595	25.9	21.6	17.5	22.9
578	21.4	77.0	.178	6.3	129.7	1687.2	1.595	25.8	21.5	17.4	23.0
579	23.2	76.5	.176	6.1	129.7	1687.2	1.595	25.8	21.6	17.4	22.9
580	23.0	76.0	.177	6.1	129.7	1687.2	1.595	25.8	21.6	17.4	22.7
581	22.2	75.8	.175	7.7	129.7	1687.2	1.595	24.6	20.5	16.6	22.2
582	21.1	76.5	.175	5.9	129.7	1687.2	1.595	26.0	21.7	17.6	22.9
583	22.9	75.5	.172	6.8	162.2	2038.1	1.783	26.2	22.4	17.7	24.0
584	23.7	74.8	.170	6.4	162.2	2038.1	1.783	26.3	22.5	17.8	23.8
585	23.8	74.8	.167	7.3	162.2	2038.1	1.783	25.6	21.9	17.3	23.6
586	23.0	75.5	.171	7.1	162.2	2038.1	1.783	25.9	22.2	17.6	23.9
587	22.5	74.8	.170	6.0	162.2	2038.1	1.783	26.7	22.8	18.1	23.9
588	23.4	75.0	.170	6.1	162.2	2038.1	1.783	26.6	22.8	18.0	23.9
589	24.5	76.0	.172	6.1	161.3	2046.7	1.779	26.8	23.0	18.1	24.3
590	23.8	75.0	.169	6.9	161.3	2046.7	1.779	25.9	22.2	17.6	23.8
591	25.1	74.8	.166	6.9	161.3	2046.7	1.779	25.8	22.1	17.5	23.7

592	24.0	75.0	.167	6.4	161.3	2046.7	1.779	26.2	22.5	17.8	23.9
593	22.2	75.5	.171	6.6	161.3	2046.7	1.779	26.3	22.6	17.8	24.0
594	23.4	75.0	.169	6.4	161.3	2046.7	1.779	26.3	22.5	17.8	23.9
595	22.1	74.5	.171	6.8	157.9	1927.7	1.760	25.9	21.8	17.5	23.2
596	22.7	75.0	.170	6.1	157.9	1927.7	1.760	26.5	22.3	17.9	23.5
597	22.8	75.3	.173	7.0	157.9	1927.7	1.760	25.9	21.9	17.5	23.4
598	23.6	74.3	.169	6.1	157.9	1927.7	1.760	26.3	22.2	17.9	23.3
599	23.6	76.0	.174	5.9	157.9	1927.7	1.760	26.9	22.7	18.2	24.0
600	24.6	75.3	.173	6.3	157.9	1927.7	1.760	26.4	22.3	17.9	23.6
601	25.8	75.5	.172	7.0	191.6	2341.7	1.939	26.9	23.4	18.2	25.1
602	25.0	76.0	.173	6.6	191.6	2341.7	1.939	27.4	23.8	18.5	25.4
603	24.3	76.0	.168	6.3	191.6	2341.7	1.939	27.5	23.9	18.6	25.4
604	24.5	76.3	.170	6.8	191.6	2341.7	1.939	27.2	23.6	18.3	25.4
605	25.2	76.3	.170	6.1	191.6	2341.7	1.939	27.7	24.1	18.7	25.6
606	23.6	73.5	.166	6.1	191.6	2341.7	1.939	27.2	23.7	18.5	24.5
607	25.7	76.0	.172	7.0	191.6	2341.7	1.939	27.0	23.5	18.2	25.3
608	22.5	75.3	.170	7.3	191.6	2341.7	1.939	26.6	23.1	18.0	24.9
609	26.0	76.5	.172	7.0	191.6	2341.7	1.939	27.1	23.5	18.3	25.5
610	24.1	74.8	.167	7.3	191.6	2341.7	1.939	26.5	23.1	18.0	24.8
611	22.1	75.3	.169	5.9	191.6	2341.7	1.939	27.7	24.1	18.8	25.2
612	23.5	75.8	.173	5.9	191.6	2341.7	1.939	27.9	24.3	18.9	25.4
613	23.4	75.0	.167	7.3	192.3	2360.7	1.942	26.5	23.1	18.0	24.9
614	25.9	74.5	.166	6.6	192.3	2360.7	1.942	27.0	23.5	18.3	24.9
615	25.9	75.3	.169	6.8	192.3	2360.7	1.942	27.0	23.5	18.3	25.1
616	23.2	75.3	.173	7.0	192.3	2360.7	1.942	26.9	23.5	18.2	25.0
617	24.9	75.0	.170	7.3	192.3	2360.7	1.942	26.6	23.2	18.1	24.9
618	25.1	75.8	.172	6.4	192.3	2360.7	1.942	27.4	23.9	18.6	25.4
619	27.9	76.5	.173	5.2	210.1	2475.4	2.030	29.3	25.6	19.8	26.4
620	26.2	77.0	.172	5.4	210.1	2475.4	2.030	29.1	25.4	19.6	26.5
621	26.0	75.5	.172	5.9	210.1	2475.4	2.030	28.4	24.8	19.2	25.9
622	23.7	75.0	.164	6.3	210.1	2475.4	2.030	27.7	24.1	18.7	25.6
623	24.8	76.0	.172	5.2	210.1	2475.4	2.030	29.2	25.5	19.7	26.2
624	25.3	75.5	.171	6.3	210.1	2475.4	2.030	27.9	24.4	18.9	25.8
625	25.4	77.3	.166	6.1	210.7	2492.6	2.033	28.3	24.7	19.0	26.5
626	28.5	76.3	.167	5.3	210.7	2492.6	2.033	28.9	25.3	19.5	26.3
627	24.2	75.3	.170	5.9	210.7	2492.6	2.033	28.3	24.8	19.2	25.8
628	25.3	74.8	.169	6.6	210.7	2492.6	2.033	27.6	24.1	18.7	25.5
629	23.9	75.3	.174	6.8	210.7	2492.6	2.033	27.6	24.2	18.7	25.6
630	25.4	74.5	.167	6.6	210.7	2492.6	2.033	27.5	24.0	18.7	25.4
631	26.0	75.5	.172	6.0	210.6	2493.7	2.032	28.3	24.8	19.2	25.9
632	23.3	76.8	.174	6.3	210.6	2493.7	2.032	28.2	24.7	19.0	26.3
633	25.3	75.0	.166	5.5	210.6	2493.7	2.032	28.5	24.9	19.3	25.8
634	25.4	76.3	.174	6.0	210.6	2493.7	2.032	28.5	24.9	19.2	26.2
635	25.2	75.3	.167	6.8	210.6	2493.7	2.032	27.4	24.0	18.6	25.6
636	24.7	76.3	.170	6.1	210.6	2493.7	2.032	28.2	24.7	19.1	26.1
637	29.0	75.8	.173	6.0	313.4	3313.2	2.479	30.8	27.7	20.8	28.1
638	28.0	75.3	.169	5.8	313.4	3313.2	2.479	30.7	27.7	20.8	28.0
639	28.6	75.0	.173	5.9	313.4	3313.2	2.479	30.7	27.7	20.8	27.9
640	28.9	75.0	.168	6.3	313.4	3313.2	2.479	30.2	27.2	20.4	27.8
641	28.1	75.5	.174	5.7	313.4	3313.2	2.479	31.1	28.0	21.0	28.1
642	30.1	76.0	.172	5.6	313.4	3313.2	2.479	31.1	28.1	21.0	28.3
643	28.0	74.8	.166	7.9	314.8	3333.5	2.485	28.7	25.9	19.5	27.3
644	31.3	75.5	.167	5.4	314.8	3333.5	2.485	31.1	28.1	21.0	28.2
645	29.6	76.0	.173	5.4	314.8	3333.5	2.485	31.4	28.3	21.2	28.3

646	30.9	75.3	.167	5.2	314.8	3333.5	2.485	31.4	28.3	21.2	28.1
647	28.4	74.8	.169	5.7	314.8	3333.5	2.485	30.8	27.8	20.9	27.8
648	29.2	75.0	.172	6.3	314.8	3333.5	2.485	30.2	27.3	20.5	27.8
649	27.8	76.0	.171	6.3	316.3	3368.9	2.491	30.4	27.6	20.6	28.1
650	28.5	75.8	.174	6.3	316.3	3368.9	2.491	30.5	27.6	20.6	28.1
651	29.4	76.0	.171	6.1	316.3	3368.9	2.491	30.6	27.7	20.7	28.2
652	29.8	75.0	.169	5.7	316.3	3368.9	2.491	30.9	28.0	20.9	27.9
653	29.1	74.5	.168	6.3	316.3	3368.9	2.491	30.1	27.2	20.4	27.6
654	28.0	74.8	.166	5.7	316.3	3368.9	2.491	30.7	27.8	20.8	27.8
655	17.2	77.0	.178	6.8	85.0	305.4	1.291	23.4	14.9	15.7	15.0
656	15.3	77.5	.175	6.1	85.0	305.4	1.291	23.8	15.2	16.0	15.3
657	14.5	76.0	.177	6.6	85.0	305.4	1.291	23.4	14.9	15.8	14.7
658	15.3	76.5	.176	6.0	85.0	305.4	1.291	23.8	15.2	16.1	15.0
659	15.5	76.8	.175	5.1	85.0	305.4	1.291	24.7	15.7	16.6	15.3
660	17.4	75.5	.175	5.9	85.0	305.4	1.291	23.7	15.1	16.1	14.6
661	15.0	75.8	.175	5.9	85.3	311.6	1.294	23.8	15.2	16.1	14.8
662	12.3	76.0	.177	6.4	85.3	311.6	1.294	23.6	15.0	15.9	14.8
663	14.2	76.3	.174	6.1	85.3	311.6	1.294	23.7	15.1	16.0	14.9
664	15.6	77.3	.179	6.8	85.3	311.6	1.294	23.5	15.0	15.8	15.1
665	15.1	75.5	.175	6.4	85.3	311.6	1.294	23.4	15.0	15.9	14.6
666	16.4	75.5	.174	7.3	85.3	311.6	1.294	22.8	14.5	15.4	14.4
667	13.6	75.5	.176	5.7	84.9	312.8	1.291	24.0	15.3	16.2	14.7
668	14.9	75.8	.177	5.7	84.9	312.8	1.291	24.0	15.4	16.3	14.8
669	12.7	76.0	.176	5.9	84.9	312.8	1.291	23.9	15.2	16.1	14.9
670	14.1	76.8	.179	6.4	84.9	312.8	1.291	23.7	15.1	16.0	15.0
671	16.0	77.0	.176	5.9	84.9	312.8	1.291	24.0	15.3	16.2	15.2
672	11.5	76.8	.180	6.0	84.9	312.8	1.291	24.0	15.3	16.2	15.1
673	13.5	75.8	.176	6.1	109.0	355.7	1.462	24.9	15.9	16.8	15.4
674	11.0	76.0	.179	6.8	109.0	355.7	1.462	24.5	15.6	16.5	15.3
675	15.3	77.5	.178	5.7	109.0	355.7	1.462	25.5	16.3	17.2	16.1
676	14.9	76.0	.178	7.5	109.0	355.7	1.462	24.0	15.3	16.2	15.2
677	13.8	76.8	.179	6.9	109.0	355.7	1.462	24.5	15.7	16.5	15.6
678	16.3	75.3	.175	7.3	109.0	355.7	1.462	23.9	15.3	16.2	14.9
679	17.3	76.0	.175	6.8	109.7	360.6	1.466	24.4	15.6	16.5	15.4
680	14.4	75.5	.176	6.8	109.7	360.6	1.466	24.3	15.6	16.5	15.2
681	16.0	75.5	.177	7.3	109.7	360.6	1.466	24.1	15.4	16.3	15.1
682	14.6	76.0	.176	6.4	109.7	360.6	1.466	24.7	15.8	16.7	15.5
683	15.3	76.0	.178	6.0	109.7	360.6	1.466	25.1	16.1	17.0	15.5
684	14.2	76.3	.180	7.9	109.7	360.6	1.466	23.8	15.2	16.1	15.2
685	14.7	75.8	.177	6.6	109.9	368.6	1.468	24.6	15.8	16.6	15.4
686	15.6	76.0	.179	6.9	109.9	368.6	1.468	24.4	15.7	16.5	15.4
687	14.0	77.3	.178	6.4	109.9	368.6	1.468	25.0	16.0	16.8	16.0
688	13.3	76.5	.175	6.0	109.9	368.6	1.468	25.1	16.1	16.9	15.8
689	17.7	77.0	.178	6.4	109.9	368.6	1.468	24.9	16.0	16.8	15.9
690	15.9	77.3	.179	6.1	109.9	368.6	1.468	25.2	16.2	17.0	16.0
691	16.9	77.0	.178	6.0	131.3	416.5	1.605	26.2	16.9	17.6	16.6
692	16.5	76.0	.176	6.6	131.3	416.5	1.605	25.5	16.4	17.2	16.1
693	17.0	76.5	.175	7.1	131.3	416.5	1.605	25.1	16.2	17.0	16.2
694	17.9	75.8	.178	6.8	131.3	416.5	1.605	25.3	16.3	17.1	16.0
695	14.9	76.0	.178	6.6	131.3	416.5	1.605	25.5	16.5	17.3	16.1
696	16.9	76.5	.180	6.8	131.3	416.5	1.605	25.5	16.4	17.2	16.3
697	12.3	76.5	.180	6.4	131.7	410.3	1.607	25.8	16.6	17.4	16.3
698	16.5	75.5	.177	6.4	131.7	410.3	1.607	25.6	16.5	17.3	16.0
699	15.9	76.5	.176	7.3	131.7	410.3	1.607	25.0	16.1	16.9	16.1

700	15.6	75.8	.176	6.8	131.7	410.3	1.607	25.3	16.3	17.1	15.9
701	15.0	76.3	.178	6.4	131.7	410.3	1.607	25.8	16.6	17.4	16.2
702	14.4	76.0	.179	6.4	131.7	410.3	1.607	25.8	16.6	17.4	16.1
703	14.3	76.3	.178	6.0	132.0	423.8	1.609	26.1	16.9	17.6	16.4
704	13.0	76.5	.177	6.6	132.0	423.8	1.609	25.6	16.6	17.3	16.4
705	11.4	74.5	.177	6.6	132.0	423.8	1.609	25.3	16.4	17.2	15.6
706	14.7	76.0	.176	5.9	132.0	423.8	1.609	26.1	16.9	17.6	16.3
707	15.5	77.0	.176	5.8	132.0	423.8	1.609	26.3	17.0	17.7	16.7
708	12.1	75.8	.178	7.3	132.0	423.8	1.609	25.0	16.2	16.9	15.9
709	19.7	76.3	.169	6.6	225.8	633.6	2.105	28.2	18.6	19.0	19.1
710	18.3	75.0	.166	5.9	225.8	633.6	2.105	28.5	18.8	19.3	18.8
711	15.1	74.5	.166	7.0	225.8	633.6	2.105	27.5	18.1	18.6	18.3
712	20.1	76.0	.172	6.6	225.8	633.6	2.105	28.3	18.7	19.1	19.0
713	17.7	76.0	.173	6.4	225.8	633.6	2.105	28.4	18.8	19.2	19.0
714	20.6	74.8	.169	6.1	225.8	633.6	2.105	28.4	18.7	19.2	18.6
715	18.6	75.0	.171	6.4	226.4	621.3	2.107	28.3	18.6	19.2	18.6
716	19.1	74.8	.166	5.7	226.4	621.3	2.107	28.7	18.9	19.5	18.7
717	18.9	74.8	.167	5.9	226.4	621.3	2.107	28.5	18.8	19.3	18.6
718	18.8	76.3	.173	6.6	226.4	621.3	2.107	28.3	18.6	19.1	19.0
719	19.4	75.8	.179	7.3	226.4	621.3	2.107	27.9	18.4	18.9	18.7
720	20.1	78.3	.180	7.0	226.4	621.3	2.107	28.5	18.7	19.1	19.6
721	20.8	76.5	.177	6.1	223.6	621.3	2.094	28.9	19.0	19.5	19.2
722	20.3	77.0	.178	6.4	223.6	621.3	2.094	28.7	18.9	19.4	19.3
723	21.2	76.5	.176	6.1	223.6	621.3	2.094	28.8	19.0	19.4	19.2
724	20.8	76.0	.177	6.1	223.6	621.3	2.094	28.8	19.0	19.4	19.0
725	22.0	75.8	.175	7.7	223.6	621.3	2.094	27.4	18.0	18.5	18.5
726	20.3	76.5	.175	5.9	223.6	621.3	2.094	29.0	19.1	19.6	19.2
727	18.3	75.5	.172	6.8	255.8	672.2	2.240	28.7	18.9	19.4	19.4
728	17.8	74.8	.170	6.4	255.8	672.2	2.240	28.8	19.0	19.5	19.2
729	20.2	74.8	.167	7.3	255.8	672.2	2.240	28.0	18.5	19.0	19.1
730	20.2	75.5	.171	7.1	255.8	672.2	2.240	28.4	18.8	19.2	19.4
731	19.2	74.8	.170	6.0	255.8	672.2	2.240	29.2	19.3	19.8	19.3
732	18.4	75.0	.170	6.1	255.8	672.2	2.240	29.2	19.3	19.8	19.4
733	19.8	76.0	.172	6.1	253.2	678.9	2.228	29.3	19.4	19.8	19.8
734	19.6	75.0	.169	6.9	253.2	678.9	2.228	28.4	18.8	19.2	19.2
735	19.0	74.8	.166	6.9	253.2	678.9	2.228	28.2	18.7	19.1	19.1
736	20.3	75.0	.167	6.4	253.2	678.9	2.228	28.7	19.0	19.5	19.3
737	19.6	75.5	.171	6.6	253.2	678.9	2.228	28.8	19.1	19.5	19.5
738	18.8	75.0	.169	6.4	253.2	678.9	2.228	28.8	19.0	19.5	19.3
739	20.9	74.5	.171	6.8	253.3	695.5	2.229	28.4	18.9	19.3	19.2
740	19.7	75.0	.170	6.1	253.3	695.5	2.229	29.1	19.3	19.7	19.5
741	19.8	75.3	.173	7.0	253.3	695.5	2.229	28.5	18.9	19.3	19.4
742	19.9	74.3	.169	6.1	253.3	695.5	2.229	29.0	19.2	19.7	19.2
743	19.5	76.0	.174	5.9	253.3	695.5	2.229	29.6	19.7	20.0	19.9
744	20.0	75.3	.173	6.4	253.3	695.5	2.229	29.1	19.3	19.7	19.6
745	19.6	75.5	.172	7.0	304.7	774.0	2.444	29.5	19.6	20.0	20.8
746	22.7	76.0	.173	6.6	304.7	774.0	2.444	30.0	20.0	20.3	21.0
747	21.4	76.0	.168	6.3	304.7	774.0	2.444	30.2	20.1	20.4	21.1
748	19.8	76.3	.170	6.8	304.7	774.0	2.444	29.8	19.8	20.1	21.1
749	20.6	76.3	.170	6.1	304.7	774.0	2.444	30.4	20.2	20.5	21.2
750	21.5	73.5	.166	6.1	304.7	774.0	2.444	29.8	19.8	20.3	20.2
751	21.8	76.0	.172	7.0	304.9	783.2	2.446	29.6	19.7	20.0	21.0
752	19.0	75.3	.170	7.3	304.9	783.2	2.446	29.2	19.4	19.7	20.7
753	22.0	76.5	.172	7.0	304.9	783.2	2.446	29.7	19.8	20.0	21.2

754	19.9	74.8	.167	7.3	304.9	783.2	2.446	29.1	19.4	19.7	20.5
755	18.3	75.3	.169	5.9	304.9	783.2	2.446	30.4	20.3	20.6	21.0
756	21.3	75.8	.173	5.9	304.9	783.2	2.446	30.7	20.4	20.7	21.2
757	20.5	75.0	.167	7.3	304.8	775.2	2.445	29.1	19.4	19.7	20.5
758	20.5	74.5	.166	6.6	304.8	775.2	2.445	29.6	19.7	20.1	20.5
759	21.5	75.3	.169	6.8	304.8	775.2	2.445	29.6	19.7	20.0	20.7
760	18.1	75.3	.173	7.0	304.8	775.2	2.445	29.5	19.6	20.0	20.7
761	21.2	75.0	.170	7.3	304.8	775.2	2.445	29.2	19.4	19.8	20.5
762	21.1	75.8	.172	6.4	304.8	775.2	2.445	30.1	20.0	20.3	21.0
763	22.8	76.5	.173	5.2	360.1	875.8	2.657	32.6	21.8	22.0	23.0
764	21.0	77.0	.172	5.4	360.1	875.8	2.657	32.4	21.7	21.8	23.1
765	21.9	75.5	.172	5.9	360.1	875.8	2.657	31.6	21.2	21.4	22.4
766	21.9	75.0	.164	6.4	360.1	875.8	2.657	30.8	20.6	20.9	22.2
767	22.9	76.0	.172	5.2	360.1	875.8	2.657	32.5	21.8	22.0	22.8
768	27.4	75.5	.171	6.4	360.1	875.8	2.657	31.1	20.8	21.1	22.3
769	22.2	77.3	.166	6.1	356.0	880.1	2.642	31.4	21.0	21.1	23.0
770	23.8	76.3	.167	5.3	356.0	880.1	2.642	32.1	21.6	21.7	22.8
771	22.2	75.3	.170	5.9	356.0	880.1	2.642	31.5	21.1	21.3	22.3
772	20.3	74.8	.169	6.6	356.0	880.1	2.642	30.6	20.5	20.8	22.0
773	21.6	75.3	.174	6.8	356.0	880.1	2.642	30.7	20.6	20.8	22.1
774	24.0	74.5	.167	7.0	356.0	880.1	2.642	30.1	20.2	20.4	21.8
775	23.9	75.5	.172	6.0	357.4	877.6	2.648	31.5	21.1	21.3	22.4
776	25.3	76.8	.174	6.4	357.4	877.6	2.648	31.4	21.0	21.2	22.8
777	21.2	75.0	.166	5.5	357.4	877.6	2.648	31.7	21.2	21.5	22.3
778	23.0	76.3	.174	6.0	357.4	877.6	2.648	31.7	21.2	21.4	22.7
779	21.9	75.3	.167	6.8	357.4	877.6	2.648	30.5	20.4	20.6	22.1
780	22.5	76.3	.170	6.1	357.4	877.6	2.648	31.4	21.0	21.2	22.6
781	24.6	75.8	.173	6.0	410.6	978.3	2.838	32.5	21.9	21.9	23.9
782	21.6	75.3	.169	5.8	410.6	978.3	2.838	32.4	21.9	22.0	23.7
783	24.4	75.0	.173	5.9	410.6	978.3	2.838	32.4	21.9	22.0	23.6
784	23.3	75.0	.168	6.3	410.6	978.3	2.838	31.8	21.5	21.6	23.5
785	23.6	75.5	.174	5.7	410.6	978.3	2.838	32.8	22.1	22.2	23.8
786	23.4	76.0	.172	5.6	410.6	978.3	2.838	32.9	22.2	22.2	24.0
787	22.9	74.8	.166	7.9	396.3	954.9	2.788	30.1	20.3	20.4	22.7
788	27.0	75.5	.167	5.4	396.3	954.9	2.788	32.6	21.9	22.0	23.5
789	24.2	76.0	.173	5.4	396.3	954.9	2.788	32.9	22.1	22.2	23.7
790	24.0	75.3	.167	5.2	396.3	954.9	2.788	32.9	22.1	22.2	23.5
791	22.3	74.8	.169	5.7	396.3	954.9	2.788	32.2	21.7	21.9	23.2
792	24.0	75.0	.172	6.4	396.3	954.9	2.788	31.7	21.3	21.5	23.2
793	22.7	76.0	.171	6.4	398.8	963.5	2.797	31.9	21.5	21.5	23.6
794	25.2	75.8	.174	6.4	398.8	963.5	2.797	31.9	21.5	21.6	23.5
795	24.1	76.0	.171	6.1	398.8	963.5	2.797	32.1	21.6	21.7	23.7
796	24.7	75.0	.169	5.7	398.8	963.5	2.797	32.3	21.8	21.9	23.4
797	23.2	74.5	.168	6.4	398.8	963.5	2.797	31.5	21.2	21.4	23.1
798	23.7	74.8	.166	5.7	398.8	963.5	2.797	32.1	21.6	21.8	23.3

9. LIST OF REFERENCES

REFERENCES

1. ALDRED, W. H. and BURCH, J. J. 1977. Telemetry and Microcomputer System Aids Investigation of Forces on Peaches During Mechanical Harvesting. ASAE Paper No. 77-1527, ASAE, St. Joseph, MI.
2. ANDERSON, G. and PARKS, R. 1984. The Electronic Potato. The British Society for Research, (Not Published).
3. DIENER, R. G., ADAMS, R.E., INGLE, M. ELLIOTT, K.C., NESSELROAD, P.E. and BLIZZARD, S.H. 1977. Bruise Energy of Peaches and Apples. ASAE Paper No. 77-1029, ASAE, St. Joseph MI.
4. FINNEY, E. E. jr. and MASSIE, R. D. 1975. Intrumentation for Testing the Response of Fruits to Mechanical Impact. ASAE Paper No. 75-3029, ASAE, St. Joseph, MI.
5. FLUCK, R.C. and AHMED, E.M. 1973. Impact Testing of Fruits and Vegetables. Transactions of the ASAE 16 (4):660-666.
6. FRIDLEY, R. B., BRADLY, R. A., RUMSEY, J. W., ADRIAN, P. A. 1967. Some Aspects of Elastic Behavior of Selected Fruits. ASAE Paper No. 67-337, ASAE, St. Joseph, MI.
7. GOFF, J.W. and TWEDE, D. 1979. Performance of Packages for the Transportation of Agricultural Products. Special Report No. 14, M.S.U. School of Packaging, E. Lansing, MI.
8. GOLDSMITH, W. 1960. Impact--the Theory and Physical Behavior of Colliding Solids. Edward Arnold Publishers. London. 369 p.
9. HALDERSON, J. L. , PETERSON, C.L. , DAIGH, R. C. 1983. A Telemetry Device for Impact Determination. Proceedings of the National Conference on Agricultural Electronics Application, Chicago, Dec. 11-13, (2): 773-780.
10. HALLEE, N. D. 1981. Telemetry Device for Monitoring the Damage Potential of Harvesting and Handling Equipment. Ph.D. Thesis, Pennsylvania State University, University Park, PA.

11. HAMANN, D.D. 1968. Analysis of Stress During Impact of Fruit Considered to be Viscoelastic. ASAE Paper No. 68-812, ASAE, St. Joseph, MI.
12. HAMMERLE, J.R. and MOHSEIN, N.N. 1965. Some Dynamic Aspects of Fruit Impacting Hard and Soft Materials. ASAE Paper No. 65-320, ASAE, St. Joseph, MI.
13. HARRISON, D. R. 1969. FM/AM Telemetry to Measure Impact Accelerations. NASA Ames Research Center, Moffet Field, CA.
14. HERTZ, H. 1896. Miscellaneous Papers. MacMillan and Company, New York.
15. HORSFIELD, B. L., FRIDLEY, R. B., and CLAYPOOL, L. L. 1972. Application of Theory of Elasticity to the Design of Fruit Harvesting and Handling Equipment for Minimum Bruising. Transaction of the ASAE 15:746-750.
16. INTEL Corporation 1986. Microcontroller Handbook. Intel corporation, 3065 Bowers Ave., Santa Clara, CA.
17. JENKINS, W. H. and HUMPHRIES, E. G. 1982. Impact Damage Assessment Technique. ASAE Paper No. 79-1560, ASAE, St. Joseph. MI.
18. KERR, G.L. and WILKIE, K.I. 1985. Damage Detection During the Handling of Fruits and Vegetables. Paper No. 85-202, CSAE, June 23-27, Annual Meeting, Charlottetown, Canada.
19. KLUG, B. A., B. R. TENNES, H. R. ZAPP, S.SIYAMI AND J.CLEMENS. 1986. Software for a Miniature Impact Data Acquisition Device. ASAE paper No. 86-3032, ASAE, St. Joseph, MI.
20. KUSZA, T.J. 1979. Apple Properties Related to packaging. Ph.D. Dissertation, Michigan State University, East Lansing, MI.
21. McDONALD, T., DELWICHE, M. J. 1983. Non-Destructive Sensing of Peach Flesh Firmness Using Impact Force Analysis. ASAE Paper No. 83-6540, ASAE, St. Joseph, MI.
22. MOHSEIN, N.N. 1970 . Physical Properties of Plant and Animal Materials. Gordon and Breach, Science Publishers, Inc., New York, NY.
23. MOHSEIN, N.N. 1971. Mechanical Properties of Fruits and Vegetables: Review of a Decade of Research Applications and Future Needs. ASAE Paper No. 71-849, ASAE, St. Joseph, MI.
24. NELSON, C.W., MOHSEIN, N.N. 1968. Maximum Allowable

Static and Dynamic Loads and Effects of Temperature for Mechanical Injury in Apples. Journal of Agric. Engng. Res. 13(4): 305-317.

25. O'BRIEN, M., R. B. FRIDLEY, J. R. GOSS and J. SHUBERT. 1973. Telemetry for Investigating Forces on Fruits During Handling. Transactions of the ASAE 16(2):245-247.

26. PAO, Y.H. 1955. Extension of the Hertz Theory of Impact to the Viscoelastic Case. Journal of Applied Physics 26(9):1083-1086.

27. PULLEN, J. M. and R. G. DIENER. 1971. A Low-Cost FET Triaxial Accelerometer with Vector Summing Capabilities. ASAE Paper No. 71-509, ASAE, St. Joseph, MI.

28. RIDER, R.C. 1969. Elastic Behavior of a Pseudo Fruit for Determining Bruise Damage to Fruit During Mechanized Handling. M.S. Thesis, University of California, Davis, CA.

29. RIDER, R.C., FRIDLEY, R.B., O'BRIEN, M. 1973. Elastic Behavior of a Pseudo-Fruit for Determining Bruise Damage to Fruit During Mechanized Handling. Transactions of the ASAE 16(2):241-244.

30. RHODES, J.E. 1960. Transducer System Frequency Requirements for Transient Measurements. Endevco Corp, TechData Report, Sept. 22.

31. SCHOORL, D. and HOLT, J.E. 1974. Bruising and Acceleration in Apple Packs. Qld. Journal of Agricultural and Animal Science. 31,83.

32. SCHOORL, D. and HOLT, J.E. 1980. Bruise Resistance Measurements in Apples. Journal of Texture Studies 11:389-394.

33. SHAHABASI, Y. 1979. Experimental and Numerical Techniques Related to the Maximum Allowable Depth of Apples in a Bulk Storage. Ph.D. dissertation, Michigan State University, East Lansing, Michigan.

34. SHUPE, W. L. and R. M. LAKE. 1970. Designing an Instrumented Test Egg for Detecting Impact Breakage. Shock and Vibration Bulletin No. 41:11-16.

35. TENNES, B. R., H. R. ZAPP AND G.K. BROWN. 1986. Produce Impact Detection and Monitoring Device. ASAE paper No. 86-3029, ASAE, St. Joseph, MI.

36. TIMOSHENKO, S. P., and GOODIER, J. N. 1951. Theory of Elasticity. McGraw-Hill, New York.

37. TURCZYN, M.T., GRANT, S.W., ASHBY, B.H. and WHEATSON, F.W. 1985. Potato Shatter Bruising During Laboratory Handling and Transportation Simulation. Unpublished report, Office Of Transportation, U.S. Dept. Of Agriculture, Washington, DC.

38. U.S.D.A. , AGRICULTURAL MARKETING SERVICE. 1964. Apples: Shipping Point Inspection Instructions. Fruit and Vegetable Division, Fresh Products Standardization and inspection Branch, Washington, DC.

39. WALKER, R. J. SCHOORL, D. and HOLT, J. E. 1978. The Vibration Bruising of Apples. Conference on Agriculture Engineering, Toowoomba, Aug. 29-31.

40. YANG, W. H. 1966. The Contact Problem for Viscoelastic Bodies. Transactions of ASME, Journal of Applied Mechanics 33(4):395-401.

General References

1. AHRENS, D. A. and SEARCY, S. W. 1984. Monitoring Grazing Activities with a data-Logging System. ASAE Paper No. 84-3029, ASAE, St. Joseph, MI.
2. BRANDENBERG, P. K. and LEE, J. L. 1985. Fundamentals of Packaging Dynamics. MTS System Corp, M.S.U. School of Packaging, East Lansing, MI.
3. BROWN, G. K. and SEGERLIND, L. J. 1975. The Location Probabilities of Surface Injuries for Some Mechanically Harvested Apples. Transactions of the ASAE, 18(1): 55-57.
4. CHEN, P., SUN, Z. 1981. Impact Parameters Related to Bruise Injury in Apples. ASAE Paper No. 81-3041. ASAE, St. Joseph, MI.
5. CHEN, P., TANG, S. and CHEN, S. 1985. Instrument for Testing the Response of Fruits to Impact. ASAE Paper No. 85-3537, ASAE, St. Joseph, MI.
6. CHESSON, J.H. and MOOR, J.L. 1983. An Automatic Recording Fruit Pressure Tester. ASAE Paper No. 83-3527, ASAE, St. Joseph, MI.
7. De BAERDEMAEKER, J. , LEMAITRE, L. and MEIRE, R. 1979. Quality Detection by Frequency Spectrum Analysis of the Fruit Impact Force. ASAE Paper No. 79-3060, ASAE, St. Joseph, MI.
8. De BAERDEMAKER, J.G. and SEGERLIND, L.J. 1974. Determination of the Viscoelastic Properties of Apple Flesh. ASAE Paper No. 74-3512, ASAE, St. Joseph, MI .
9. DELWICHE, M. J. and BOWERS, S. V. 1985. Signal Processing of Fruit Impact Forces for Firmness Detection. ASAE Paper No. 85-3029, ASAE, St. Joseph, MI.
10. DELWICHE, M.J., HOOD, C.E., LAMBERT, W.R. and McLEOD, M.F. Microcomputer Applications for Automated Sorting of Peaches. 1981. ASAE Paper No. 81-1608, ASAE, St. Joseph, MI.

11. DELWICHE, M.J. 1986. Theory of Fruit Firmness Sorting by Impact Forces. ASAE Paper No. 86-3027, ASAE, St. Joseph, MI.
12. FRANKE, J. E. and ROHRBACH, R. P. 1979. A Nonlinear Impact Model for a Sphere with a Flat Plate. ASAE Paper No. 79-1566, ASAE, St. Joseph, MI.
13. FRIDLEY, R.B., GOEHLICH, H., CLAYPOOL, L.L. and ADRIAN, P.A. 1964. Factors Affecting Impact Injury to Mechanically Harvested Fruit. Transactions of the ASAE 11(1):409-411.
14. GOFF, J.W. and PIERCE, S.R. 1969. A Procedure for Determining Damage Boundaries. Shock and Vibration Bulletin, Vol. 40, Part 6, pp. 127-131.
15. HALDERSON, J.L. and SKROBACKI, A. 1986. Dynamic Performance of an Impact Telemetry System. ASAE Paper No. 86-3030, ASAE, St. Joseph, MI.
16. HALDERSON, J.L. and HADERLIE, L.C. 1985. Mechanical Killing of Potato Vines. ASAE Paper No. 85-1073, ASAE, St. Joseph, MI.
17. HOLT, J.E. and SCHOORL, D. 1977. Bruising and Energy Dissipation in Apples. Journal of Texture Studies 7: 421-432.
18. HOLT J.E. and SCHOORL, D. 1978. The Prediction of Fruit Bruising from Fruit, Packing and Handling Studies. Conference on Agriculture Engineering, Toowoomba, Aug. 29-31.
19. JARIMOPAS, B., MANOR, G. and SARIG, Y. 1984. Mechanical Behavior and Bruising of Apple Under Quasi-Static Loading. ASAE Paper No. 84-1096, ASAE, St. Joseph, MI.
20. McDONALD, T. Non-Destructive Sensing of Peach Flesh Firmness Using Analysis of Forces. 1984. M.S. Thesis, Clemson University, Clemson, SC.
21. MINDLIN, R.D., 1945. Dynamics of Package Cushioning. Bell System Technical Journal, 24: 353-461.
22. MOHSEININ, N.N. 1971. Mechanical Properties of Fruits and Vegetables: Review of a Decade of Research Applications and Future Needs. ASAE Paper No. 71-849, ASAE, St. Joseph, MI.
23. NAHIR, D., SCHMILOVITCH, Z. and RONEN, B. 1986. Tomato Grading by Impact Force Response. ASAE Paper No. 86-3028, ASAE, St. Joseph, MI.
24. SIYAMI, S., TENNES, B.R., ZAPP, H.R., BROWN, G.K., KLUG, B. and CLEMENS, J. 1986. Microcontroller Based Data Acquisition System for Impact Measurement. ASAE Paper No. 86-3031, ASAE, St. Joseph, MI.